DESIGN OF CHITOSAN-ALGINATE NANOPARTICLES CONTAINING CURCUMIN DIETHYL DISUCCINATE

Mr. Settapon Bhunchu

A Dissertation Submitted in Partial Fulfillment of the Requirements
for the Degree of Doctor of Philosophy Program in Nanoscience and Technology
(Interdisciplinary Program)
Graduate School
Chulalongkorn University
Academic Year 2015

การออกแบบอนุภาคนาโนไคโตซาน-อัลจิเนตที่บรรจุเคอร์คิวมินไดเอทิลไดซักซิเนต

นายเศรษฐพล บุญชู

วิทยานิพนธ์นี้เป็นส่วนหนึ่งของการศึกษาตามหลักสูตรปริญญาวิทยาศาสตรดุษฎีบัณฑิต
สาขาวิชาวิทยาศาสตร์นาโนและเทคโนโลยี (สหสาขาวิชา)
บัณฑิตวิทยาลัย จุฬาลงกรณ์มหาวิทยาลัย
ปีการศึกษา 2558

Thesis Title	DESIGN OF CHITOSAN-ALGINATE NANOPARTICLES CONTAINING CURCUMIN DIETHYL DISUCCINATE
By	Mr. Settapon Bhunchu
Field of Study	Nanoscience and Technology
Thesis Advisor	Assistant Professor Pranee Rojsitthisak, Ph.D.
Thesis Co-Advisor	Associate Professor Pornchai Rojsitthisak, Ph.D.

Accepted by the Graduate School, Chulalongkorn University in Partial Fulfillment of the Requirements for the Doctoral Degree

.....Dean of the Graduate School

(Associate Professor Sunait Chutintaranond, Ph.D.)

THESIS COMMITTEE

.....Chairman

(Associate Professor Vudhichai Parasuk, Ph.D.)

.....Thesis Advisor

(Assistant Professor Pranee Rojsitthisak, Ph.D.)

.....Thesis Co-Advisor

(Associate Professor Pornchai Rojsitthisak, Ph.D.)

.....Examiner

(Phanphen Wattanaarsakit, Ph.D.)

.....Examiner

(Associate Professor Warangkana Warisnoicharoen, Ph.D.)

.....Examiner

(Assistant Professor Police Lieutenant Walaisiri Muangsiri, Ph.D.)

.....External Examiner

(Associate Professor Ubonthip Nimmannit, Ph.D.)

เศรษฐพล บุญชู : การออกแบบอนุภาคนาโนไคโตซาน-อัลจิเนตที่บรรจุเคอร์คิวมินไดเอทิลไดซักซิเนต (DESIGN OF CHITOSAN-ALGINATE NANOPARTICLES CONTAINING CURCUMIN DIETHYL DISUCCINATE) อ.ที่ปรึกษาวิทยานิพนธ์หลัก: ผศ. ดร. ปราณี โรจน์สิทธิศักดิ์, อ.ที่ปรึกษาวิทยานิพนธ์ร่วม: รศ. ภก. ดร. พรชัย โรจน์สิทธิศักดิ์, 131 หน้า.

เคอร์คิวมินไดเอทิลไดซักซิเนตเป็นโปรดรักส์ของเคอร์คิวมินอยด์ที่มีความคงตัวในพลาสมาของมนุษย์ และสามารถช่วยในการนำเข้าสู่เซลล์และมีความเป็นพิษต่อเซลล์มะเร็งได้มากกว่าเคอร์คิวมินและโปรดรักส์ของเคอร์คิวมินอนย์ชนิดอื่น ดังนั้นเคอร์คิวมินไดเอทิลไดซักซิเนตจึงมีศักยภาพในการพัฒนาเป็นสารต้านมะเร็งได้ ในงานวิจัยนี้จึงมุ่งเน้นการหาสภาวะที่เหมาะสมในการเตรียมไคโตซาน/อัลจิเนตนาโนพาร์ติเคิลสำหรับบรรจุเคอร์คิวมินไดเอทิลไดซักซิเนตโดยใช้การทดลองแบบบ็อกซ์-เบ็ห์นเคน (Box-Behnken statistical design) และการออกแบบพื้นผิวตอบสนอง (response surface methodology) เพื่อเพิ่มประสิทธิภาพทางการรักษาของเคอร์คิวมินไดเอทิลไดซักซิเนต ไคโตซาน/อัลจิเนตนาโนพาร์ติเคิลสำหรับบรรจุเคอร์คิวมินไดเอทิลไดซักซิเนตเตรียมด้วยวิธีอิมัลชันชนิดน้ำมันในน้ำร่วมกับวิธีการเกิดเจล แบบไอออนิก (ionotropic gelification) โดยเริ่มจากการคัดกรองปัจจัยหลักที่มีผลต่อการเตรียมนาโนพาร์เคิลและหาสภาวะที่เหมาะสมเบื้องต้นด้วยวิธีการออกแบบการทดลองแบบปรับตั้งค่ากระบวนการทีละค่า จากผลการศึกษาพบว่า อัตราส่วนระหว่างไคโตซานต่ออัลจิเนต, ความเข้มข้นของ Pluronic® F127 และ ความเข้มข้นของเคอร์คิวมินไดเอทิลไดซักซิเนต เป็นปัจจัยหลักที่มีผลต่อการเตรียมโนพาร์ติเคิล โดยสภาวะการเตรียมนาโนพาร์ติเคิลที่เหมาะสมเบื้องต้นคือ อัตราส่วนระหว่างไคโตซานต่ออัลจิเนต เท่ากับ 015:1, ความเข้มข้นของ Pluronic® F127 เท่ากับ ร้อยละ 1 โดยมวลต่อปริมาตรและความเข้มข้นของเคอร์คิวมินไดเอทิลไดซักซิเนต 1 มิลลิกรัม/มิลลิลิตร นาโนพาร์ติเคิลที่เตรียมขึ้นจากสภาวะดังกล่าวมีความคงตัวทางกายภาพโดยสามารถเก็บไว้ที่อุณหภูมิ 4 องศาเซลเซียส เป็นเวลา 3 เดือน นอกจากนี้นาโนพาร์ติเคิลที่พัฒนาขึ้นยังสามารถนำเคอร์คิวมินไดเอทิลไดซักซิเนตเข้าสู่เซลล์มะเร็งลำไส้ชนิด Caco-2 ได้เพิ่มสูงขึ้นอย่างมีนัยสำคัญเมื่อเปรียบเทียบกับสารละลายเคอร์คิวมินไดเอทิลไดซักซิเนต งานวิจัยนี้ยังเพิ่มความแม่นยำในการหาสภาวะที่เหมาะสมในการเตรียมนาโนพาร์ติเคิลด้วยวิธีการออกแบบบอกซ์-เบ็ห์นเคนและการออกแบบพื้นผิวตอบสนอง โดยศึกษาสารลดแรงตึงผิวชนิดไม่มีประจุ 2 ชนิด ได้แก่ Tween® 80 และ Pluronic® F127 จากผลการศึกษาพบว่าสภาวะที่เหมาะสมในการเตรียมนาโนพาร์ติเคิลตำรับที่ใช้สารลดแรงตึงผิวชนิด Tween® 80 คือ อัตราส่วนระหว่างไคโตซานต่ออัลจิเนต 0.05:1, ความเข้มข้นของ Tween® 80 ร้อยละ 4.05 โดยมวลต่อปริมาตรและความเข้มข้นของเคอร์คิวมินไดเอทิลไดซักซิเนต 1.5 มิลลิกรัม/มิลลิลิตร และสำหรับนาโนพาร์ติเคิลตำรับที่ใช้สารลดแรงตึงผิวชนิด Pluronic® F127 คือ อัตราส่วนระหว่างไคโตซานต่ออัลจิเนต 0.15:1, ความเข้มข้นของ Pluronic® F127 ร้อยละ 0.65 โดยมวลต่อปริมาตรและความเข้มข้นของเคอร์คิวมินไดเอทิลไดซักซิเนต 1.5 มิลลิกรัม/มิลลิลิตร ผลการวิเคราะห์ด้วย FTIR, TGA และ XRD ยืนยันได้ว่าเคอร์คิวมินไดเอทิลไดซักซิเนตถูกบรรจุลงในนาโนพาร์ติเคิลและไม่เกิดการเสียสภาพภายหลังการบรรจุ นอกจากนี้ยังพบว่านาโนพาร์ติเคิลที่บรรจุเคอร์คิวมินไดเอทิลไดซักซิเนตสามารถเข้าสู่เซลล์และมีความเป็นพิษต่อเซลล์เซลล์มะเร็งเต้านมทดสอบชนิด MDA-MB-231 ได้ดีกว่าสารละลายเคอร์คิวมินไดเอทิลไดซักซิเนตอย่างมีนัยสำคัญ และจากผลการศึกษาด้านความคงตัวทางกายภาพและเคมีพบว่านาโนพาร์ติเคิลที่เตรียมขึ้นมีความคงตัวเมื่อเก็บในรูปสารละลายที่อุณหภูมิ 4 องศาเซลเซียส นาน 3 เดือน

สาขาวิชา วิทยาศาสตร์นาโนและเทคโนโลยี ลายมือชื่อนิสิต .....

ปีการศึกษา 2558 ลายมือชื่อ อ.ที่ปรึกษาหลัก .....

ลายมือชื่อ อ.ที่ปรึกษาร่วม .....

5487849720 : MAJOR NANOSCIENCE AND TECHNOLOGY
KEYWORDS: CHITOSAN, ALGINATE, CURCUMIN DIETHYL DISUCCINATE, BOX-BEHNKEN DESIGN

SETTAPON BHUNCHU: DESIGN OF CHITOSAN-ALGINATE NANOPARTICLES CONTAINING CURCUMIN DIETHYL DISUCCINATE. ADVISOR: ASST. PROF. PRANEE ROJSITTHISAK, Ph.D., CO-ADVISOR: ASSOC. PROF. PORNCHAI ROJSITTHISAK, Ph.D., 131 pp.

Curcumin diethyl disuccinate (CDD) is a succinate prodrug of curcuminoids that has better stability in human plasma and improved *in vitro* cellular uptake and cytotoxicity compared to curcumin and other succinate prodrugs. Therefore, CDD has a potential for further development as an anticancer agent. In this study, we focuses on optimization of the formulation of CDD-loaded chitosan/alginate nanoparticles using Box-Behnken statistical design and response surface methodology to enhance the therapeutic efficacy of CDD. Oil-in-water emulsification followed by ionotropic gelification was used to prepare the CDD-loaded nanoparticles. One-variable-at-a-time approach was used as a parameter screening technique and pre-optimization for CDD-loaded nanoparticles. The chitosan/alginate mass ratio, and concentrations of Pluronic® F127 and CDD were the major affecting parameters. The pre-optimaized formulation of nanoparticles was a chitosan/alginate mass ratio of 0.15:1, a Pluronic® F127 concentration of 1% (w/v) and a CDD concentration of 1 mg/ml. The pre-optimized CDD-loaded nanoparticles could stored at 4°C up to 3 months. In addition, the CDD-loaded nanoparticles showed significantly higher cellular uptake in Caco-2 cell line compared to free CDD. To determine the interaction among the parameters, the Box-Behnken experimental design and response surface methodology were used to design and optimize the CDD-Nanoparticles with two types of non-ionic surfactants including Tween® 80 and Pluronic® F127. The optimized formulation of CDD-loaded chitosan/alginate nanoparticles based on Tween® 80 was chitosan/alginate mass ratio of 0.05:1, Tween® 80 concentration of 4.05% (w/v) and CDD concentration of 3 mg/ml. On the other hand, the optimalized formulation based on Pluronic® F127 was chitosan/alginate mass ratio of 0.05:1, Pluronic® F127 content of 0.65% (w/v) and CDD concentration of 1.5 mg/ml. The encapsulation of CDD in the nanoparticles was confirmed using FTIR, TGA and XRD. . *In vitro* cytotoxicity and cellular uptake studies showed that CDD-loaded chitosan/alginate nanoparticles using Pluronic® F127 as a stabilizer had significantly higher cytotoxicity and cellular uptake in human breast adenocarcinoma MDA-MB-231 cells, compared to free CDD. Physical and chemical stability studies indicated that the optimally formulated CDD-loaded chitosan/alginate nanoparticles were stable at 4°C for 3 months.

Field of Study: Nanoscience and Technology
Academic Year: 2015

Student's Signature .....
Advisor's Signature .....
Co-Advisor's Signature .....

ACKNOWLEDGEMENTS

This thesis would not have been to complete without the assistance and support of numerous individuals. I would like to express my deepest gratitude to my advisor, Assistant Professor Pranee Rojsitthisak, Ph.D. and my co-advisor, Associate Professor Pornchai Rojsitthisak, Ph.D. for their excellent instruction, guidance, encouragement and support throughout this thesis.

My gratitude is also extended to Associate Professor Vudhichai Parasuk, Ph.D., Associate Professor Warangkana Warisnoicharoen, Ph.D., Assistant Professor Walaisiri Muangsiri, Ph.D., Dr. Phanphen Wattanaarsakit, Ph.D. and Associate Professor Ubonthip Nimmannit, Ph.D. for serving as thesis-committee.

My appreciation is also expressed to Associate Professor Ian S. Haworth, Ph.D. (University of Southern California), Professor Qian Wang, Ph.D. (University of South Carolina), and Professor Suwabun Chirachanchai (Petroleum and Petrochemical College, Chulalongkorn University) for their support and comments throughout this work.

Sincere thanks are also extended to the members in SWB research groups, Petroleum and Petrochemical College, Chulalongkorn University, for their assistance and friendship. And I am thankful to the members in Wang research group. Department of Chemistry and Biochemistry, University of South Carolina, who have made me feel so welcome during my research period in United State of America.

Finally, the greatest gratitude and indebtedness are expressed to my parent for their support, unlimited love, understanding and everything given to my life.

The funding is acknowledged from the Graduate School and Center of Innovative Nanotechnology, Chulalongkorn University for a Scholarship and the 90th Anniversary of Chulalongkorn University Fund and Ratchadaphiseksomphot Endowment Fund of Chulalongkorn University (RES560530014-AM) for providing research funds.

CONTENTS

Page

Page

Page

Page

Page

LIST OF FIGURES

Page

Page

Page

LIST OF TABLES

Page

Page

PART I

THESIS CONTENT

1. Overview of the publications

Over the past few decades, there has been an increased interest in nanoparticulate drug carrier systems. In particular, nanoparticles formulated from naturally occurring polymers. For example, chitosan/alginate nanoparticles have received an increasing public attention in the fields of drug delivery and pharmaceutics, because of their biodegradable, biocompatible, non-toxic properties. In addition, chitosan/alginate nanoparticles have also been widely studied for the encapsulation of various bioactive compounds with promising results.

Curcumin diethyl disuccinate (CDD), a succinate prodrug of curcumin, has been shown to exhibit various pharmacological properties such as analgesic, anti-inflammatory and anticancer activities. Currently, the research related with the improvement of pharmaceutical properties of CDD by encapsulation in chitosan/alginate nanoparticulate systems has not yet been investigated. Therefore, this research focuses on the formulation and optimization of chitosan/alginate nanoparticles for encapsulation of CDD using the statistical experimental design. The preparation parameters affecting the characteristics of CDD-loaded chitosan/alginate nanoparticles are also discussed.

The response surface methodology (RSM) and Box-Behnken experimental design are useful in simultaneously analyzing variables when the variable interactions are very complicated. Many studies demonstrated the value of RSM for establishing the optimal formulation in various drug delivery systems. Therefore, in this study, Box-Behnken design was chosen for statistical optimization and evaluation of the main effects, interaction and quadratic effects.

The aims of the dissertation were to design and optimize the independent variables in order to achieve desired particle size, zeta potential, encapsulation efficiency and loading capacity for CDD-loaded nanoparticles. Finally, *In vitro* cellular uptake and cytotoxicity of CDD-loaded chitosan/alginate nanoparticles were examined by confocal laser scanning microscopy in human epithelial colorectal adenocarcinoma Caco-2 cells and human breast cancer cells. This dissertation contains 4 research publications as follows:

The first publication provides an overview of the use of nanoparticulate drug delivery systems for cancer therapy. The first part of the review was discussed on the application of different types of nanoparticles in cancer treatment. The subsequent sections focused on the characteristics and applications of chitosan, alginate and chitosan/alginate nanoparticles with anticancer drugs in cancer treatment. Based on our findings, we conclude that chitosan and alginate are suitable for the development of polymeric nanoparticles as a potential drug delivery system of CDD and could be applied for hydrophobic bioactive compounds.

The second publication investigated the effects of preparation parameters on the characteristics of chitosan/alginate nanoparticles containing CDD using the traditional optimization technique, namely one-variable-at-a-time. The results indicated that the crucial factors affecting the characteristics of nanoparticles were chitosan/alginate mass ratio, type and concentration of non-ionic surfactant and concentration of CDD. The prepared CDD-loaded nanoparticles under the optimum conditions stored at 4°C were physically stable up to 3 months and also showed a significantly higher cellular uptake in Caco-2 cell line compared to free CDD. However, one-variable-at-a-time used in this experiment was time consuming and expensive when a large number of parameters were considered. In order to overcome these difficulties and improve the ability to determine the interaction among the parameters, the statistical experimental designs, i.e. Box-Behnken experimental design and response surface methodology, were employed for optimization as presented in the third and the forth publications.

Based on the results shown in the second publication, Pluronic® F127 and Tween® 80 showed higher encapsulation efficiency and loading capacity compared to Cremophor RH40™. In addition, Pluronic® F127 and Tween® 80 are non-toxic and non-irritant. Therefore, Pluronic® F127 and Tween® 80 were chosen for the further study as presented in publication 3 and publication 4, respectively.

The third publication based on the formulation optimization using response surface methodology. The results demonstrated that response surface methodology was found to be an effective technique for optimization of the preparation of chitosan/alginate nanoparticles using a limited number of experiments. The optimized formulation of nanoparticles containing CDD had a chitosan/alginate mass ratio of 0.05:1, a CDD concentration of 3 mg/ml, and a Tween® 80 content of 4.05% (w/v).

According to the forth publication, the results demonstrated that CDD-loaded nanoparticles were successfully optimized and developed using Box-Behnken experimental design coupled with response surface methodology. *In vitro* cytotoxicity and cellular uptake studies also confirmed that the optimized CDD-loaded nanoparticles showed relatively higher cytotoxicity efficacy and cellular uptake to MDA-MB-231 breast cancer cells than free CDD.

All publications were presented in Part II and the original articles were attached in appendices as partial fulfillment of the requirements for the Degree of Doctor of Philosophy, Program in Nanoscience and Technology, Graduate School, Chulalongkorn University.

2. Background and problem statement

Recently, nanoparticulate drug carrier systems have received great interest in cosmeticutical and pharmaceutical applications due to their abilities to improve bioavailability, stability, pharmacokinetic and pharmacodynamic properties of therapeutic agents [1, 2]. Nanoparticulate drug carrier systems also improve poor aqueous solubility of hydrophobic drugs in the aqueous medium for parenteral administration [3]. In addition, they have been used for delivery drugs to target sites

by attaching the specific ligands resulting in the reduction of side effects to healthy cells or organs [4, 5]. The examples of nanoparticulate drug carrier systems are liposomes, niosomes, nanoemulsion, solid lipid nanoparticles and polymeric nanoparticles, etc. The selection of nanoparticulate drug carrier systems depends on properties of drugs, routes of administration, target environments and pharmaceutical applications. In this dissertation, polymeric nanoparticles were chosen due to their ability to protect drugs from biodegradation and to increase drug stability.

Polymeric nanoparticles are effective carriers for delivery of various bioactive compounds such as DNA, peptides and proteins to target cells or tissues [6-8]. Drugs incorporated in polymeric nanoparticles include chemotherapeutic agents [9, 10], antimicrobial agents [11], anti-ischemic drug [12], etc. The advantage of polymeric nanoparticles is their ability to improve the physicochemical and biopharmaceutical properties of drugs, resulting in an increase in therapeutic efficacy [13, 14]. For example, they enhance water solubility, chemical and metabolic stability, and bioavailability of drugs [15]. Polymeric nanoparticles can be designed to provide different formulations for various administration routes, site specific drug delivery and controlled release, depending on polymers and preparation methods [16-18].

Polymers used as matrices or shells of polymeric nanoparticles can be synthetic and naturally occurring polymers. Among these polymers, alginate and chitosan are commonly employed because they possess many desirable properties such as nontoxicity, biocompatibility, biodegradability, high hydrophilicity, and good film forming ability [8, 19, 20].

Alginate is an anionic biopolymer derived from marine brown algae. It is unbranched block copolymers of β-D-mannuronic acid and α-L-guluronic acid residues linked by (1→4) glycosidic linkages as shown in Figure. 1 [21]. Alginate has been extensively used as a carrier for therapeutic agents, and has received much attention due to many favorable characteristics including biodegradability, biocompatibility, mucoadhesive, and mild gelation condition [22]. In the presence of divalent cations or cationic polymers, alginate forms hydrogels for controlled release and drug delivery

system. For example, calcium ions interact with guluronic acid residues of alginate and form eggbox structures between two neighboring alginate chains or inside the chain [12].

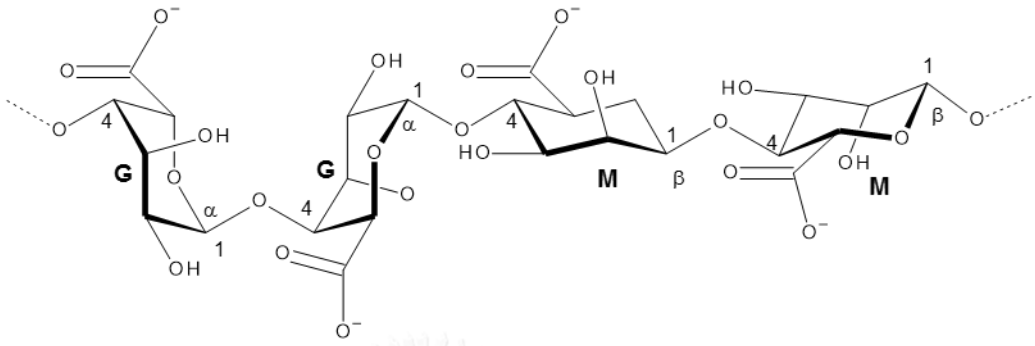

Figure 1 Chemical structure of alginate. G: guluronic acid; M: mannuronic acid [23].

Although, alginate has been extensively used for controlled release and drug delivery system, they have some limitations that may reduce therapeutic efficacy such as low stability in the alkaline environment [24] and loss of encapsulated drugs by leaking through the pores of alginate particles [25]. To overcome these limitations, alginate particles should be modified or stabilized with cationic polymers such as chitosan [20, 26, 27].

Chitosan is a cationic biopolymer comprising D-glucosamine and N-acetyl-D glucosamine linked by β(1→4) glycosidic linkages as presented in Figure. 2 [23]. Chitosan is commercially produced by alkaline extraction of chitin [28]. Chitosan can form complexes with anionic biopolymers and used for controlled release and drug delivery systems [29-32]. For example, chitosan forms complexes with alginate by ionotropic gelation [32, 33]. The formation occurs because of electrostatic interaction between carboxylic groups of alginate and amino groups of chitosan [34]. To get the size in nanometer scale, the mass ratio of alginate/$CaCl_2$/chitosan should be 10:1.7:1 [35]. For encapsulation of hydrophobic drug, surfactant should be used in the formulation [27] and non-ionic surfactants is frequently chosen because it is less toxic comparing to anionic and cationic surfactants [36-38].

The use of chitosan as second counter ions could reduce pores of alginate particles and the leakage of encapsulated drug [39]. In addition, chitosan could improve the physical stability of alginate nanoparticles. Nagarwal et al. [40], Lertsutthiwong et al. [27] and Motwani et al. [34] suggested that chitosan/alginate nanoparticles performed more effective controlled release than nanoparticles made of either chitosan or alginate alone. In addition, chitosan also improved other properties of alginate particles such as permeability, stability and shelf-life during storage and half-life in biological fluids [26]. However, only few studies have been reported on the use of chitosan/alginate nanoparticles for encapsulation of hydrophobic drug especially natural therapeutic compounds.

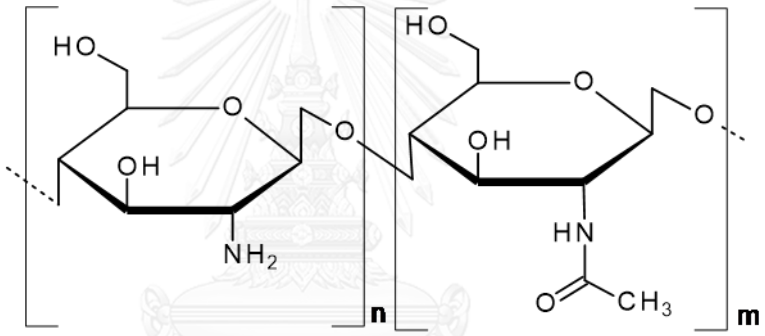

Figure 2 Chemical structure of chitosan [23].

Curcumin is one of the most important natural bioactive compounds and extensively used in South Asia as a food ingredient and a traditional medicine as a topical household remedy for the treatment of sprains, swelling, and wounds [41]. Curcumin (also named diferuloyl methane) or 1,7-bis(4-hydroxy-3-methoxyphenyl)-1,6-heptadiene-3,5-dione is a hydrophobic polyphenol extracted from rhizomes of turmeric (*Curcuma longa* L.) [42]. Curcumin was predominantly used for the treatment of a wide variety of diseases because of its wide spectra of pharmacological activities such as antioxidant, radical scavenging [43, 44], antibacterial, antifungal, antiviral [45], antiinflammatory [46], anticarcinogenic and chemopreventive properties [47]. In addition, curcumin also performs thrombosis suppressing [48], myocardial infarction protective [49], nephron- and hepato-protective [50, 51], antirheumatic and

hypoglycemic properties [42]. Although curcumin has been found to be safe at very large dose and has a potential to be used as a health-promoting agent, it has not been approved as a therapeutic agent [3]. Curcumin is poor water solubility, low bioavailability and intense staining color [52]. These limit the development of curcumin for pharmaceutical and biochemical applications. Therefore, several approaches to overcome these problems have been investigated either by formulation [21, 53-56] or conjugation of curcumin [57-60]. For example, the enhancement of water solubility and stability of curcumin was accomplished by encapsulation of curcumin in various media such as micelles [61], hydrogel [62], microcapsules [63], nanocapsules [21] and nanoparticles [64-66]. In addition, the properties of curcumin can be improved by interaction or complexation with macromolecules [67], and chemical alteration [60, 68]. Wichitnithad et al. [59] synthesized succinate prodrugs of curcuminoids by aldol condensation of 2,4-pentanedione with different benzaldehydes and subsequent esterification with a methyl or ethyl ester of succinyl chloride. The succinate prodrugs of curcuminoids were determined on the stability and anticolon cancer property. Curcumin diethyl disuccinate (CDD) (Figure. 3) was found to be more stable than curcumin in phosphate buffer at pH 7.4. In addition, CDD exhibited the highest anticolon cancer activity compared to other synthesized succinate prodrugs and curcumin. CDD also showed antinociceptive activity [59]. However, nanoparticle formulations of CDD for improvement of its pharmacological properties and delivery system has not yet been investigated. Therefore, this study focuses on the formulation of polymeric nanoparticles for CDD using natural biopolymers, i.e. alginate and chitosan as polymer materials due to their biodegradability, biocompatibility, non-toxicity, hemocompatibility and mucoadhesive properties [34].

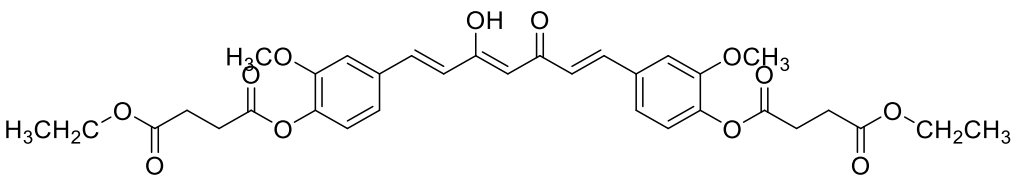

Figure 3 The chemical structure of curcumin diethyl disuccinate [69].

Process optimizing refers to enhancing the performance of a system, or product in order to obtain the maximum advantage from it. Commonly, the meaning of process optimization is discovering conditions at which to apply a procedure or methodology that produces the best possible response [70]. Traditionally, process optimization has been carried out by investigating the effect of one parameter at a time on an experimental response. While only one parameter is changed, others are kept at a constant level. This optimization method is called one-variable-at-a-time. Its major disadvantage is that it does not include the interactive effects among the variables studied. As a consequence, this technique does not depict the complete effects of the parameter on the response [71-73]. Another disadvantage of the one-variable-at-a-time optimization method is the large number of experiments are required to conduct the research, which leads to an increase the time, expenses and consumption of reagents and materials.

To overcome these problems, the process optimization should be carried out using multivariate statistic techniques. Among the most relevant multivariate techniques used in process optimization is response surface methodology (RSM), which is a collection of mathematical and statistical techniques based on the fit of a polynomial equation to the experimental data. RSM has a significant application in the design, development, and formulation of new products, as well as in the enhancement of existing product design. Usually, RSM including factorial experimental design and regression analysis can be used to evaluate the effective parameters and to generate mathematical models in order to investigate the interactions and to select the optimum conditions of a desirable response [74, 75]. RSM with several types of mathematic models are also widely used for modeling of drug formulation due to the complexity of formulation ingredients and processing parameters of drug formulations. RSM defines the effect of the independent variables, alone or in combination, on the process. Furthermore, in analyzing the effects of the independent variables, RSM generates a mathematical model that accurately describes the overall process [76]. The effectiveness of RSM methodology in optimizing of drug formulations in

pharmaceutical sciences has been documented in the literatures [39, 77-79], and it has been successfully applied for modeling and optimization of the preparing conditions for several drug formulations.

Before applying the RSM methodology, it is necessary to choose which design should be carried out for this study. There are some experimental matrices for this purpose. Experimental design for first-order models (e.g., factorial designs) can be used when the data set does not present any curvature [80]. However, to estimate a response function with an experimental data that cannot be described by linear functions, experimental designs for quadratic response surfaces such as three-level factorial, Box–Behnken, central composite, and Doehlert designs should be used.

Box–Behnken experimental designs [81] are response surface designs, especially made based on only three-coded levels -1, 0, and +1, whereas central composite made based on five levels. They are formed by combining two-level factorial designs with incomplete block designs. This procedure creates designs with desirable statistical properties but, most importantly, with only a fraction of the experiments required for a three-level factorial. Because there are only three levels, the quadratic model is appropriate. The coefficients of the quadratic model may be calculated using standard regression techniques [82].

In addition, the Box-Behnken experimental design was specially selected in optimization of drug formulations since it requires fewer runs than a central composite and Doehlert experimental designs, in cases of three or four factors [83]. This cubic design is characterized by set of points lying at the midpoint of each edge of a multidimensional cube and center point replicates (n = 3) whereas the ‘missing corners’ as shown in Figure. 4(c) help the experimenter to avoid the combined factor extremes. This property prevents a potential loss of data in those cases [84] Table 1 shows some applications of the Box–Behnken mathematical design in drug formulation developments.

Table 1 Some applications of Box–Behnken design in drug formulation development.

Type of carriers	Drugs	Objective of study	References
PLGA nanoparticles	Lorazepam	Establishing the optimum conditions for to optimize lorazepam loaded PLGA nanoparticles formulation	Sharma et al.[85]
Solid-lipid nanoparticles	Chloramphenicol	To optimize preparation process a solid lipid nanoparticle (SLN) of chloramphenicol for ocular delivery	Hao et al.[86]
Polymeric lipid nanoparticles	Itraconazole	To optimize a polymeric lipid hybrid nanoparticles (Lipomer) containing hydrophobic antifungal drug Itraconazole and to improve intestinal permeability.	Gajra et al.[87]
PEG-PLGA nanoparticles	Docetaxel	To optimize a solid lipid nanoparticle (SLN) of docetaxel for delivery to SKOV3 tumor cell lines.	Noori-Koopaei et al. [88]

Table 1 Some applications of Box–Behnken design in drug formulation development (continue).

Type of carriers	Drugs	Objective of study	References
Chitosan and Magnetic-chitosan nanoparticles	Tacrine	Establishing the optimum conditions of chitosan and magnetic-chitosan nanoparticles of tacrine for Alzheimer treatment.	Elmizadeh et al.[89]
Carbopol 934P gel	Diclofenac and Curcumin	To optimize and formulation of gels of diclofenac and curcumin for transdermal drug delivery	Chaudhary et al.[90]

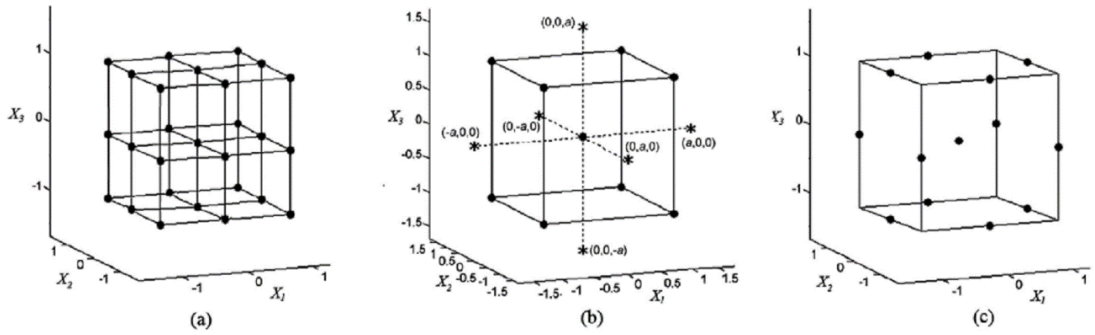

Figure 4 Response surface design based on three-variables, three-levels; (a) three-level full factorial design; (b) Central composite design and (c) Box-Behnken design in graphics [91].

A design matrix comprising of 15 experimental runs was constructed, for which the non-linear computer generated quadratic model is defined as:

$$Y = b_0 + b_1X_1 + b_2X_2 + b_3X_3 + b_{12}X_1X_2 + b_{13}X_1X_3 + b_{23}X_2X_3 + b_{11}X_1^2 + b_{22}X_2^2 + b_{33}X_3^2$$

Where Y is the measured response associated with each factor level combination; b_0 is an intercept; b_1 to b_{33} are regression coefficients computed from the observed experimental values of Y from experimental runs; and X_1, X_2 and X_3 are the coded levels of independent variables. The terms X_1X_2 and X^2_i (i = 1, 2 or 3) represent the interaction and quadratic terms, respectively [34].

Therefore, in this dissertation, RSM and Box-Behnken mathematical design is chosen for statistical optimization and evaluation of the main effects, interaction and quadratic effects of the formulation ingredients on the characteristics of CDD-loaded chitosan-alginate nanoparticulate formulations.

3. Research objectives

The overall objective of this study was to prepare, characterize and optimize the formulation of chitosan-alginate nanoparticles containing CDD using response surface methodology. The specific objectives are classified according to publications as described below:

Publication 1: To overview the drug delivery systems for cancer treatment, the use of biopolymeric alginate-chitosan nanoparticles and its the important characteristics for anticancer drug delivery.

Publication 2: To investigate the effects of the type and concentration of non-ionic surfactants, the chitosan/alginate mass ratio, and the concentration and rate of CDD addition into the formulation on the characteristics of nanoparticles. In addition, *in vitro* cellular uptake of nanoparticles containing CDD was examined by confocal laser scanning microscopy in human epithelial colorectal adenocarcinoma Caco-2 cells.

Publication 3: To design and optimize the CDD-loaded chitosan/alginate nanoparticles prepared with Tween® 80 formulation using Box-Behnken experimental design and response surface methodology. The significant formulation and preparation parameters obtained from publication 2 were applied to design and optimize the nanoparticles.

Publication 4: To design and optimize the CDD-loaded chitosan/alginate nanoparticles prepared with Pluronic® F127 formulation using Box-Behnken experimental design and response surface methodology. The crucial affecting parameters obtained in publication 2 and the basic information about statistical optimization technique in publication 3 were applied to design and optimize the nanoparticles. The chemical and physical stability of the optimized nanoparticles were subsequently studied. In addition, we also investigated - *in vitro* cytotoxicity and cellular uptake using MDA-MB-231 breast cancer cell lines.

4. Scope of study

The work focused on the design and optimization of CDD-loaded nanoparticles using Box-Behnken experimental design and response surface methodology. The influence of preparation parameters on the characteristics of CDD-loaded nanoparticles including chitosan/alginate mass ratio, type and concentration of non-ionic surfactants, CDD concentration rate of CDD addition into the formulations were

investigated. *In vitro* cellular uptake and cytotoxicity of CDD-loaded chitosan/alginate nanoparticles were also examined by confocal laser scanning microscopy in human epithelial colorectal adenocarcinoma Caco-2 cells and human breast cancer cells.

5. Advantages of the dissertation

The optimal formulation of CDD-loaded chitosan/alginate nanoparticles provided by the Box-Behnken experimental design and response surface methodology showed the effective drug carries in drug delivery system with *in vitro* cytotoxicity against various types of cancer cells. The obtained formulation could be applied as the prototype for further development of nanoparticles containing hydrophobic drugs.

PART II

THE MANUSCRIPTS OF THE DISSERTATION

CHAPTER I

BIOPOLYMERIC ALGINATE-CHITOSAN NANOPARTICLES AS DRUG DELIVERY CARRIER FOR CANCER THERAPY

Settapon Bhunchu[1], Pranee Rojsitthisak[2*]

[1]Ph.D. Program in Nanoscience and Technology (International), Graduate School, Chulalongkorn University, Bangkok 10330, Thailand

[2]Metallurgy and Materials Science Research Institute, Chulalongkorn University 10330, Bangkok, Thailand

Published in Pharmazie 2014, 69: 563-570.

Abstract

Nanoparticulate drug delivery systems enhance cancer treatment by direct entry of nanometer particles into the fenestration in the vasculature of cancer cells. Nanoparticles for encapsulation of anticancer drugs are preferably prepared using natural polymers as carriers, with polysaccharides being particularly favorable. Alginate and chitosan polysaccharides have been widely used in nanoparticulate drug delivery systems because of their biodegradable, biocompatible, non-toxic and bioadhesive properties. In this review, we present an overview of drug delivery systems for cancer treatment, describe the use of biopolymeric alginate-chitosan nanoparticles for anticancer drug delivery, and discuss the important characteristics of these nanoparticles for use in drug delivery.

Keywords: Alginate; Chitosan; Nanoparticles; Drug delivery system; Cancer therapy Stability

1.1. Introduction

Surgery, chemotherapy and radiation are widely used for cancer therapy, but have limitations such as destruction of healthy cells, cytotoxicity, inflammatory effects, and skin burning from radiation [79, 92]. A nanoparticulate drug delivery system (NPDDS) offers an alternative approach to delivery of anticancer drugs that may improve their pharmacological and therapeutic properties [79, 93-95]. A NPDDS can protect an anticancer drug against degradation during delivery to the target tissue and also provide a therapeutic level of the drug at specific organ sites. Various types of nanoparticles have been used in drug delivery systems, including polymeric nanoparticles, nanovesicles and nanoemulsions (Figure 5) [96]. In such nanoparticles, the use of natural biopolymers (and especially polysaccharides) is preferable owing to their non-toxicity, biodegradability, biocompatibility, and protective and hydrophilic properties [97]. Biopolymeric hydrogel nanoparticles are formulated by an interaction between anionic and cationic biopolymers [98-101]. The hydrogel nanoparticles have good characteristics for encapsulation of drugs and delivery to a target site [27, 34, 102, 103].

Most attempts at use of anticancer drugs in a drug delivery system have involved hydrophobic drugs encapsulated into an aqueous nanoparticulate system, with the goal of delivering the drug to the target site and releasing the full potential of the encapsulated drug [104]. The biodegradable, biocompatible and non-toxic properties required for the polymers in these systems are met by natural biopolymers such as alginate and chitosan. In this review, we provide an overview of the use of drug delivery systems in cancer treatment and of biopolymeric alginate-chitosan nanoparticles as anticancer drug carriers. We also discuss the important characteristics of alginate-chitosan nanoparticles for use in a drug delivery system.

1.2. Drug delivery systems for cancer treatment

Cancer is a group of diseases related to abnormal cell growth and uncontrollable cell division. Cancer cells can also spread to other parts of the body *via* the blood

stream and lymphatic system, and consequently destroy healthy cells [105]. Anand et al. [106] reported that 90–95% of cancers occur due to environmental pollutants, radiation, infection, tobacco use, poor diet and obesity, and 5–10% due to genetics. Surgery is the primary treatment for all types of cancer, but is not suitable when cancer cells have spread to other parts of the body. Side effects of pain, fatigue, bleeding, infection and lymphedema may also occur. Chemotherapy and radiotherapy also have side effects such as destruction of healthy cells, toxicity and loss of hair [92, 107]. Therefore, new cancer therapies are required and there is growing interest in NPDDS development for delivery of anticancer drugs to a target organ.

A drug delivery system is used for administration of a drug to achieve a therapeutic effect with safety and convenience to patients [104]. A NPDDS is a modified drug delivery system using nanotechnology for (i) improvement of specific drug targeting and delivery efficiency, (ii) reduction of side effects, (iii) improved safety and biocompatibility, and (iv) faster and lasting development of medicines [79, 95]. NPDDSs have been widely studied for anticancer drugs [108-110] because of their versatile properties. For example, nanoparticles of size 10–100 nm are suitable for intravenous delivery because the nanoparticles are smaller than the diameter of intravenous capillaries (5–6 μm), and thus can pass through the blood circulation and distribute *in vivo* [111, 112]. Nanoparticles can also penetrate through tissues to approach sites that larger particles cannot reach. For example, Bawa [113] reported that chemotherapeutic drug-nanoparticles can be delivered into tumor cells *via* leaky holes in the microvasculature, with an extended circulation time and accumulation of the drug within the tumor cells.

Nanoparticles can be classified as natural or synthetic [95, 114]. Examples of synthetic nanoparticles include carbon black, carbon nanotubes, fullerenes, quantum dots, metals, metal oxides and semiconductors. However, synthetic nanoparticles may be toxic to humans, animals and the environment [115, 116], and thus natural nanoparticles are used for biomedical applications. Various biopolymers have been used in such nanoparticles, including poly(3-hydroxybutyrate), poly(lactic acid), poly(e-

caprolactone), and copolymers of polyglycolide, alginate and chitosan [117]. Examples of nanoparticles produced from various biopolymers for cancer treatment are shown in Table 2. Among these biopolymers, chitosan and alginate are of particular interest for drug delivery to cancer cells because of their biodegradable, biocompatible, hydrophilic, mucoadhesive and protective properties [93, 117-119].

(A)

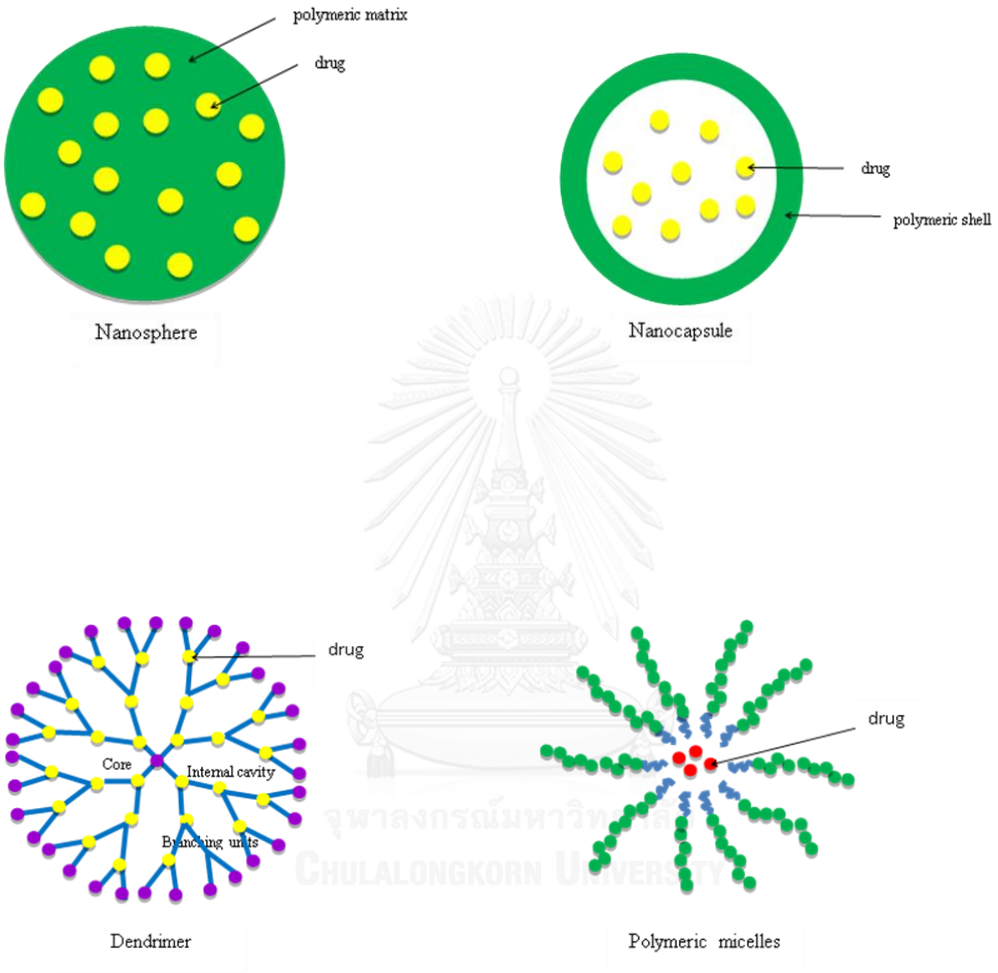

Figure 5 Types of nanoparticles used in nanoparticulate drug delivery systems: (a) polymeric nanoparticles, (b) nanovesicles and (c) nanoemulsions.

(B) (C)

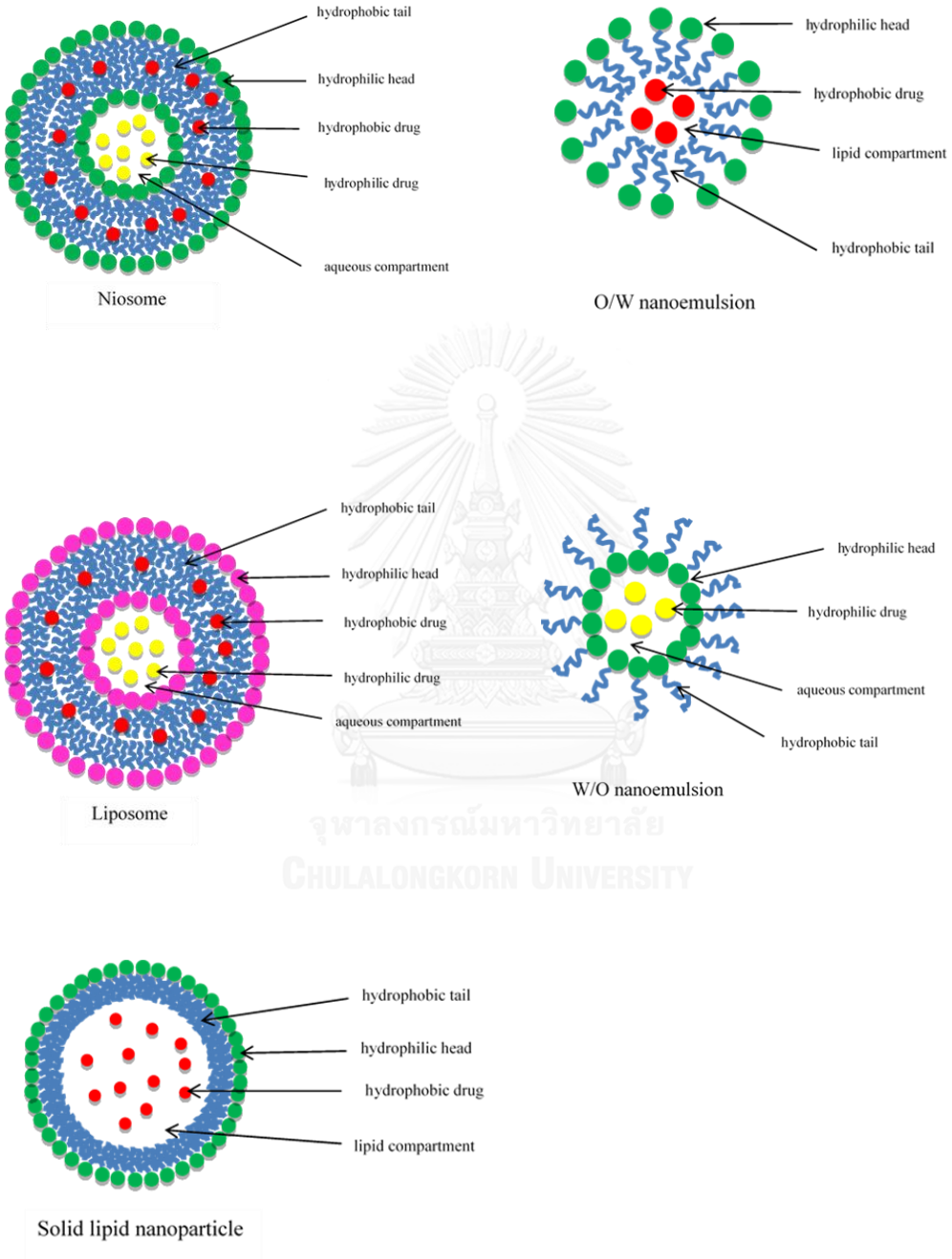

Figure 5 Types of nanoparticles used in nanoparticulate drug delivery systems: (a) polymeric nanoparticles, (b) nanovesicles and (c) nanoemulsions (continued).

Table 2 Examples of polymeric nanoparticles for cancer treatment.

Polymer	Preparation technique	Anticancer drug	Outcome of study	Reference
Gelatin	Desolvation	Paclitaxel	Rapid drug release from gelatin nanoparticles was observed (~90% released at 37 °C after 2 h).	Lu et al. [120]
Poly(butylcyanoacrylate) (PBC)	Anionic polymerization	Doxorubicin	Concentration of doxorubicin in the brain after systemic administration increased about 60-fold by incorporating doxorubicin into PBC nanoparticles coated with polysorbate 80.	Gulyaev et al. [121]
Poly(lactic-coglycolic acid) (PLGA)	Nanoprecipitation	9-Nitrocamptothecin	Nanoparticles improved the release profile and sustained release of the drug up to 160 h.	Derakhshandeh et al. [122]
PLGA	Interfacial deposition	Paclitaxel	Incorporation of paclitaxel in PLGA nanoparticles enhanced the cytotoxicity of paclitaxel compared to a commercial formulation taxol®.	Fonseca et al. [123]

Table 2 Examples of polymeric nanoparticles for cancer treatment (continued).

Polymer	Preparation technique	Anticancer drug	Outcome of study	Reference
PLGA	Solvent displacement	Xanthones	Nanoparticles containing xanthones showed good physical stability at 4°C for 3–4 months.	Teixeira et al. [124]
PLGA	Interfacial deposition	Rose bengal	PLGA nanoparticles improved the half-life of rose bengal in the blood stream compared to free drug solution.	Redhead et al. [125]
PLGA	Double emulsion and Solvent evaporation	Triptorelin	Encapsulation efficiency varied from 4% to 83% depending on the interaction between the drug molecule and copolymer. The release profile of Triptorelin from PLGA nanoparticles did not show burst effects.	Nicoli et al. [126]

Table 2 Examples of polymeric nanoparticles for cancer treatment (continued).

Polymer	Preparation technique	Anticancer drug	Outcome of study	Reference
PLGA	Solvent evaporation	Dexamethasone	Highest drug loading was obtained using 10 mg of dexamethasone and 100 mg PLGA (75:25) in a mixture of acetone-dichloromethane 1:1 (v/v) and complete drug release was observed after 4 h incubation at 37 °C.	Gómez-Gaete et al. [127]
Chitosan	Microemulsion	Doxorubicin conjugated with dextran	Nanoparticles enhanced permeability and the retention effect of doxorubicin. Nanoparticles improved therapeutic efficacy and minimized side effects of doxorubicin.	Mitra et al. [128]
Chitosan	Novel emulsion droplet coalescence	Gadopentetic acid	Gadopentetic acid was successfully incorporated into chitosan nanoparticles by a novel emulsion droplet coalescence method.	Tokumitsu et al. [129]

Table 2 Examples of polymeric nanoparticles for cancer treatment (continued).

Polymer	Preparation technique	Anticancer drug	Outcome of study	Reference
Chitosan	Novel emulsion droplet coalescence	Gadopentetic acid	Chitosan nanoparticles prolonged retention of gadopentetic acid in the tumor tissue. Chitosan nanoparticles had high affinity to tumor cells, resulting in greater accumulation in the cells	Shikata et al. [130]
Alginate and chitosan	Ionotropic pre-gelation followed by polycationic cross-linking	Curcumin	Composite nanoparticles can deliver a hydrophobic drug like curcumin to cancer cells.	Das et al. [102]

Table 2 Examples of polymeric nanoparticles for cancer treatment (continued).

Polymer	Preparation technique	Anticancer drug	Outcome of study	Reference
Alginate and chitosan	Pre-gel preparation	Antisense oligonucleotide	Alginate/chitosan nanoparticles have the potential to be used as antisense oligonucleotide delivery vectors. The optimal formulation for preparation of alginate/chitosan nanoparticles was alginate/chitosan ratio of 1, $CaCl_2$/alginate ratio of 0.2% and chitosan amine groups/antisense phosphate groups (N/P) ratio of 5 at pH 5.3.	Gazori et al. [98]
Alginate and chitosan	Ionotropic gelation	Carboplatin	Nanoparticles showed high drug loading, fast release of the drug during the first 24 h, followed by sustained release. High cellular drug uptake and sustained intracellular drug retention were observed.	Parveen et al. [131]

1.3. Biopolymeric alginate-chitosan nanoparticles as anticancer drug delivery systems

1.3.1. Alginate

Alginate is an anionic polysaccharide consisting of linear copolymers of α-L-guluronate and β-d-mannuronate residues linked by (1–4) glycosidic linkages (Figure 6) [99]. Alginate has many desirable properties, such as biodegradability, biocompatibility, non-toxicity, gelation and mucoadhesion [132-134], and is hemocompatible and does not accumulate in organs due to *in vivo* degradation. Thus, alginate has been used in numerous biomedical applications, and especially in drug delivery systems [34, 134].

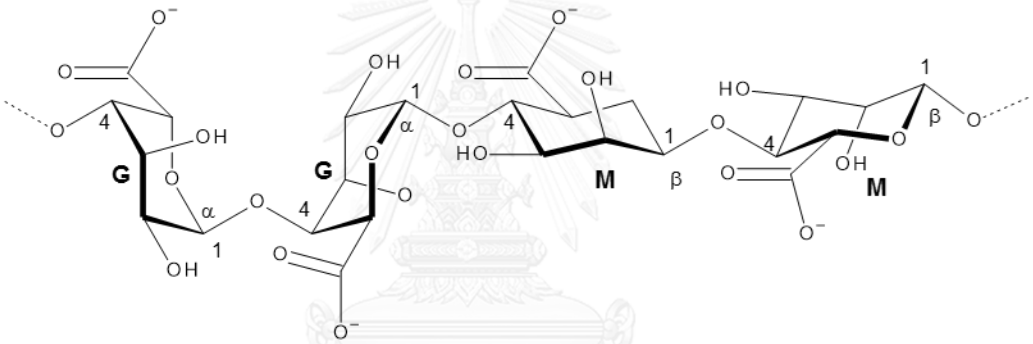

Figure 6 Chemical structure of alginate. G: guluronic acid; M: mannuronic acid.

1.3.2. Chitosan

Chitosan is a cationic polysaccharide consisting of copolymers of d-glucosamine and N-acetyl-d-glucosamine units linked by D-(1–4) glycosidic linkages (Figure 7) [99]. The biocompatibility, non-toxicity, gelation, biodegradability, and membrane permeability of chitosan makes it a polymer of choice for medical and pharmaceutical applications [35, 103, 119, 135, 136]. Chitosan can be degraded by human enzymes, especially lysozyme, and can be fabricated into various forms, such as films, beads, microparticles and nanoparticles [137].

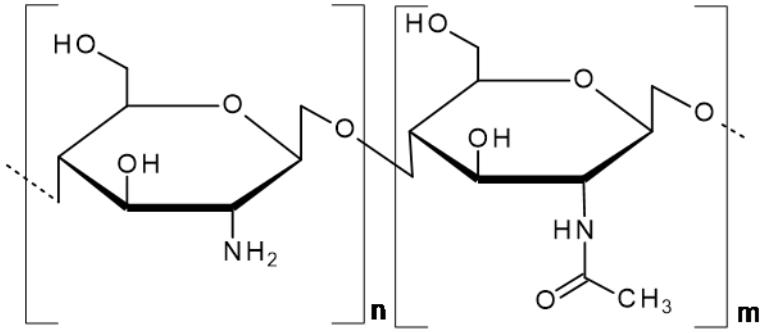

Figure 7 Chemical structure of chitosan.

1.3.3. Alginate and chitosan in drug delivery systems

Alginate and chitosan are of interest as biomaterials for use in drug delivery systems due to their versatile properties including non-immunogenicity [138]. Chitosan can interact with negatively charged polymers such as alginate and form hydrogels with desirable features for drug encapsulation and drug delivery [99, 100, 102, 103, 138]. Alginate- chitosan nanoparticles are formed by ionotropic gelation based on an interaction between carboxylate groups of alginate and amino groups of chitosan. Alginate-chitosan nanoparticles protect the encapsulated drug from enzymatic degradation, deliver the drug to the target organ, and permit controlled release of the drug [139]. Many studies have focused on the preparation of alginate-chitosan nanoparticles containing various anticancer drugs and targeting different types of cancer cells [102, 131], as shown in Table 3. In addition, chitosan and alginate can be fabricated in the form of microparticles and multilayers.

Table 3 Forms of chitosan and alginate for encapsulation of anticancer drugs and targeting of different types of cancer cells.

Form	Polymer	Anticancer drug	Targeted organ/cancer cell	Reference
Nanoparticles	Chitosan	Doxorubicin	Murine macrophage cell line	Mitra et al. [128]
		Gadolinium	L929 mouse fibroblast cells, B16F10 melanoma cells	Shikata et al. [130]
			SCC-VII squamous cell carcinoma.	Jain and Jain [140]
	Chitosan	5-Flurouracil (5FU)	HT-29 colon cancer cell line	Nagarwal et al. [40]
	Alginate/chitosan	5-Flurouracil (5FU)	Epithelial cells of eyes (ocular delivery)	Das et al. [102]
	Alginate/chitosan	Curcumin	Human cervical cancer cell line (HeLa)	Gazori et al. [141]
	Alginate/chitosan	Antisense oligonucleotides	T47D breast cancer cell line	Parveen et al. [131]
	Alginate/chitosan	Carboplatin	Retinoblastoma cell line	

Table 3 Forms of chitosan and alginate for encapsulation of anticancer drugs and targeting of different types of cancer cells.

Form	Polymer	Anticancer drug	Targeted organ/cancer cell	Reference
Microparticles	Alginate/chitosan	Tamoxifen	Gut-associated lymphoid tissue	Coppi and Iannuccelli [118]
	Alginate/chitosan	Interleukin-2	Human lung squamous carcinoma SQ-5, and AOI cells Human lung adenocarcinoma A549 cells	Liu et al. [142]
Multilayers	Alginate/chitosan	5-Aminosalicylic acid	Colon tissue	Mladenovska et al. [143]
	Alginate/chitosan	Doxorubicin	-	Peng et al. [144]
	Alginate/chitosan	Doxorubicin	HepG2 tumor cell line	Zhao et al. [145]

1.3.4. Characteristics of alginate-chitosan nanoparticles for drug delivery systems

1.3.4.1. Particle size

Particle size and size distribution of nanoparticles are used for process control or delivery of a drug to target cells, and these characteristics affect the stability, drug loading and drug release of the nanoparticles [95]. Typically, the cell uptake efficiency of nanoparticles is higher than that of microparticles due to their small size and good mobility. Nanoparticles are also suitable for both cellular and intracellular targeting. Das et al. [102] demonstrated that curcumin-loaded alginate/chitosan/PF127 nanoparticles with a mean size of 100 nm could be internalized in the HeLa cell line (cervical cancer). Parveen et al. [131] found that the drug release profile of carboplatin-loaded alginate-chitosan nanoparticles in a retinoblastoma cell line included fast release of 25% of the drug in the first 24 h, followed by sustained release. These results demonstrate that anticancer drug-loaded alginate/chitosan nanoparticles can sustain the antiproliferative activity of a drug in a dose- and time-dependent manner.

1.3.4.2. Surface properties

Reduction of opsonization and prolongation of the circulation time increase the efficiency of drug targeting and can be achieved by formulation of nanoparticles with a hydrophilic and biodegradable copolymer or coating of the nanoparticles with hydrophilic polymers and surfactants, such as polyoxamers, polyethylene glycol (PEG), polysorbate 80 (Tween® 80) and polyethylene oxide [95]. Alginate-chitosan nanoparticles are biodegradable copolymers with hydrophilic characteristics that reduce opsonization and prolong the circulation time *in vivo*. Das et al. [102] showed that curcumin-loaded alginate/chitosan/PF127 nanoparticles were effective for passive targeting of cancer cells and prolonged the period the drug spends in the circulation.

The zeta potential or surface charge determines the stability of nanoparticles in suspension due to the electrostatic potential between the particles [21, 27]. A zeta potential higher than ± 30 mV produces a stable suspension due to the surface charges preventing aggregation of the particles [95]. For example, the zeta potential of

carboplatin-loaded alginate-chitosan nanoparticles prepared by Parveen et al. [131] was about + 36 mV and no aggregation was observed. Similar results were reported by Coppi and Lannucelli [118] for tamoxifen-loaded alginate-chitosan nanoparticles, which also had a zeta potential of about + 36 mV. The positive surface charge may also improve the association of the alginate/chitosan nanoparticles with the cell surface and increase uptake into cancer cells, since most epithelial cells carry a negative charge [118].

1.3.4.3. Drug loading and encapsulation efficiency

A successful NPDDS requires a high drug loading capacity, which can be achieved by reduction of the quantity of matrix material. High drug loading can be accomplished during preparation of nanoparticles and incubation after formation of the particles. Drug loading and entrapment efficiency depend on the method of preparation and the physicochemical properties of the drug [96, 97, 135]. Agnihotri et al. [135]showed that chitosan-based particles could be used for encapsulation of both water-soluble and water-insoluble drugs, with an encapsulation efficiency of 99% for cisplatin. Coppi and Iannuccelli [118] found that a 92% drug loading capacity could be achieved using alginate-chitosan nanoparticles. These results show that alginate and chitosan are good choices as polymers for formulation of nanoparticles for inclusion of anticancer drugs.

1.3.4.4. Drug release from alginate-chitosan nanoparticles

Many techniques are used for determination of drug release profiles, including dialysis bag diffusion, reverse dialysis bag diffusion, agitation by ultracentrifugation or centrifugation, side-by-side diffusion cells with a membrane, and ultrafiltration [146]. Among these techniques, the dialysis method is preferred. Effective release of the encapsulated drug from the alginate-chitosan nanoparticles after internalization into the cancer cells is a key issue in making effective nanoparticles for drug delivery and targeting. Singh and Lillard Jr [95] demonstrated that burst release of carboplatin from alginate-chitosan nanoparticles occurred within 12 h and that later sustained release also occurred. In a study of curcumin-loaded alginate/chitosan/PF127 nanoparticles,

Das et al. [102] showed that about 36% of the curcumin was released in the first 12 h and 51% in 24 h, followed by sustained release until 72 h, after which the release rate dropped and a total of 75% was released in 96 h. Various mathematic models are used to study the drug release mechanism, including use of the regression coefficient (R^2) to indicate the level of release [147]. For example, the release of curcumin from alginate/chitosan/PF127 nanoparticles had a high R^2 value (0.9421), which indicates good release and a prolonged period in the circulation [102]. Due to the rate of drug release, alginate-chitosan nanoparticles are good candidates as anticancer drug nanocarriers for targeting of cancer cells.

1.3.4.5. Cytotoxicity and cellular uptake of alginate-chitosan nanoparticles

Alginate-chitosan nanoparticles can be used to deliver anticancer drugs to target cancer cells and induce cell death. Parveen et al. [131] found that carboplatin-loaded alginate-chitosan nanoparticles affected the viability of the human retinoblastoma cell line Y79. The antiproliferative activity and apoptosis rate of cancer cells induced by the carboplatin-loaded alginate-chitosan nanoparticles were greater than those with the native (unencapsulated) drug. This activity increased with incubation time when the cancer cells were treated with a low dose of carboplatin loaded into the alginate-chitosan nanoparticles. Moreover, the IC_{50} of the carboplatin-loaded alginate-chitosan nanoparticles was lower than that of native carboplatin [131]. Curcumin-loaded alginate-chitosan-PF127 nanoparticles were successfully delivered into HeLa cells based on the green fluorescence in fluorescent microscopy images of these cells after treatment with the nanoparticles [102].

1.4. Conclusion

Anticancer drugs are typically toxic and harmful to healthy cells, which is a major disadvantage of chemotherapy. To overcome this problem, drug delivery systems are required as novel therapy. Nanoparticles are preferable for delivery of anticancer drugs due to their ease of intracellular uptake and the increased efficacy of therapy. The smaller size of nanoparticles allows penetration across blood capillaries and uptake

into cancer cells with high efficiency. Such a nanoparticulate drug delivery system can be used to deliver drugs to target organs and improve important parameters such as oral bioavailability, stability of chemotherapy agents against enzymatic degradation, reduction of drug toxicity, and therapeutic efficacy. Biodegradable polymers such as alginate and chitosan are useful for preparation of nanoparticles and are a good choice as anticancer drug nanocarriers in drug delivery systems that may replace conventional cancer chemotherapy.

CHAPTER II

EFFECTS OF PREPARATION PARAMETERS ON THE CHARACTERISTICS OF CHITOSAN-ALGINATE NANOPARTICLES CONTAINING CURCUMIN DIETHYL DISUCCINATE

Settapon Bhunchu[1], Pornchai Rojsitthisak[2], Pranee Rojsitthisak[1,3*]

[1]Ph.D. Program in Nanoscience and Technology (International)[1], Graduate School, Chulalongkorn University, Bangkok 10330, Thailand

[2]Department of Food and Pharmaceutical Chemistry, Faculty of Pharmaceutical Sciences, Chulalongkorn University, Bangkok 10330, Thailand

[3]Metallurgy and Materials Science Research Institute, Chulalongkorn University 10330, Bangkok, Thailand

Published in Journal of Drug Delivery Science and Technology 2015, 28: 64-72.

Abstract

Chitosan-alginate nanoparticles for encapsulation of curcumin diethyl disuccinate (CDD) were prepared by o/w emulsification and ionotropic gelation. The influence of parameters, including type and concentration of non-ionic surfactants, chitosan/alginate mass ratio, and concentration and rate of CDD addition into the formulation, on the characteristics of the nanoparticles were investigated. The results indicate that chitosan and alginate can be used as polymer matrices for encapsulation of CDD and that the characteristics of the nanoparticles depend on the preparative method. To obtain CDD-nanoparticles with a high encapsulation efficiency, loading capacity and yield, the nanoparticles should be prepared using 1% (w/v) Pluronic® F127, a chitosan/alginate mass ratio of 0.15:1, and dropwise addition of 1 mg/ml CDD at a rate of 20 ml/h under vigorous stirring. Data from FT-IR and DSC analysis showed that there was no chemical reaction between CDD and the polymers; only physical mixing occurred and the drug was loaded in the amorphous phase inside the nanoparticle matrix. The CDD-nanoparticles prepared under optimal conditions were stable in storage at 4°C for 3 months. *In vitro* cellular internalization study demonstrated CDD-nanoparticles had significantly higher cellular uptake in Caco-2 cells compared to free CDD. Thus, the chitosan-alginate nanoparticles improved cellular uptake.

Keywords: Chitosan; Alginate; Curcumin diethyl disuccinate; Nanoparticles; Stability

2.1. Introduction

Curcumin is a natural bioactive compound extracted from rhizomes of turmeric (*Curcuma longa L.*) [42]. Curcumin is widely used as an ingredient in household medicine in Southern Asia because of its antibacterial and antifungal (Wang et al., 2009) antioxidant and radical scavenging [148], antiviral [149], anti-inflammatory [150], anti-carcinogenic and chemopreventive properties [151]. Curcumin is also hepatoprotective [152], anti-thrombotic [153], protective against myocardial infarction [154], and has anti-rheumatic and hypoglycemic properties [155]. However, curcumin has poor water solubility and low bioavailability [106] and this has limited its pharmaceutical use. Approaches to overcome these problems include formulation development [53, 55, 56, 156] and synthesis of curcumin conjugates [53, 55, 56, 59, 60, 152, 156]. For example, improvement of the water solubility and stability of curcumin can be achieved by encapsulation of curcumin in media such as surfactant micelles [157], polymeric micelles [156], hydrogels [53], microcapsules [56], and nanoparticles [55]. The properties of curcumin can also be improved by interaction or complexation with macromolecules [55] and chemical alteration [60]. For example, Wichitnithad et al. [59] synthesized succinate prodrugs of curcuminoids by aldol condensation of 2,4-pentanedione with different benzaldehydes and esterification with a methyl or ethyl ester of succinyl chloride, and determined the stability and anti-colon cancer efficacy. Curcumin diethyl disuccinate (CDD) (Figure 8) was found to be much more stable than curcumin in phosphate buffer at pH 7.4 and had the highest anticolon cancer activity compared to other succinate prodrugs and curcumin [59]. CDD also possesses antinociceptive activity [59, 60].

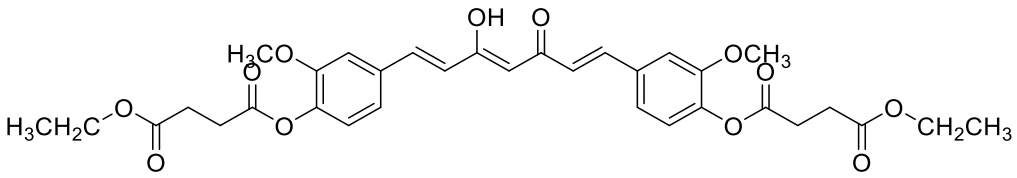

Figure 8 Structure of curcumin diethyl disuccinate (CDD) [60].

Formulation of CDD in nanoparticles may enhance its pharmacological properties and delivery. In this study, we examined preparation of nanoparticles for encapsulation of CDD using natural biopolymers (alginate and chitosan) that are biodegradable, biocompatible, non-toxic, hemocompatible and mucoadhesive [34]. Alginate and chitosan are widely used to deliver therapeutic agents such as peptides, proteins and polynucleotides. Entrapment in the biopolymers maintains the physicochemical structure and pharmacological activity of these agents and protects them from enzymatic degradation [158]. Moreover, these formulations have advantages including prolongation of the therapeutic agents in the circulation, controlled release, reduced leaching, and the potential for encapsulation of both hydrophilic and hydrophobic biomolecules [34, 159]. Therefore, alginate and chitosan biopolymers have become important components in drug delivery systems.

Alginate is an anionic biopolymer derived from marine brown algae. It is an unbranched block copolymer of β-D-mannuronic acid and α-L-guluronic acid residues linked by (1→4) glycosidic linkages [21]. Alginate is of interest due to its biodegradability, biocompatibility and mucoadhesiveness [160]. Alginate nanoparticles can be obtained through gelation with divalent cations such as calcium ions [157, 160]. This simple gelation approach allows alginate to be used to produce a pre-gel with calcium ions that consists of small aggregates of gel particles, and subsequent addition of cationic polymers produces a polyelectrolyte complex coating [27]. Alginate has been extensively used in controlled release and drug delivery systems, but these have some limitations that may reduce therapeutic efficacy, including low stability, especially in alkaline conditions [161], and loss of encapsulated drugs by leakage through the pores of alginate particles [162].Therefore, alginate particles require modification with cationic polymers such as poly-L-lysine (PLL) to prepare stable nanoparticles. However, PLL is relatively toxic and immunogenic for use in a peripheral route, and currently chitosan is used as an alternative cationic polymer [163].

Chitosan is a cationic biopolymer comprising D-glucosamine and *N*-acetyl-D-glucosamine linked by β(1→4) glycosidic linkages [27]. It has been widely used as a

drug delivery vehicle for pharmaceutical applications, including mucosal, ocular and topical delivery, and controlled release and targeting systems [164]. Chitosan can form complexes with anionic biopolymers such as alginate that are used for controlled release and drug delivery [165]. Chitosan-alginate complexes are prepared by ionotropic gelation [166], in which the electrostatic interaction of carboxylic acid groups of alginate with amino groups of chitosan results in gel formation [34]. Zhang et al. [167] showed that use of chitosan polymers as secondary counterions reduced the pore sizes of alginate particles and decreased the leakage of encapsulated drug, and Lertsutthiwong et al. [27] had previously found that use of chitosan improved the physical stability of alginate nanoparticles. Motwani et al. [34] suggested that chitosan-alginate nanoparticles resulted in more effective controlled release than chitosan or alginate alone. Chitosan also improves the permeability, the stability and shelf-life during storage, and the half-life of alginate particles in biological fluids [30], and Das et al. [102] suggested that the chitosan-alginate nanocomposites are good candidates as novel carriers for delivery of hydrophobic drugs to cancer cells.

Chitosan-alginate nanoparticles have not been used for encapsulation and delivery of CDD. In this study, we examined the effects of the type and concentration of non-ionic surfactants, the chitosan/alginate mass ratio, and the concentration and rate of CDD addition into the formulation on the particle size, size distribution, zeta potential, encapsulation efficiency, loading capacity, yield and physical stability (4°C and 25°C) of the nanoparticles. The interaction and compatibility of CDD and other components in the formulation were analyzed by Fourier Transform Infrared Spectrometry (FT-IR) and Differential Scanning Calorimetry (DSC). *In vitro* cellular uptake of nanoparticles containing CDD was examined by confocal laser scanning microscopy in human epithelial colorectal adenocarcinoma Caco-2 cells.

2.2. Experimental

2.2.1. Materials

CDD was synthesized as described in Wichitnithad et al. [59]. Chitosan (molecular weight) was purchased from Aquatic Nutrition Lab Co. Ltd., Samut Sakorn, Thailand. The medium viscosity alginic acid sodium salt isolated from brown algae (molecular weight 80,000-120,000 g/mol and low guluronic acid content: *FG* = 0.39) was purchased from Sigma, St. Louis, MO, USA. Ultrapure water was obtained with MilliQ equipment (Waters, USA). Tween® 80 was purchased from Acros Organics, Thermo Fisher Scientific, NJ, USA. Pluronic® F127 and Cremophor RH40™ were purchased from BASF Corporation, Ludwigshafen, Germany. Tetrahydrofuran was of HPLC grade. All other chemicals were of analytical grade.

2.2.2. Cell culture

Caco-2 cells (ATCC No. HTB37, American Type Culture Collection) were maintained in complete growth medium containing 1% (v/v) glutamine, 1% (v/v) nonessential amino acids, 1% (v/v) antibiotic penicillin-streptomycin solution, 0.2% (v/v) antifungal amphotericin B solution (fungizone) and Dulbecco's modified Eagle's medium (DMEM), supplemented with 10% (v/v) heat inactivated fetal bovine serum (FBS). Cells were maintained at 37°C in a saturated humid atmosphere containing 95% air in a 5% CO_2.

2.2.3. Preparation of chitosan-alginate nanoparticles containing CDD

Chitosan-alginate nanoparticles containing CDD were prepared using o/w emulsification and ionotropic gelation with modifications [27]. Briefly, 1 ml of acetonic CDD solution at an appropriate concentration was added dropwise into 20 ml of sodium alginate solution (0.6 mg/ml) containing a non-ionic surfactant using an automatic syringe pump (NE 100, New Era, Pump System Inc. USA) at an addition rate of 20 ml/h under mechanical stirring at 1000 rpm for 30 min, followed by dropwise addition of 4 ml of 0.67 mg/ml $CaCl_2$ solution and continuous stirring for 30 min. After sonication at a frequency of 45 kHz and sonic power of 80 W (CP230D, Ultrasonic Bath,

Crest Ultrasonics Corp., USA) for 15 min, 4 ml of chitosan solution of various concentrations (0.15-0.45 mg/ ml in 1% (v/v) acetic acid) was added dropwise into the resultant calcium-alginate pre-gel with continuous stirring at 1000 rpm for 30 min. The suspension was equilibrated overnight to allow the nanoparticles to form a uniform particle size. The chitosan-alginate nanoparticles containing CDD were obtained as a dispersion in aqueous solution.

2.2.4. Variation and optimization of the formulation parameters

The characteristics of the chitosan-alginate nanoparticles were examined in formulations using various types and concentrations of non-ionic surfactants (Pluronic® F127, Cremophor RH40™ and Tween® 80); chitosan/alginate mass ratios of 0.05:1, 0.10:1 and 0.15:1; concentrations of CDD of 1, 2 and 3 mg/ml; and rates of CDD addition of 10-30 ml/h. Each parameter was varied while the other parameters remained constant. Selection of the optimum formulation was based on the particle size, size distribution (polydispersity index, PDI), zeta potential, encapsulation efficiency, and loading capacity of the nanoparticles.

2.2.5. Characterization of nanoparticles

The particle size and size distribution based on PDI and zeta potential were determined using a Zetasizer model Nano-ZS (Malvern Instruments, England). The morphology of nanoparticles containing CDD was visualized by transmission electron microscopy (TEM, model H-9500, Hitachi High Technology America Inc., USA). Nanoparticle suspensions were diluted 50-fold with ultrapure water and dropped onto Formvar-coated copper grids. The amount of CDD in the formulated chitosan-alginate nanoparticles was assayed using HPLC according to USP36-NF31 with modifications (Rockville, 2013). Briefly, the sample was maintained at 20°C before injection onto the HA 166 (C18, 4.6 x 150 mm, 5 mm) column, which was maintained at 40°C. The mobile phase consisted of a mixture of 1 mg/ml citric acid in water and tetrahydrofuran (40:60, v/v). The sample injection volume was 20 µl and elution was isocratic at a flow rate of 1.0 ml/min. Detection was carried out at 400 nm. The total chromatographic analysis time per sample was 4 min, with CDD eluting at a retention time of 3.38 min. The

amount of CDD in nanoparticles was calculated as the difference between the total amount of initial CDD added in the formulation and the amount of CDD found in supernatant after ultracentrifugation at 45,000 rpm at 4°C for 1 h. The encapsulation efficiency was calculated from the amount of CDD in nanoparticles, as a percentage of the total amount of CDD initially added in the formulation. The loading capacity was calculated from the amount of CDD in nanoparticles, as a percentage of the total dry mass of nanoparticles. The nanoparticle yield was calculated from the actual weight of freeze-dried nanoparticles, as a percentage of the theoretical weight of the nanoparticles. The equations are as follows:

$$\text{Encapsulation efficiency (\%)} = \frac{\text{CDD initial} - \text{CDD in supernatant} \times 100}{\text{CDD initial}} \quad (1)$$

$$\text{Loading capacity (\%)} = \frac{\text{CDD initial} - \text{CDD in supernatant} \times 100}{\text{total dry mass of nanoparticles}} \quad (2)$$

$$\text{Nanoparticle yield (\%)} = \frac{\text{weight of freeze - dried nanoparticles} \times 100}{\text{theoretical weight of the nanoparticles}} \quad (3)$$

The interaction and compatibility of CDD with other components in the nanoparticle formulation were analyzed by FT-IR (Perkin Elmer, Norwalk, CT, USA). Spectra were recorded in transmittance mode at 4000-400 cm^{-1}, with a resolution of 4 cm^{-1} and a scan number of 32 times/sample at ambient temperature [168]. The physical state of CDD in nanoparticles was analyzed by DSC (DSC 200 F3Maia®, Netzsch, Germany). The instrument conditions followed the method described by Sarmento et al. with modifications [169]. An appropriate amount of lyophilized nanoparticles was sealed in an aluminum pan and scanned in a temperature range of 20-350°C with a heating rate of 10°C /min. An inert atmosphere was maintained by purging nitrogen with a flow rate of 20 ml/min.

The physical stability of the chitosan-alginate nanoparticles containing CDD was determined by assessment of the particle size and zeta potential after storage at 4°C and 25°C for 3 months.

2.2.6. *In vitro* cellular internalization study

Caco-2 cells were harvested with DMEM and cultured in a 96-well plate at a density of 5 x 10^3 cells/200 ml/well. After the cells were incubated at 37°C for 24 h, DMEM was removed. The cells were then washed with 200 ml DMEM and equilibrated for 1 h in an incubator. After removal of DMEM, 2 ml of free CDD, empty nanoparticles and nanoparticles containing CDD at predefined concentrations were introduced into each well containing 200 ml of DMEM. After incubation for 72 h, the cells were rinsed with 0.01 M PBS buffer (pH 7.4) to remove excess nanoparticles and free CDD. Subsequently, the cells were imaged by confocal laser scanning microscopy (Nikon, D-ECLIPSE C1, Japan) using a FITC filter (Ex (λ) 400 nm, Em (λ) 470 nm). Images were processed using Nikon software.

2.2.7. Statistical analysis

All experiments were performed in triplicate. Results are expressed as mean ± standard deviation. Statistical analysis was performed by one-way ANOVA using MS-Excel with $p < 0.05$ considered to be significant.

2.3. Results and discussion

2.3.1. Effects of type and concentration of surfactant

The choice of surfactant is one of the most important factors affecting the characteristics of chitosan-alginate nanoparticles containing CDD. In this study, we focused on non-ionic surfactants because of their improved safety compared to anionic or cationic surfactants. Various non-ionic surfactants are widely used in cosmetic and pharmaceutical applications [170]. In this study, three non-ionic surfactants, Pluronic® F127, Cremophor RH40™ and Tween® 80, were examined to

determine the most effective surfactant for preparation of nanoparticles containing CDD.

The characteristics of the nanoparticles as a function of the type of non-ionic surfactant are shown in Table 4. Pluronic® F127 gave the smallest size and size distribution (PDI), compared to Cremophor RH40™ and Tween® 80. These results are similar to the findings of Kim et al. [171] showing that Poloxamer 407 (Pluronic® F127) was more efficient than Tween® 80 in decreasing size and PDI. Wu et al. [172] suggested that within an acceptable range of zeta potential (20 to 30), a nanoparticle suspension made using Pluronic® F127 was stable. Thus, Pluronic® F127 may enhance stability, as well as improving encapsulation efficiency, loading capacity and the yield of nanoparticles (Table 4).

These results might be explained by the hydrophilicity-lipophilicity balance (HLB) values of 22, 17 and 15 for Pluronic® F127, Cremophor RH40™ and Tween® 80, respectively. The surfactant with the higher HLB value is more soluble in water and is likely to enhance the solubility of the drug [173]. Therefore, greater drug encapsulation is observed with Pluronic® F127. Das et al. [102] suggested that the presence of Pluronic® F127 in the formulation enhances encapsulation due to its amphiphilic and self-assembling nature in the aqueous phase, with formation of a hydrophobic core. Based on these results, Pluronic® F127 was chosen for further experiments.

The particle size, PDI and yield of nanoparticles (Table 5) increased proportionally with the concentration of Pluronic® F127 ($p < 0.05$), whereas the zeta potential became less negative. This might be due to the interaction between Pluronic® F127 and the polymer network, since Pluronic® F127 can form micelles surrounding insoluble drug with its polar head groups facing the polymer networks. Therefore, a higher concentration of Pluronic® F127 improves the chance of interaction with polymers and results in a larger particle size. This phenomenon may account for the change in zeta potential, since the interaction with Pluronic® F127 neutralizes the negative charge of the nanoparticles. The increase in concentration of Pluronic® F127 from 0.5% to 1% also enhanced the encapsulation efficiency by about 15%, but this decreased at above

1% (w/v) Pluronic® F127. Othayoth et al. [174] also found that addition of Pluronic® F127 at an appropriate concentration led to a high encapsulation efficiency of drug in nanoparticles. This may be because the solubility of the drug in the aqueous phase is increased by increasing the concentration of Pluronic® F127, which consequently results in better encapsulation in hydrophilic polymers [175]. The reduced encapsulation efficiency at a higher level of Pluronic® F127 may be due to the surfactant increasing the viscosity of the system and producing large particles with low surface area, as suggested by Arora et al. [176]. Therefore, Pluronic® F127 concentrations of 1% (w/v) were chosen for preparation of nanoparticles containing CDD. The encapsulation efficiency and loading capacity of the chitosan-alginate nanoparticles was relatively low because hydrophilic polymers (chitosan and alginate) were used to encapsulate a relatively hydrophobic molecule (CDD).

Table 4 Effect of non-ionic surfactants on the characteristics of nanoparticles with a chitosan/alginate mass ratio of 0.15:1, a surfactant concentration of 1% (w/v), and a CDD concentration of 1 mg/ml (n = 3).

Type of surfactant	Particles size (nm)	PDI	Zeta potential (mV)	Encapsulation efficiency (%)	Loading capacity (%)	Nanoparticle yield (%)
Pl Pluronic® F127	414 ± 16	0.63 ± 0.05	-22.1 ± 1.4	54.9 ± 1.3	3.33 ± 0.08	86.5 ± 3.2
Cremophor RH40™	477 ± 12	0.77 ± 0.02	-18.1 ± 0.5	24.5 ± 1.0	1.64 ± 0.19	77.5 ± 6.9
Tween 80®	555 ± 13	1.00 ± 0.00	-17.8 ± 0.4	28.2 ± 0.5	2.16 ± 0.03	72.4 ± 2.2

Table 5 Effect of Pluronic® F127concentration on the characteristics of nanoparticles with a chitosan/alginate mass ratio of 0.15:1 and a CDD concentration of 1 mg/ml (n = 3).

Pluronic® F127 (%(w/v))	Particles size (nm)	PDI	Zeta potential (mV)	Encapsulation efficiency (%)	Loading capacity (%)	Nanoparticle yield (%)
0.5	355 ± 15	0.53 ± 0.07	-24.4 ± 1.4	46.7 ± 0.6	3.47 ± 0.11	72.3 ± 1.4
1.0	414 ± 16	0.63 ± 0.05	-22.1 ± 1.4	54.9 ± 1.3	3.33 ± 0.08	86.5 ± 3.2
1.5	688 ± 13	1.00 ± 0.00	-19.8 ± 0.4	34.1 ± 5.4	2.07 ± 0.32	88.2 ± 2.8

Table 6 Effect of chitosan/alginate mass ratio on the characteristics of nanoparticles with 1% (w/v) Pluronic® F127and 1 mg/ml CDD (n = 3).

Chitosan/alginate mass ratio	Particles size (nm)	PDI	Zeta potential (mV)	Encapsulation efficiency (%)	Loading capacity (%)	Nanoparticle yield (%)
0.05:1	281 ± 18	0.37 ± 0.06	-26.4 ± 0.2	33.2 ± 2.6	2.58 ± 0.17	72.4 ± 2.2
0.10:1	352 ± 14	0.47 ± 0.06	-24.2 ± 0.3	48.3 ± 2.8	3.33 ± 0.27	77.0 ± 3.0
0.15:1	414 ± 16	0.63 ± 0.05	-22.1 ± 1.4	54.9 ± 1.3	3.33 ± 0.08	86.5 ± 3.2

2.3.2. Effect of chitosan/alginate mass ratio

The influence of the chitosan/alginate mass ratio on the characteristics of the nanoparticles is shown in Table 6. The particle size and PDI significantly increased with an increase in the chitosan/alginate mass ratio ($p < 0.05$). However, an increase in the mass ratio above 0.15:1 produced aggregated particles and an opaque suspension. This might be due to formation of a compact membrane of chitosan on the surface of the nanoparticles, leading to a rapid increase in the particle size and PDI. The zeta potential of the nanoparticles is negative because alginate is the core material in these nanoparticles. An increase in the chitosan/alginate mass ratio results in more positive charges neutralizing the negative charges on the nanoparticle surface. An increase in the mass ratio also resulted in increases in the encapsulation efficiency and yield of nanoparticles ($p < 0.05$). Sarmento et al. [136] showed that chitosan coated on the surface of alginate nanoparticles reduced leakage of encapsulated drug from nanoparticles. Similarly, Bathool et al. [177] found that a high chitosan content improved the encapsulation efficiency and the nanoparticle yield. Loading capacity differed slightly with a change in the mass ratio (Table 6). These results show that a chitosan/alginate mass ratio of 0.15:1 is required to produce particles of size <1000 nm, PDI < 1 and zeta potential -20 to -30 with high encapsulation efficiency, loading capacity and yield.

2.3.3. Effects of concentration and rate of CDD addition into the formulation

The effect on the characteristics of the chitosan-alginate nanoparticles of incorporation of concentrations of 1, 2 and 3 mg/ ml of CDD was investigated at a fixed Pluronic® F127 level of 1% (w/v) and a chitosan/alginate mass ratio of 0.15:1. Turbidity and particle aggregation started to occur at CDD >1 mg/ml. This indicates that 1% Pluronic® F127 was insufficient to produce small nanoparticles at CDD >1 mg/ml because the surfactant could not fully cover the surface area of the droplets. This caused the nanoparticles to tend to aggregate [178], which resulted in a low encapsulation efficiency [176]. Therefore, 1 mg/ml CDD was selected as the

concentration for determination of the effect of the rate of CDD addition into the nanoparticle formulation.

The influence of the rate of CDD addition on the characteristics of nanoparticles is shown in Table 7. CDD addition at 10 ml/h and 20 ml/h did not significantly affect the particle size, PDI and zeta potential of the nanoparticles ($p > 0.05$), but a rate of 30 ml/h had a significant effect on these parameters. This may be because an increase in the rate of CDD (or organic phase) addition increases the micelle population, and at a high rate of addition there might be inadequate mixing, leading to an increase in particle size and PDI [179]. These results indicate that a rate of 20 ml/h for CDD addition to the formulation is optimal for further parameter optimization.

Table 7 Effect of rate of CDD addition on the characteristics of nanoparticles with a constant chitosan/alginate mass ratio of 0.15:1, 1% (w/v) Pluronic® F127, and 1 mg/ml CDD (n = 3).

Rate of addition (ml/h)	Particles size (nm)	PDI	Zeta potential (mV)
10	440 ± 15	0.57 ± 0.02	-24.1 ± 0.9
20	414 ± 16	0.47 ± 0.06	-24.2 ± 0.3
30	695 ± 12	0.86 ± 0.08	-23.4 ± 1.3

TEM images of chitosan-alginate nanoparticles containing CDD produced under optimal conditions of a chitosan/alginate mass ratio of 0.15:1, 1% (w/v) Pluronic® F127 and 1 mg/ml CDD added at 20 ml/h are shown in Figure 9. The nanoparticles were spherical and had a narrow size distribution. The particle size obtained by TEM was in agreement with data obtained from dynamic light scattering (Table 7).

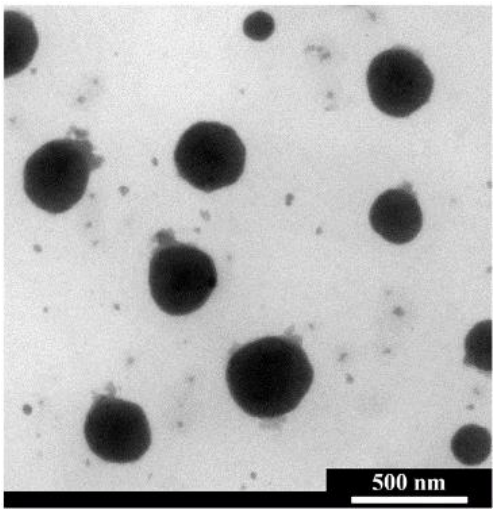

Figure 9 TEM image of chitosan-alginate nanoparticles containing CDD formed under optimal conditions

2.3.4. Drug-excipient compatibility

2.3.4.1. Fourier Transform Infrared Spectrometry

The interactions between CDD and polymers in the nanoparticles were characterized by FT-IR. FT-IR spectra of chitosan, alginate, chitosan-alginate nanoparticles, Pluronic® F127, chitosan-alginate Pluronic® F127 nanoparticles, CDD, and chitosan-alginate- Pluronic® F127 nanoparticles containing CDD are shown in Figure 10.

The FT-IR spectrum of chitosan (Figure 10(A)) had a broad band at 3290 cm^{-1} corresponding to O-H and N-H stretching. The band at 2872 cm^{-1} represents C-H stretching of the aliphatic hydrocarbon side chain. The peak for carbonyl (C=O) stretching of the secondary amide (amide I band) occurred at 1645 cm^{-1} [180]. The bands at 1486 and 1378 cm^{-1} correspond to C-N stretching of the amide and C-O stretching of the ether bond, respectively. The peaks at 1024 cm^{-1} are due to the secondary hydroxyl group (characteristic peak of –CH-OH in cyclic alcohols, C-O stretch) and primary hydroxyl group (characteristic peak of -CH_2-OH in primary alcohols, C-O

stretch) [181]. After complexation with alginate, the peaks at 2872, 1645, 1486 and 1378 cm^{-1} shifted by a few wave numbers (cm^{-1}) (Figure 10(D)).

In the spectrum of alginate (Figure 10(B)), the broad band at 3257 cm^{-1} is due to O-H stretching of the hydroxyl group. The strong absorption bands at 1594 cm^{-1} and 1404 cm^{-1} were assigned as asymmetric and symmetric stretching vibrations of carboxylate groups (COO-), respectively. The band around 1024 cm^{-1} was assigned as C-O-C stretching in the cyclic saccharide structure [182]. After complexation with chitosan, the bands at 1594 cm^{-1} and 1404 cm^{-1} shifted slightly to 1591 $cm^{-1}$and 1408 cm^{-1} and the band around 3500-3100 cm^{-1} became broader in comparison with that in chitosan alone, which indicates greater hydrogen bonding (Figure 10(D)).

After complex formation between chitosan-alginate blank particles and Pluronic® F127, bands are present for C-H bending at 1342 cm^{-1} and C-H stretching at 2882 cm^{-1} (Figure 10(E)). In the spectrum of CDD (Figure 10(G)), there are no signals due to phenolic hydroxyl groups of curcumin since these are succinylated, giving the band at 3000-3500 cm^{-1}. The peak at 2974-2935 cm^{-1} is due to C=H stretching in the ethylene spacer of ethyl succinate. The bands at 1763 and 1726 cm^{-1} are caused by C=O stretching of the aliphatic and phenolic esters, respectively, that at 1627 cm^{-1} is due to C=O stretching of the 1,3-diketone, and the bands at 1508 cm^{-1} and 1462 cm^{-1} are assigned to C=C stretching of aromatic rings. After incorporation of CDD in the chitosan-alginate- Pluronic® F127 nanoparticles (Figure 10(F)), the spectrum was similar to that for the blank nanoparticles (Figure 10(E)), except for a shift of some bands, as observed by overlay of the spectra of the blank and CDD nanoparticles.

A comparison between authentic CDD and the CDD nanoparticles indicated disappearance of the bands at 1763 and 1726 cm^{-1} observed in CDD alone. This suggests that micelle formation in nanoparticles results in loss of some signals. There were also additional bands in the spectrum of the CDD nanoparticles, including at 3368 cm^{-1} for OH stretching in alginate and chitosan, and 1360 and 2882 cm^{-1} for C-H bending and C-H stretching of Pluronic® F127. However, several characteristics of CDD were also present in the spectrum of CDD nanoparticles, including the band at 1605 cm^{-1}

(broadened signal) for the 1,3-diketone, the C=C stretching of aromatic rings at 1466 cm^{-1}, and a hidden peak at 1605 cm^{-1}. These findings conclusively show CDD entrapment in the chitosan-alginate-Pluronic® F127nanoparticles at the molecular level and imply that micelle formation in the nanoparticle preparation did not cause breakdown of the CDD structure [168].

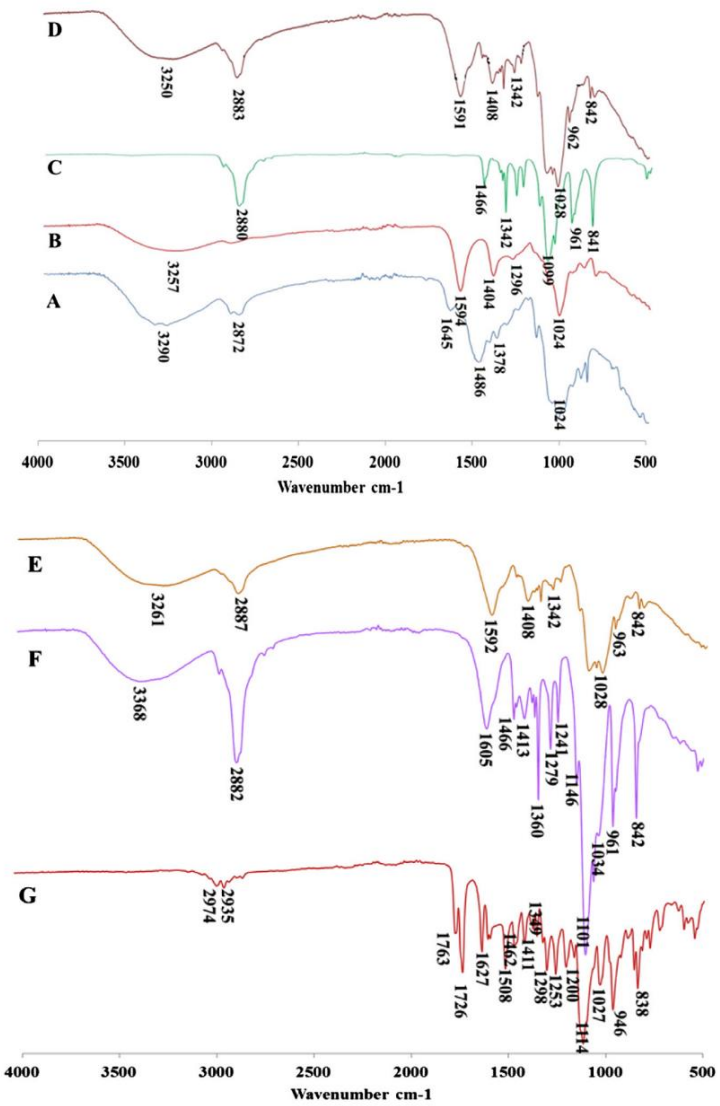

Figure 10 FT-IR spectra of (A) chitosan; (B) alginate; (C) pluronic F-127; (D) chitosan-alginate nanoparticles; (E) chitosan-alginate- Pluronic® F127 nanoparticles; (F) chitosan-alginate-Pluronic® F127 nanoparticles containing CDD; and (G) curcumin diethyl disuccinate (CDD).

2.3.4.2. Differential Scanning Calorimetry (DSC)

To examine the physical state of CDD in nanoparticles, pure CDD, Chitosan-alginate nanoparticles, chitosan-alginate-Pluronic® F127nanoparticles, and nanoparticles containing CDD with the optimal formulation were investigated using DSC. As shown in Figure 11, an endothermic peak was observed at the melting point of pure CDD as a sharp peak at 92°C, and an exothermic peak occurred at 272°C. In blank nanoparticles with Pluronic® F127, there was an endothermic peak at 130°C and exothermic peaks at 180°C and 240°C. A physical mixture of CDD and chitosan-alginate-Pluronic® F127nanoparticles and nanoparticles containing CDD showed the same endothermic peak at the same temperature. In these cases, no endothermic peak (melting peak) of CDD was observed. The absence of the melting endothermic peak of CDD suggests that CDD was encapsulated in the nanoparticles and was present in an amorphous form as a molecular dispersion or in a disordered crystalline phase inside the nanoparticle matrix [183].

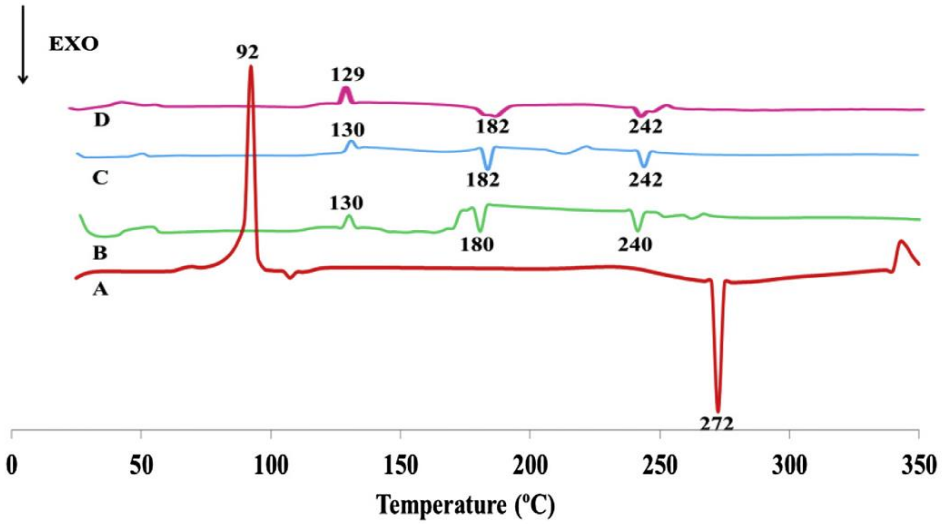

Figure 11 Differential scanning calorimetry thermograms of (A) pure CDD, (B) chitosan-alginate-Pluronic® F127 nanoparticles, (C) physical mixture of CDD, chitosan, alginate, and Pluronic® F127 and (D) chitosan-alginate-Pluronic® F127 nanoparticles containing CDD.

2.3.5. Physical stability study

Changes in particle size, PDI and zeta potential were used to determine the physical stability of the nanoparticles after storage at room temperature (25°C) and at 4°C for three months. The physical stability data in Figure 12 show that the particle size and zeta potential of the nanoparticles did not change significantly during storage at 4°C for 3 months ($p > 0.05$), whereas these parameters changed significantly after 1 month at 25°C. Thus, nanoparticles containing CDD prepared under optimum conditions should be stored at 4°C.

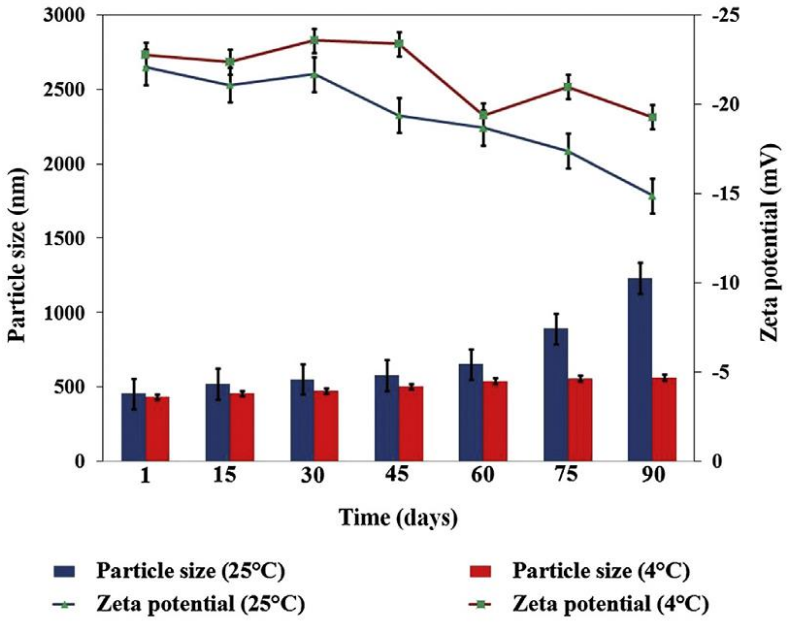

Figure 12 Physical stability of optimized nanoparticles after storage at room temperature (25°C) and 4°C for three months.

2.3.6. *In vitro* cellular internalization

Cellular internalization of nanoparticles containing CDD was evaluated in Caco-2 cells. Confocal laser scanning microscope images of control cells without exposure to

CDD, cells incubated with free CDD, empty nanoparticles, and nanoparticles containing CDD are shown in Figure 13 CDD itself was fluorescent under a confocal laser scanning microscope, whereas the control cells and empty nanoparticles were not fluorescent. In contrast, nanoparticles containing CDD had fluorescence throughout the cytoplasm. This indicates that the nanoparticles containing CDD were taken up by the cell and are located inside the cell. The intensity of the green fluorescence inside cells treated with nanoparticles containing CDD was also much greater than that of free CDD (Figure 13), which indicates enhanced uptake of nanoparticles containing CDD compared to that of free CDD. This is significant for further applications of nanoparticles containing CDD. These images confirm cellular internalization of the nanoparticles containing CDD and the successful delivery of CDD into Caco-2 cells.

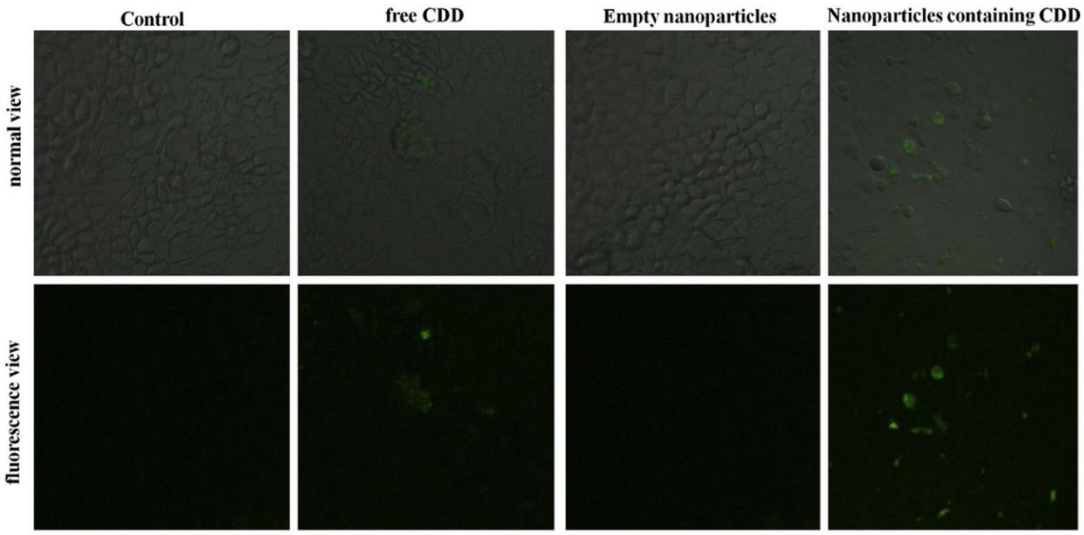

Figure 13 Cellular internalization of free CDD and chitosan-alginate nanoparticles containing CDD viewed by confocal laser scanning microscopy in Caco-2 cells.

2.4. Conclusion

Chitosan-alginate nanoparticles have the potential to be used for encapsulation of CDD using o/w emulsification and ionotropic gelation. The characteristics of nanoparticles containing CDD are strongly dependent on the preparation parameters; i.e. type and concentration of surfactants, chitosan/alginate mass ratio, and

concentration and rate of CDD addition. To get the highest encapsulation efficiency, loading capacity and yield of nanoparticles, the optimal formulation should have a chitosan/alginate mass ratio of 0.15:1, a CDD concentration of 1 mg/ml, and 1% Pluronic® F127 (w/v), with CDD addition at 20 ml/h. There was no reaction of CDD with other compounds in the formulation. Only physical mixing occurred during nanoparticle preparation. Nanoparticles produced using the optimal conditions showed good physical stability at 4°C. Confocal laser microscopy showed that the chitosan-alginate nanoparticles improve cellular uptake of CDD in Caco-2 cells, in comparison with free CDD.

CHAPTER III

RESPONSE SURFACE METHODOLOGY TO OPTIMIZE THE PREPARATION OF CHITOSAN/ALGINATE NANOPARTICLES CONTAINING CURCUMIN DIETHYL DISUCCINATE

Settapon Bhunchu[1], Pornchai Rojsitthisak[2], Pranee Rojsitthisak[1,3*]

[1]Ph.D. Program in Nanoscience and Technology (International), Graduate School, Chulalongkorn University, Bangkok 10330, Thailand

[2]Department of Food and Pharmaceutical Chemistry, Faculty of Pharmaceutical Sciences, Chulalongkorn University, Bangkok 10330, Thailand

[3]Metallurgy and Materials Science Research Institute, Chulalongkorn University 10330, Bangkok, Thailand

Published in Advanced Materials Research 2015, 1119: 398-402.

Abstract

Curcumin diethyl disuccinate (CDD) is a succinate prodrug of curcumin that has better anti-colon cancer and antinociceptive activities than curcumin and improved stability in phosphate buffer at pH 7.4. However, formulation of CDD for pharmaceutical use is limited. Therefore, this study focused on preparation of chitosan/alginate nanoparticles containing CDD and optimization of the formulation using response surface methodology. Chitosan/alginate nanoparticles were prepared by o/w emulsification and ionotropic gelification. The optimized formulation of nanoparticles containing CDD had a chitosan/alginate mass ratio of 0.05:1, a CDD concentration of 3 mg/ml, and a Tween® 80 content of 4.05% (w/v). Response surface methodology was found to be an effective technique for optimization of the preparation of chitosan/alginate nanoparticles using a limited number of experiments.

Keywords: Response surface methodology; Curcumin diethyl disuccinate; Chitosan; Alginate; Nanoparticles; Box-Behnken statistical design

3.1. Introduction

Curcumin diethyl disuccinate (CDD) is a succinate prodrug of curcumin that is synthesized by aldol condensation of 2,4-pentanedione with benzaldehyde and esterification with the methyl or ethyl ester of succinyl chloride (Wichitnithad et al., 2011). CDD has better properties than curcumin in terms of stability in phosphate buffer at pH 7.4, and anti-colon cancer and antinociceptive activities (Wichitnithad et al., 2011, Wongsrisakul et al., 2010). However, formulation of CDD for pharmaceutical use is limited and encapsulation of CDD in nanoparticles has not been reported. The current study used nanoparticles produced from chitosan and alginate biopolymers because of their biocompatibility, biodegradability, non-toxicity and good film formation [27].

Response surface methodology (RSM) was applied to make the study systematic and limit the number of experiments. RSM is a combination of statistical and mathematic techniques based on the fit of a polynomial equation to experimental data, which describes the behavior of a data set and facilitates testing of a large number of factors simultaneously with the purpose of prediction of the optimized formulation. RSM has many advantages over the one-variable-at-a-time approach, which is the traditional optimization method [184]. Box-Behnken statistical design (BBD) is a good design for RSM and an effective tool for optimization.

With this background, the study was undertaken to examine the parameters (i.e. chitosan/alginate mass ratio, concentrations of CDD and Tween® 80) affecting the characteristics of chitosan/alginate nanoparticles containing CDD, with optimization of formulation development using BBD.

3.2. Methodology

3.2.1 Materials

Chitosan of molecular weight 220,000 Da and 90% degree of deacetylation was purchased from Aquatic Nutrition Lab, Samut Sakorn, Thailand. Alginate with medium viscosity was purchased from Sigma, St Louis, MO, USA. CDD was synthesized as described in reference [59]. All other chemicals were of analytical grade.

3.2.2. Preparation of Chitosan/Alginate Nanoparticles Containing CDD

Chitosan/alginate nanoparticles containing CDD were prepared using o/w emulsification followed by ionotropic gelification using a modified version of the method described by Lertsutthiwong et al. [27]. Briefly, acetonic CDD solution was added dropwise into alginate solution containing Tween® 80 under vigorous stirring. After sonication for 15 min, $CaCl_2$ solution was added to the resulting o/w emulsion followed by addition of chitosan solution and the mixture was continuously stirred for 30 min. The resulting nanoparticle suspension containing CDD was then equilibrated overnight before characterization.

3.2.3. Experimental Design

Independent variables, including chitosan/alginate mass ratio (X_1) of 0.05:1 - 0.15:1, CDD (X_2) of 1-3 mg/ml and Tween® 80 (X_3) content of 3-5% (w/v) were defined as low (-), medium (0) and high (+). Based on Box-Behnken statistical design using Design-Expert (Version 7.0.0, Stat Ease, USA), 15 experiments including 12 factorial points with 3 replicates at the center point were used to estimate the pure error sum of squares (Motwani et al., 2008). The levels and design matrix are shown in Table 8.

Table 8 Variables and responses with their levels and constraints.

	Level			Constrains
	Low	Medium	High	
Independent variables (factors)				
X_1 = chitosan/alginate mass ratio	0.05:1	0.10:1	0.15:1	
X_2 = CDD concentration (mg/ml)	1	2	3	
X_3 = Tween® 80 (%w/v)	3	4	5	
Dependent variables (responses)				
Y_1 = Particle size (nm)				Minimize
Y_2 = Zeta potential (mV)				$\geq \pm 20$ mV
Y_3 = Encapsulation efficiency (%)				Maximize
Y_4 = Loading capacity (%)				Maximize

3.3. Characterization

The morphology of nanoparticles containing CDD was visualized using transmission electron microscopy (TEM; Hitachi High Technology America Inc., USA). Particle size and zeta potential were measured using a Zetasizer model Nano-ZS (Malvern Instruments, England).

The amount of CDD in chitosan/alginate nanoparticles was assayed using HPLC according to the method of Wichitnithad et al. (Wichitnithad et al., 2011) with modification. Briefly, the sample was injected onto the HA 166 C18 column (4.6 x 150 mm i.d., 5-µm particle size) at a column temperature of 40°C. The mobile phase consisted of a mixture of 1 mg/ml citric acid in water and tetrahydrofuran (40:60, v/v). The injection volume of the sample was 20 µl and elution was isocratic with a flow rate of 1.0 ml/min. Detection was carried out at 400 nm. The amount of CDD in nanoparticles was calculated as the difference between the total amount of CDD added in the formulation and the amount of CDD found in supernatant after ultracentrifugation. The encapsulation efficiency was calculated from the amount of CDD in nanoparticles as a percentage of the total amount of CDD added in the

formulation. The loading capacity was calculated from the amount of CDD in nanoparticles as a percentage of the total dry mass of nanoparticles.

3.4. Results and Discussion

BBD was applied to determine the optimal level of factors (independent variables) that gave responses (dependent variables) in terms of minimized particle size at the desirable range of zeta potential, maximized encapsulation efficiency and loading capacity, as described in Table 8.

Table 9. shows the observed responses of chitosan/alginate nanoparticles containing CDD at each design point. The ranges were 315 - 925 nm for particle size (Y_1), (-11) - (-31) mV for zeta potential (Y_2), 12% - 48% for encapsulation efficiency (Y_3), and 1.3% - 11% for loading capacity (Y_4). In addition, particle size increased as the chitosan/alginate mass ratio and the concentration of Tween® 80 increased, whereas CDD concentration did not show a significant effect. A less negative zeta potential was observed when a higher chitosan/alginate and Tween® 80 content were used in the formulation. This may be explained by greater adsorption of chitosan (cationic polymer) on the surface of nanoparticles resulting in neutralization of the charges of the nanoparticles.

The loading capacity and encapsulation efficiency of nanoparticles increased as the chitosan/alginate mass ratio and CDD and Tween® 80 concentrations increased. These results were also confirmed by 3D response surface plots of encapsulation efficiency, as shown in Figure 14.

Table 9 Design point and observed responses of chitosan/alginate nanoparticles containing CDD.

Run no.	Independent variables			Dependent variables			
	X_1	X_2 (mg/ml)	X_3 (% (w/v))	Y_1 (nm)	Y_2 (mV)	Y_3 (%)	Y_4 (%)
1	0.05:1	1	4	315 ± 26	-27 ± 1.9	23 ± 6.7	3.8 ± 1.1
2	0.15:1	1	4	588 ± 62	-16 ± 0.2	48 ± 8.5	5.3 ± 1.1
3	0.05:1	3	4	375 ± 17	-22 ± 0.1	48 ± 1.9	9.6 ± 0.4
4	0.15:1	3	4	598 ± 20	-13 ± 0.9	45 ± 4.7	10.8 ± 1.2
5	0.05:1	2	3	358 ± 30	-31 ± 1.4	12 ± 12.8	2.7 ± 3.1
6	0.15:1	2	3	572 ± 51	-18 ± 0.6	32 ± 9.2	5.6 ± 1.5
7	0.05:1	2	5	485 ± 32	-24 ± 2.8	34 ± 9.2	7.41± 2.3
8	0.15:1	2	5	925 ± 25	-11 ± 0.3	43 ± 7.4	7.0 ± 1.1
9	0.10:1	1	3	464 ± 50	-24 ± 0.4	14 ± 3.6	1.3 ± 0.3
10	0.10:1	3	3	443 ± 49	-23 ± 0.9	37 ± 3.7	8.5 ± 1.4
11	0.10:1	1	5	660 ± 38	-18 ± 1.0	36 ± 13.5	3.2 ± 0.9
12	0.10:1	3	5	750 ± 42	-20 ± 1.0	46 ± 5.3	10.6 ± 1.2
13	0.10:1	2	4	506 ± 17	-21 ± 0.1	24 ± 3.7	3.7 ± 0.7
14	0.10:1	2	4	513 ± 18	-21 ± 0.6	27 ± 8.9	4.1± 1.5
15	0.10:1	2	4	514 ± 48	-23 ± 1.1	28 ± 13.6	4.4 ± 2.2

To fit the model matching the constraints in Table 8, regression of each response was analyzed by testing the sequential model sum of squares, lack of fit and model summary statistics using Design-Expert software, as shown in Table 10. Based on a high F-value and a *p*-value <0.05, particle size, encapsulation efficiency and loading capacity were fitted to a quadratic second-order polynomial model and zeta potential was fitted to a linear model. The equations are as follows:

$$Y_1 = 529.09 + 143.74X_1 + 17.05X_2 + 122.99X_3 - 12.46X_1X_2 + 56.43X_1X_3 + 12.46X_2X_3 - 26.99X_1^2 - 32.88X_2^2 + 83.09X_3^2 \quad (1)$$

$$Y_2 = -20.83 + 5.91X_1 + 1.12X_2 + 2.75X_3 \quad (2)$$

$$Y_3 = 28.59 + 6.38X_1 + 6.77X_2 + 8.00X_3 - 6.97X_1X_2 + 3.01X_1X_3 - 3.13X_2X_3 + 6.09X_1^2 + 9.28X_2^2 - 1.90X_3^2 \quad (3)$$

$$Y_4 = 4.05 + 0.65X_1 + 3.24X_2 + 1.24X_3 - 0.075X_1X_2 - 0.83X_1X_3 + 0.055X_2X_3 + 1.54X_1^2 + 1.77X_2^2 - 0.072X_3^2 \quad (4)$$

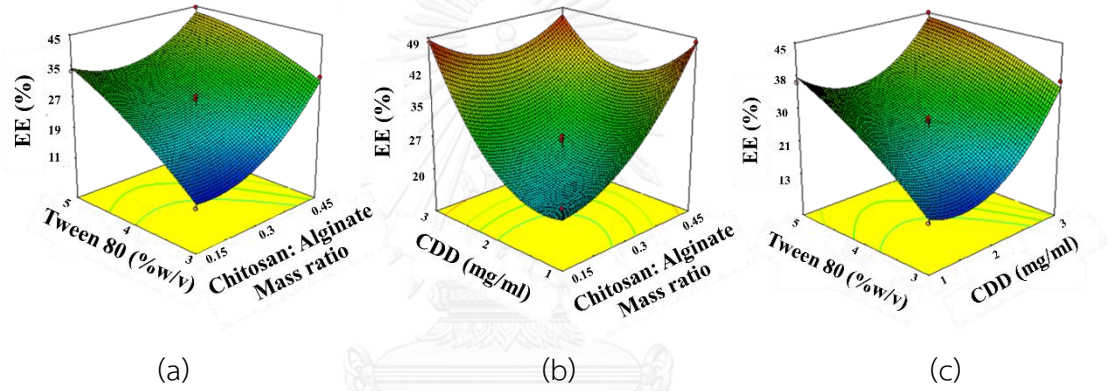

(a) (b) (c)

Figure 14 3D response surface plots of encapsulation efficiency (EE) as a function of (a) Tween® 80 concentration and chitosan/alginate mass ratio; (b) CDD concentration and chitosan/alginate mass ratio, and (c) Tween® 80 and CDD concentrations.

Table 10 Fitting a regression model for responses of 15 formulations

Responses	Sequential model sum of squares			Lack of fit		Model summary statistics				
	Models	*F*-value	*p>F*	*F*-value	*p>F*	R^2	Adjusted R^2	Predicted R^2	SD (%)	CV (%)
Particle size (Y_1)	Linear	18.99	0.0001	8.30	0.1121	0.8382	0.7940	0.6590	7.19	13.15
	Second order	1.12	0.3984	8.68	0.1069	0.8859	0.8008	0.4156	7.09	12.95
	Quadratic	41.08	0.0004	1.44	0.4348	0.9867	0.9626	0.8446	3.32	5.60
Zeta potential (Y_2)	Linear	39.15	<0.0001	4.94	0.1798	0.9144	0.8910	0.8241	1.72	2.28
	Second order	0.61	0.6260	5.96	0.1506	0.9303	0.8781	0.6605	1.82	8.76
	Quadratic	0.74	0.5707	8.04	0.1126	0.9518	0.8651	0.2799	1.92	9.21

Table 10 Fitting a regression model for responses of 15 formulations (continue).

Responses	Sequential model sum of squares			Lack of fit		Model summary statistics				
	Models	*F*-value	*p>F*	*F*-value	*p>F*	R^2	Adjusted R^2	Predicted R^2	SD (%)	CV (%)
Encapsulation efficiency (Y_3)	Linear model	5.82	0.0124	19.72	0.0592	0.6137	0.5083	0.2553	8.30	5.10
	Second order	1.48	0.2927	18.92	0.0510	0.7513	0.5648	0.0232	7.81	13.61
	Quadratic	36.98	0.0005	1.63	0.4028	0.9852	0.9586	0.8224	2.41	2.79
Loading capacity (Y_4)	Linear model	15.27	0.0003	22.61	0.0431	0.8063	0.7535	0.6653	1.48	5.21
	Second order	0.35	0.7879	29.90	0.0327	0.8290	0.7008	0.4261	1.63	7.77
	Quadratic	30.61	0.0008	5.64	0.1543	0.9822	0.9501	0.7407	0.66	1.34

Using RSM and a desirability factor of 95%, the following independent variables were suggested by the software for preparation of the optimal nanoparticle formulation: chitosan/alginate mass ratio of 0.05:1, CDD concentration of 3 mg/ml, and Tween® 80 concentration of 4.05% (w/v). The optimized formulation was prepared and compared with the predicted properties calculated for the formulation. The acceptable agreement between the observed and predicted properties, and the negligible % error validated the models and indicated adequate precision for the prediction of optimized conditions using the domain levels chosen for the independent variables (Table 11).

Table 11 Predicted and actual properties obtained from the optimized nanoparticle formulation.

Response	X_1	X_2 (mg/ml)	X_3 (%w/v)	Y_1 (nm)	Y_2 (mV)	Y_3 (%)	Y_4 (%)
Predicted	0.05: 1	3	4.05	361	-26	49	10
Actual	0.05: 1	3	4.05	353 ± 13	-25 ± 2	47 ± 4	10 ± 0.6
% Error				2.1	1.7	3.3	2.1

The morphology and size distribution of the nanoparticles in the optimized formulation are shown in Figure 15. A spherical shape with a narrow size distribution was observed. The zeta potential of the nanoparticles was in the desirable range (Table 11), which indicated that good physical stability was obtained [172]. FT-IR spectra of the optimized nanoparticles indicated no marked changes in the IR peaks of the functional groups of CDD when incorporated with excipients, compared to pure CDD (Figure 16). This indicates that polymers did not react with the drug during preparation. That is, only a physical mixture was formed and there was no chemical interaction between the components.

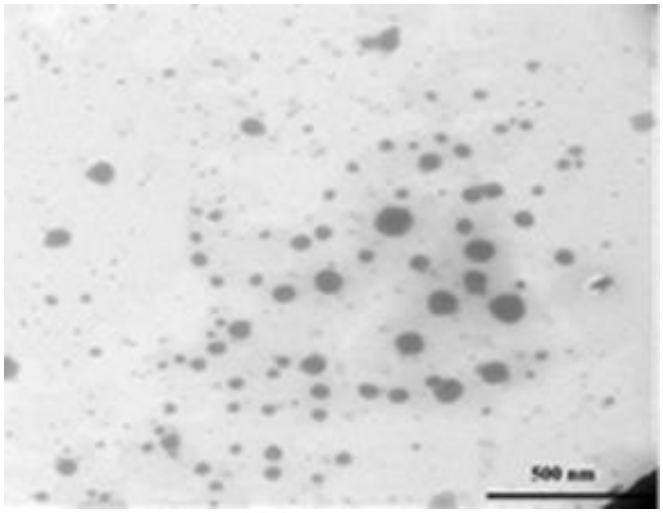

Figure 15 TEM image of nanoparticle in the optimized formulation.

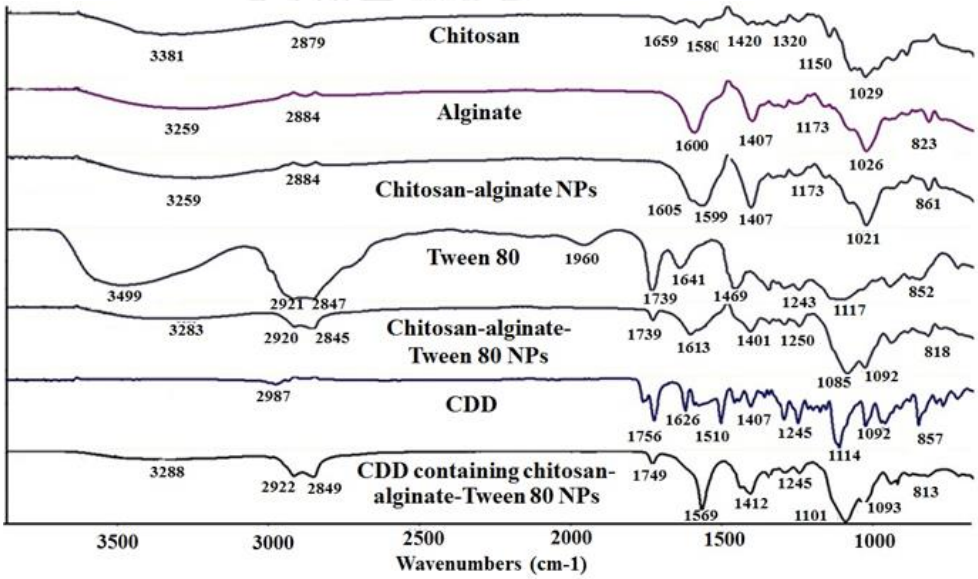

Figure 16 FT-IR spectra of the optimized nanoparticle formulation.

FT-IR spectra of the optimized nanoparticles indicated no marked changes in the IR peaks of the functional groups of CDD when incorporated with excipients, compared to pure CDD (Figure 16). This indicates that polymers did not react with the drug during preparation. That is, only a physical mixture was formed and there was no chemical interaction between the components.

3.5. Conclusion

Response surface methodology is an effective technique for optimization of chitosan/alginate nanoparticles containing CDD. The optimized formulation had a chitosan/alginate mass ratio of 0.05:1, a CDD concentration of 3 mg/ml, and a Tween® 80 concentration of 4.05% (w/v). The optimized nanoparticles had a size of 353 nm, a zeta potential of -25 mV, an encapsulation efficiency of 47%, and a loading capacity of 10%.

Acknowledgments

This study was supported by the Ratchadaphiseksomphot Endowment Fund of Chulalongkorn University (RES560530014-AM) and the 90th Anniversary of Chulalongkorn University fund.

CHAPTER IV

DESIGN OF CHITOSAN/ALGINATE NANOPARTICLES CONTAINING CURCUMIN DIETHYL DISUCCINATE OF CYTOTOXICITY IN MDA-MB-231 HUMAN BREAST CANCER CELLS

Settapon Bhunchu[1], Pornchai Rojsitthisak[2], Chawanphat Muangnoi[2], Pranee Rojsitthisak[1,3*]

[1]Ph.D. Program in Nanoscience and Technology (International)[1], Graduate School, Chulalongkorn University, Bangkok 10330, Thailand

[2]Department of Food and Pharmaceutical Chemistry, Faculty of Pharmaceutical Sciences, Chulalongkorn University, Bangkok 10330, Thailand

[3]Metallurgy and Materials Science Research Institute[2], Chulalongkorn University 10330, Bangkok, Thailand

Under review Progress in Natural Science: Materials International.

Abstract

Curcumin diethyl disuccinate (CDD) is a succinate prodrug of curcuminoids that has better stability in human plasma and improved in vitro cytotoxicity compared to curcumin. Therefore, CDD has the potential for further development as an anticancer agent. In this study, we focused on optimization of the formulation of CDD-loaded chitosan/alginate nanoparticles using Box-Behnken statistical design to enhance the therapeutic efficacy of CDD. Oil-in-water emulsification followed by ionotropic gelification was used to prepare the CDD-loaded chitosan/alginate nanoparticles. A formulation with a 0.05:1 chitosan/alginate mass ratio, 0.65% (w/v) Pluronic® F127 and 1.5 mg/ml CDD was found to be optimal. FTIR, TGA and XRD confirmed the encapsulation of CDD molecules in the nanoparticles. *In vitro* cytotoxicity and cellular uptake studies showed that CDD-loaded chitosan/alginate nanoparticles had significantly higher cytotoxicity and cellular uptake in human breast adenocarcinoma MDA-MB-231 cells, compared to free CDD. Physical and chemical stability studies indicated that the optimally formulated CDD-loaded chitosan/alginate nanoparticles were stable at 4°C for 3 months.

Keywords: Chitosan; Alginate; Curcumin diethyl disuccinate; Nanoparticles; Box-Behnken statistical design

4.1. Introduction

Nanotechnology is an emerging technology that can be used in a broad range of research areas, including material, medical and pharmaceutical sciences [185]. The major focus of nanotechnology research in the pharmaceutical sciences is the design of more selective and effective nanoparticles that can be used as carriers of bioactive compounds for enteral and parenteral administration, with protection of these compounds from enzymatic degradation, metabolism and cellular efflux and extension of shelf-life [34], Nanoparticles can also be used to deliver bioactive compounds to their target at the appropriate time and dosage [37].

Bioactive compounds extracted from plants have become alternatives for treatment of various diseases due to their low toxicity and lack of side effects [186]. Curcumin, the major component of Turmeric (*Curcuma longa* L.), has been extensively used as a flavor, coloring in food, preservative and household medicine in Southern Asia for a century. Curcumin has pharmacological effects including anti-oxidant, anti-inflammatory, anti-tumor, anti-HIV and anti-infectious activities [186, 187]. However, curcumin also has limitations due to its low water solubility, low stability, poor bioavailability and rapid intestinal and hepatic degradation and metabolism [155, 188]. Therefore, several approaches have been used to overcome these limitations, including development of nanoparticle formulations of curcumin [189] and chemical conjugation to give curcumin prodrugs [59].

Curcumin diethyl disuccinate (CDD) (Figure 17) is a succinate prodrug of curcuminoids that is synthesized by aldol condensation of 2,4-pentanedione with benzaldehyde and esterification with the methyl or ethyl ester of succinyl chloride. Compared to other succinate prodrugs of curcuminoids and to curcumin itself, CDD has better stability in human plasma and improved anti-colon cancer activity [59]. These properties may be further improved by encapsulation of CDD in nanoparticles.

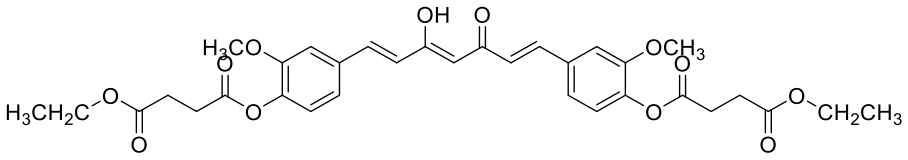

Figure 17 Structure of curcumin diethyl disuccinate.

Nanoparticles can be formulated from synthetic biodegradable polymers, lipids, proteins, and polysaccharides [190]. Alginate and chitosan are polysaccharides that have been extensively used for controlled release and delivery of bioactive compounds to target sites [20, 23, 27, 190].

Alginate is a hydrophilic polysaccharide extracted from marine brown algae. It is a linear copolymer of β-D-mannuronic acid and α-L-guluronic acid linked by 1,4-glycosidic bonds [27]. Alginate is of interest in pharmaceutical applications due to its gel formation, biocompatibility, non-toxicity, biodegradability and mucoadhesiveness [191]. Alginate nanoparticles can be obtained by inducing gelation with divalent cation [21, 100, 192]. This simple gelling property allows alginate to be used to produce a pre-gel consisting of very small aggregates of particles, followed by addition of an aqueous polycationic solution to make a polyelectrolyte complex [27]. For example, poly-L-lysine (PLL), a cationic natural polymer, has been used in combination with alginate to prepare nanoparticles [35]. However, PLL is toxic and immunogenic for administration by injection, and chitosan can be used as an alternative cationic polymer.

Chitosan is a linear polysaccharide consisting of D-glucosamine and *N*-acetyl-D glucosamine units linked by β(1→4) glycosidic linkages. Chitosan has versatile properties of biodegradability, biocompatibility, mucoadhesiveness, non-toxicity and good film formation [23]. For example, leakage of drugs from alginate nanoparticles is reduced when chitosan is used as a secondary counterion source [167]. Chitosan can enhance the desirable properties of alginate particles, such as controlled release, permeability, stability and half-life in physiological fluids [167]. Our previous work

(Bhunchu et al, unpublished data) demonstrated that use of lower molecular weight chitosan produced smaller chitosan/alginate nanoparticles with higher encapsulation and loading capacity of CDD at an optimal $CaCl_2$/alginate mass ratio of 0.2:1. In addition, chitosan/alginate nanoparticles improved uptake of CDD in caco-2 cells [69]. However, a systematic study of the optimal formulation of CDD-loaded chitosan/alginate nanoparticles is required. Therefore, in the current study, Box-Behnken statistical design was used to design and optimize CDD-loaded chitosan/alginate nanoparticles using response surface methodology. The influence of the chitosan/alginate mass ratio and concentrations of Pluronic® F127 and CDD on the characteristics of the nanoparticles was examined, and the in vitro cytotoxicity and cellular uptake of the optimized CDD-loaded nanoparticles in MDA-MB-231 breast cancer cells were investigated.

4.2. Materials and Methods

4.2.1. Materials

Medium viscosity sodium alginate of molecular weight 80,000-120,000 g/mol and low guluronic acid content (*FG* = 0.39) was purchased from Sigma, St. Louis, MO, USA. Chitosan of molecular weight 83,000 g/mol and a degree of deacetylation of about 85% was purchased from Aquatic Nutrition Lab Co. Ltd., Samut Sakorn, Thailand. Pluronic® F127 was supplied by BASF Chemical Company, Ludwigshafen, Germany. CDD was synthesized as described in Wichitnithad et al [59]. Tetrahydrofuran (THF) was of HPLC grade and other chemicals were of analytical grade.

4.2.2. Cell culture

Human caucasian breast adenocarcinoma MDA-MB-231 cells were obtained from the American Type Culture Collection (ATCC, Manassas, VA). Briefly, 3×10^3 cells/200 μl/well were seeded in 96-well plates with Dulbecco's Modified Eagle's Medium (DMEM) supplemented with 10% (v/v) heat inactivated fetal bovine serum (FBS) and 1% (v/v) penicillin-streptomycin solution. Cells were incubated at 37°C in a saturated humid atmosphere containing 95% air and 5% CO_2.

4.2.3. Preparation of CDD-loaded nanoparticles

CDD-loaded nanoparticles were prepared using o/w emulsification followed by ionotropic gelation as described by Lertsutthiwong et al [27] with modifications. Briefly, 1 ml of acetonic CDD solution at an appropriate concentration was added dropwise into 20 ml of sodium alginate solution (0.6 mg/ml) containing Pluronic® F127 as a stabilizer using an automatic syringe pump (NE 100, New Era, Pump System Inc. USA) at a rate of 20 ml/h. After continuous magnetic stirring at 1,000 rpm for 10 min, 4 ml of $CaCl_2$ solution (0.67 mg/ml) was added dropwise to the resulting o/w emulsion and continuously stirred for 30 min. After sonication at a frequency of 45 kHz and sonic power 80 W for 15 min using an ultrasonic bath (CP 230, Crest Ultrasonics Corp., Ewing, NJ, USA), 4 ml of chitosan solution was added to the resulting calcium/alginate pre-gel and stirred for 30 min. The nanoparticle suspensions were equilibrated overnight in the dark to allow formation of a uniform particle size. The CDD-loaded nanoparticles were finally obtained as a dispersion in aqueous solution.

4.2.4. Experimental design

Testing of multiple variables simultaneously requires a systematic and detailed experimental design that can eliminate the large number of experimental runs required in the traditional one-variable-at-a-time method. Systemic optimization procedures such as response surface methodology (RSM) are carried out by selecting an objective function finding the most important factors and investigating the relationship between responses and factors [81]. Previous work (Bhunchu et al [69]) indicated that formulation parameters such as chitosan/alginate mass ratio, Pluronic® F127 and CDD concentrations were the main factors affecting the characteristics of CDD-loaded nanoparticles in terms of particle size, size distribution, encapsulation efficiency and loading capacity. Therefore, Box-Behnken design was used to optimize the formulation parameters and evaluate the main effects, interaction effects and quadratic effects of the formulation factors on the particle size (Y_1), zeta potential (Y_2), encapsulation efficiency percentage (Y_3) and loading capacity percentage (Y_4) of CDD-loaded

nanoparticles. Chopra et al [83] suggested that the Box Behnken model requires fewer experimental runs than the central composite design model. The cubic design is characterized by a set of points lying at the midpoint of each edge of a multidimensional cube and center point replicates (*n* = 3), with the 'missing corners' helping to avoid combined factor extremes. Box-Behnken design provides a suitable means of optimizing and testing for a wide range of applications in the food and pharmaceutical industries [193].

Table 12 Factors and their levels for the Box-Behnken design.

Factors	Level used, Actual (coded)		
	Low (-1)	Medium (0)	High (+1)
X_1 = chitosan/alginate mass ratio	0.05:1	0.10:1	0.15:1
X_2 = Pluronic® F127 (%w/v)	0.5	1	1.5
X_3 = CDD (mg/ml)	0.5	1	1.5
Responses:	Constrains		
Y_1 = Particle size (nm)	Minimize		
Y_2 = Zeta potential (mV)	$Y_3 \geq \pm 20$		
Y_3 = Encapsulation efficiency (%)	Maximize		
Y_4 = Loading capacity (%)	Maximize		

4.2.5. Characterizations of CDD-loaded nanoparticles

Particles size and zeta potential were measured using a Zetasizer model Nano-ZS (Malvern Instruments, UK). The amount of CDD in nanoparticles was assayed by HPLC according to USP36- NF31 with some modification. The CDD-loaded nanoparticles were separated from the aqueous medium by ultracentrifugation at 45,000 rpm at 4°C for 1 h and lyophilized at -50°C for 24 h to obtain powdered nanoparticles. The lyophilized nanoparticles were then extracted in 1 ml of the mobile phase of 1 mg/ml citric acid in water and tetrahydrofuran (40:60, v/v)) under vortex for 1 min, followed by centrifugation at 14,000 rpm for 30 min. The supernatant was then collected for analysis. The 20-ml sample was injected onto the HA 166 (C_{18}, 4.6×150 mm, 5 μm) column, which was maintained at 40°C. The elution was isocratic at a flow rate of 1.0

ml/min and detection was carried out at 400 nm. The total chromatographic analysis time per sample was 4 min, with CDD eluting at a retention time of 3.38 min. The encapsulation efficiency and loading capacity were calculated as follows:

$$\text{Encapsulation efficiency (\%)} = \frac{\text{total amount of CDD in the nanoparticles}}{\text{total amount of CDD initially added in the formulation}} \times 100 \quad (2)$$

$$\text{Loading capacity (\%)} = \frac{\text{total amount of CDD in the nanoparticles}}{\text{total dry mass of nanoparticles}} \times 100 \quad (3)$$

Thermal properties of nanoparticles were analyzed using a thermogravimetric analyzer (TGA, model STA 409 PG/4/G Luxx, Netzsch, USA) using a heating rate of 5°C/min from 30 to 800°C under a nitrogen atmosphere with a flow rate of 10 ml/min. The interaction of CDD and excipients was analyzed by Fourier Transform Infrared Spectrometry (FT-IR, model ALPHA; Bruker, Philadelphia, PA, USA) in ATR mode. The analysis was carried out in spectral transmittance mode at 4000-400 cm^{-1} with a speed of 4 mm/s and resolution of 2 cm^{-1}. The physical state of CDD in the nanoparticle matrix was determined by wide-angle X-ray diffraction (XRD, model PW3710; Philips, The Netherlands). Samples were irradiated with monochromatized CuKα radiation (1.542 Å) and analyzed at 2θ range of 20-60° at a scanning speed of 0.2° 2θ/step. The detector was operated at a voltage of 40 kV and a current of 30 mA. The morphology of the CDD-loaded nanoparticles was visualized by transmission electron microscopy (TEM, model H-9500; Hitachi High Technology America Inc., USA)

4.2.6. Data analysis and model validation

ANOVA was used for statistical analysis of the polynomial equations generated by Design Expert® software. A total of 15 experimental runs in triplicate at center points were generated by Box-Behnken design. The mathematic model for mixture design includes linear, interaction and quadratic components. The best fitting mathematic model was selected based on several statistical parameters, including the multiple correlation coefficient (R^2), adjusted R^2, predicted R^2, standard deviation (SD), coefficient of variation (CV) and the predicted residual sum of squares (PRESS)

calculated in Design Expert® software. PRESS and CV indicate how well the model fits the data, and should be small for the chosen model relative to other models (Kim et al., 2007). Three dimensional response surface plots were generated in Design Expert® software using an intensive grid search over the whole experimental region. The optimal formulation was selected to validate the chosen experimental domain and polynomial equations, and was prepared and evaluated for various response properties. The resultant experimental values of the responses were compared with the predicted values to calculate the % prediction error. Linear regression plots between actual and predicted values of the responses were produced using MS-Excel 2013.

4.2.7 *In vitro* cytotoxicity assay

The cytotoxicity of CDD in MDA-MB-231 cells was determined using a 3-(4,5-dimethylthiazol-2- yl)-2, 5-diphenyl tetrazolium bromide (MTT) based colorimetric assay. This method is used to analyze the cytotoxicity of bioactive compounds based on the capacity of living cells to metabolize the yellow water soluble substrate MTT to an insoluble dark blue formazan product [194]. The MTT assay was carried out using the method described by Umthong et al. [195]. MDA-MB-231 cells were cultured in DMEM supplemented with 10% (v/v) heat inactivated fetal bovine serum (FBS) and 1% (v/v) antibiotic penicillin-streptomycin solution and incubated at 37°C in a humid atmosphere containing 95% air and 5% CO_2 until the cells reached 80% confluence. The cells were seeded in 96-well plates at 3×10^3 cells/well and incubated in the same atmosphere for 24 h. The cells were then washed with DMEM and treated with 200 µl of fresh DMEM containing a CDD-loaded nanoparticle suspension, blank chitosan/alginate nanoparticles or free CDD at drug concentrations ranging from 0.3-5 µg/ml and incubated for 72 h. Dimethyl sulfoxide (DMSO) and blank nanoparticles were used as positive and negative controls, respectively. MTT was then added to each well and incubated for 4 h, followed by removal of the solution. DMSO was added and thoroughly mixed for 10 min before measurement of absorbance at 540 nm using

a microplate reader (Molecular Devices, USA). Cell growth without nanoparticles was evaluated as a control. Cell viability was calculated as follows:

$$\text{Cell viability (\%)} = \frac{\text{OD}_{\text{sample}}}{\text{OD}_{\text{control}}} \times 100 \quad (4)$$

The results are shown as the half maximal inhibitory concentration (IC_{50}), which is the concentration of sample required to kill 50% of the cancer cells compared with the negative control.

4.2.8 *In vitro cellular* uptake study

MDA-MB-231 cells were cultured in 96-well plates at 3×10^3 cells/well at 37°C for 24 h. DMEM was then removed from each well. The cells were washed with 200 µl of DMEM and equilibrated for 1 h in an incubator at 37°C. A 2-µl sample of free CDD, blank chitosan/alginate nanoparticles or CDD-loaded nanoparticles was introduced into each well in 200 µl of DMEM and incubated for 72 h. The cells were then washed with 0.01 M phosphate-buffered solution (pH 7.4) to remove excess nanoparticles or free CDD, followed by addition of fresh PBS buffer. The cells were then visualized by confocal laser scanning microscopy (Nikon, D-ECLIPSE C1, Japan) using a green channel with excitation at 400 nm and emission at 470 nm. Images were processed with the aid of Nikon software. Cellular uptake was expressed as the fluorescence intensity associated with CDD-loaded nanoparticles versus the fluorescence intensity associated with free CDD.

4.2.9. Stability study

The stability of the nanoparticle suspension was determined based on ASEAN guidelines (2005) for stability of drug products. The CDD-loaded nanoparticle suspension was stored in amber bottles in the dark at 4°C and 25°C for 3 months. The particle size, zeta potential, encapsulation efficiency and loading capacity of the nanoparticle suspensions were determined at specific time intervals.

4.3. Result and discussion

4.3.1. Formation of CDD-loaded chitosan/alginate nanoparticles

Preparation of CDD-loaded chitosan/alginate nanoparticles by o/w emulsification and ionotropic gelation under mild conditions at room temperature was simple, rapid and reliable. The CDD encapsulation efficiency (~17-45%) and loading capacity (~1-5%) of the nanoparticles were low due to the hydrophilic and hydrophobic characters of the nanoparticle matrices and CDD, respectively. Li et al [100] also concluded that use of hydrophilic polymeric nanoparticles for encapsulation of hydrophobic compounds is difficult and that the encapsulation mechanism is unclear. Therefore, the challenge of this study was to maximize the encapsulation efficiency and loading capacity using chitosan/alginate nanoparticles by optimization of the preparation process using statistical design.

Previous work showed that Pluronic® F127 should be used as a stabilizer in the preparation process because of the poor water solubility of CDD, and that 1% (w/v) Pluronic® F127 gave the smallest particles with the highest encapsulation efficiency and loading capacity, compared to Tween® 80 and Cremophor RH40™ [69]. Therefore Pluronic® F127 was chosen for this study, with Box-Behnken design and RSM used for optimization of the formulation (Table 12). Chitosan/alginate mass ratio and Pluronic® F127 and CDD concentrations were used as the main factors affecting the characteristics (responses) of the nanoparticles, and the most important responses were particle size, zeta potential, encapsulation efficiency and loading capacity. Chitosan/alginate mass ratios of 0.05:1 to 0.15:1 were examined because below this lower mass ratio resulted in the reduction of encapsulation efficiency, whereas beyond 0.15:1 the particles aggregate and form microparticles. For Pluronic® F127, <0.5% (w/v) is insufficient to stabilize the CDD-loaded nanoparticle suspension and >1.5% (w/v) produces a viscous system due to particle aggregation. The solubility of CDD in acetone is 1.5 mg/ml, and therefore CDD concentrations of 0.05 to 1.5 mg/ml were examined. Thus, the 15 experiments in Table 12 were performed using a three-factor, three-level design.

The results (Table 13) showed that the particle size mainly depended on the chitosan/alginate mass ratio and Pluronic® F127 concentration. The minimum size of 279 nm occurred at a chitosan/alginate mass ratio of 0.05:1 and 0.5% (w/v) Pluronic® F127 (formulation 1), and the maximum size of 645 nm corresponded to the highest chitosan/alginate mass ratio (0.15:1) and highest Pluronic® F127 concentration (1.5% w/v) (formulation 4). The zeta potential was mainly affected by the chitosan/alginate mass ratio and became less negative with a higher mass ratio at fixed Pluronic® F127 and CDD concentrations. For example, at 0.50% (w/v) Pluronic® F127 and 1 mg/ml CDD, the zeta potential changed from -27.8 to -19.8 mV when the chitosan/alginate mass ratio increased from 0.05:1 to 0.15:1 (formulations 1 vs. 2). The highest encapsulation efficiency of the nanoparticles was observed at a chitosan/alginate mass ratio of 0.1:1, 1% (w/v) Pluronic® F127 and 1 mg/ml CDD (formulations 13- 15), and the highest loading capacity of about 5% occurred at a 0.1:1 chitosan/alginate mass ratio, 0.5% (w/v) Pluronic® F127 and 1.5 mg/ml CDD (formulation 11).

Table 13 Factors and observed responses in Box-Behnken design (n = 3).

Runs	Factors			Responses			
	X_1	X_2 (%w/v)	X_3 (mg/ml)	Y_1 (nm)	Y_2 (mV)	Y_3 (%)	Y_4 (%)
1	0.05	0.50	1.00	279 ± 71	-27.8 ± 0.3	38.71 ± 2.78	3.43 ± 0.34
2	0.15	0.50	1.00	434 ± 17	-19.8 ± 1.4	17.08 ± 2.27	1.41 ± 0.21
3	0.05	1.50	1.00	308 ± 22	-17.5 ± 0.2	25.42 ± 1.12	2.14 ± 0.04
4	0.15	1.50	1.00	645 ± 24	-12.4 ± 0.5	13.64 ± 0.87	1.06 ± 0.11
5	0.05	1.00	0.50	285 ± 22	-24.9 ± 1.3	24.52 ± 1.91	1.25 ± 0.12
6	0.15	1.00	0.50	558 ± 16	-16.5 ± 1.2	19.09 ± 4.32	0.76 ± 0.16
7	0.05	1.00	1.50	340 ± 33	-23.2 ± 0.1	39.97 ± 2.37	4.45 ± 0.35
8	0.15	1.00	1.50	585 ± 16	-17.1 ± 0.3	16.55 ± 1.82	2.83 ± 0.25
9	0.10	0.50	0.50	427 ± 26	-25.7 ± 0.5	35.16 ± 0.96	1.16 ± 0.08
10	0.10	1.50	0.50	615 ± 29	-13.4 ± 0.8	23.38 ± 1.43	2.48 ± 0.13
11	0.10	0.50	1.50	482 ± 15	-20.8 ± 0.5	40.12 ± 3.04	5.25 ± 0.28

Table 13 Factors and observed responses in Box-Behnken design (*n* = 3)

Runs	Factors			Responses			
	X_1	X_2 (%w/v)	X_3 (mg/ml)	Y_1 (nm)	Y_2 (mV)	Y_3 (%)	Y_4 (%)
12	0.10	1.50	1.50	607 ± 27	-17.2 ± 1.2	37.37 ± 3.29	3.21 ± 0.24
13[a]	0.10	1.00	1.00	505 ± 19	-21.0 ± 0.7	45.11 ± 1.43	3.78 ± 0.12
14[a]	0.10	1.00	1.00	529 ± 7	-20.6 ± 0.4	43.44 ± 1.31	3.51 ± 0.05
15[a]	0.10	1.00	1.00	519 ± 14	-22.3 ± 0.5	44.31 ± 1.03	3.57 ± 0.11

[a] *Indicates the center point of the design.*

4.3.2. Fitting data to model

Responses for all 15 formulations were simultaneously fitted to linear, interaction (2FI) and quadratic models using Design Expert® software. To evaluate the effect of formulation parameters on each response (Y_1-Y_4), a polynomial equation with ANOVA was used. The comparative values of R^2, adjusted R^2, predicted R^2, SD, CV and PRESS are shown in Table 14. Responses Y_1-Y_4 best followed a quadratic model based on the high values of R^2, adjusted R^2 and predicted R^2 and the low values of SD, PRESS and CV. Only significant ($p<0.05$) coefficients are included in the polynomial equations. PRESS is a particularly important measure of fit of the model to the points in the design. The smaller the PRESS statistic, the better the model fits to the data points [196].

4.3.3. Response surface analysis by polynomial equation

Response surfaces analyzed by polynomial equation are useful for determination of the interaction effects of two factors on the responses while the third factor is kept constant [197]. In the polynomial equation, a positive value indicates a synergistic effect through which the response increases proportional to the factor. In contrast, a negative value indicates an inverse relationship (antagonistic effect) between the response and factors. The criteria for selection of the suitable model are highest *F*-value and adequate precision, but lowest lack of fit *F*-value, and the adjusted R^2 and predicted R^2 should be close to 1 (Tables 14 and 15).

The best quadratic model for particle size, zeta potential, encapsulation efficiency and loading capacity was as follows:

$$Y_1 = 517.67 + 128.62X_1 + 66.75X_2 + 16.13X_3 + 45.33X_1X_2 - 12X_1X_3 - 20.75X_2X_3 - 95.83X_1^2 - 5.08X_2^2 + 15.17X_3^2 \quad (5)$$

$$Y_2 = -21.33 + 4.21X_1 + 3.46X_2 + 1.26X_3 - 0.73X_1X_2 - 0.6X_1X_3 - 2.17X_2X_3 - 0.42X_1^2 - 1.54X_2^2 + 0.52X_3^2 \quad (6)$$

$$Y_3 = 44.33 - 7.75X_1 - 4.13X_2 + 4.13X_3 + 2.5X_1X_2 - 4.5X_1X_3 - 2.25X_2X_3 - 14.79X_1^2 - 5.54X_2^2 + 4.54X_3^2 \quad (7)$$

$$Y_4 = 3.63 - 0.68X_1 - 0.33X_2 + 1.25X_3 + 0.23X_1X_2 - 0.33X_1X_3 - 0.82X_2X_3 - 1.18X_1^2 - 0.48X_2^2 + 0.13X_3^2 \quad (8)$$

Table 14 Summary of results of regression analysis responses.

Model	*F*-value	SD	R^2	Adjusted-R^2	Predicted-R^2	PRESS	CV (%)	Remark
Particle size (Y_1)								
Linear	36.39	65.99	0.7803	0.7203	0.5594	65.99	13.98	-
Interaction (2FI)	6.44	68.38	0.8284	0.6997	0.2119	68.38	14.49	-
Quadratic	74.76	17.93	0.9926	0.9793	0.9003	17.93	3.80	Suggested
Zeta potential (Y_2)								
Linear	25.39	1.77	0.8738	0.8394	0.7544	66.78	1.77	-
Interaction (2FI)	29.26	1.22	0.9564	0.9237	0.8717	34.89	1.22	-
Quadratic	67.67	0.67	0.9919	0.9772	0.9469	14.43	0.67	Suggested

Remark: Only significant terms are included.

Table 14 Summary of results of regression analysis responses (continue).

Model	*F*-value	SD	R^2	Adjusted-R^2	Predicted-R^2	PRESS	CV (%)	Remark
Encapsulation efficiency (Y_3)								
Linear	2.62	9.79	0.4166	0.2575	0.0435	1728.34	9.79	-
Interaction (2FI)	1.26	10.77	0.4865	0.1013	0.5033	2716.39	10.77	-
Quadratic	80.29	1.58	0.9931	0.9808	0.9256	134.50	1.58	Suggested
Loading capacity (Y_4)								
Linear	6.73	0.92	0.6474	0.5512	0.3498	17.06	0.92	-
Interaction (2FI)	4.59	0.86	0.7749	0.6061	0.2429	19.87	0.86	-
Quadratic	68.33	0.21	0.9919	0.9774	0.8954	2.74	0.21	Suggested

Remark: Only significant terms are included.

Table 15 Summary results of lack of fit and adequate precision of each response.

Model	Sum of square	Lack of fit *F*-value	*p*-value Prob > *F*	Adequacy precision	Remark
Particle size (Y_1)					
Linear model	47604.52	36.39	0.0270	11.467	-
Interaction model (2FI)	37116.02	42.56	0.0231	8.507	-
Quadratic model	1317.25	3.02	0.2585	26.687	Suggested
Zeta potential (Y_2)					
Linear model	32.79	4.77	0.0852	16.802	-
Interaction model (2FI)	10.32	2.25	0.0388	18.433	-
Quadratic model	0.69	0.30	0.8270	28.205	Suggested

Table 15 Summary results of lack of fit and adequate precision of each response.

Model	Sum of square	Lack of fit *F*-value	*p*-value Prob > *F*	Adequacy precision	Remark
Encapsulation efficiency (Y_3)					
Linear model	1049.52	49.98	0.0198	4.698	-
Interaction model (2FI)	923.27	65.95	0.0150	3.653	-
Quadratic model	7.75	1.11	0.5069	23.089	Suggestion
Loading capacity (Y_4)					
Linear model	9.21	43.84	0.0225	8.128	-
Interaction model (2FI)	5.86	41.86	0.0235	7.070	-
Quadratic model	0.16	2.36	0.3117	27.977	Suggestion

According to equation (5), X_1, X_2, $X_1 X_2$ and X_1^2 were significant (p<0.05). The effects are presented as 3-dimensional response surface plots in Figure 18. The chitosan/alginate mass ratio (Figure 18 (a)) and Pluronic® F127 concentration (Figure 18 (c)) both had positive effects on particle size, whereas the CDD concentration did not have a significant effect (Figure 18 (b), 2(c)). ANOVA also indicated that the particle size strongly depended on the chitosan/alginate mass ratio and Pluronic® F127. Therefore, low levels for these two factors were favorable for preparation of CDD-loaded nanoparticles. This might be due to Pluronic® F127 forming micelles surrounding the hydrophobic CDD with its hydrophilic groups facing the alginate polymer network. An increase in the Pluronic® F127 concentration increased the chance of interaction with alginate, resulting in a larger particle size. Addition of chitosan to the alginate nanoparticle suspension led to formation of chitosan network on the surface of the alginate nanoparticles, again resulting in a larger particle size. To avoid aggregation of large particles, Pluronic® F127 should not be higher than 1% (w/v) [171].

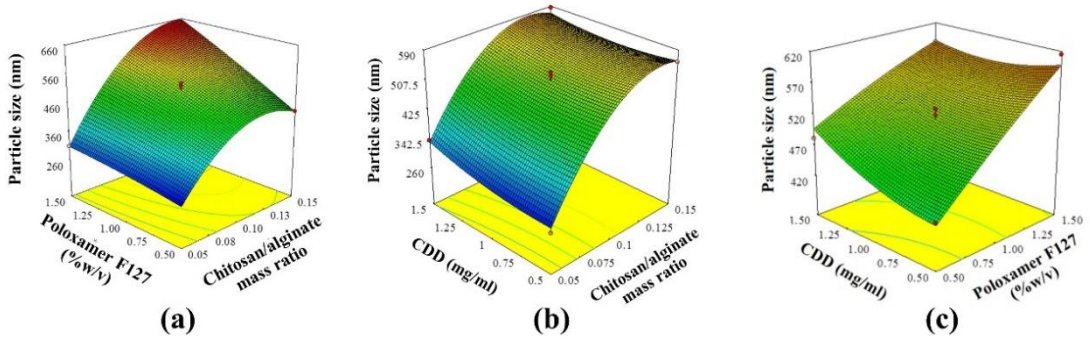

Figure 18 Three dimensional response surface plots showing the effect on particle size (Y_1) of (a) chitosan/alginate mass ratio (X_1) and Pluronic® F127 concentration (X_2); (b) chitosan/alginate mass ratio (X_1) and CDD concentration (X_3); (c) Pluronic® F127 concentration (X_2) and CDD concentration (X_3).

In equation (6), all three factors of chitosan/alginate mass ratio (X_1), Pluronic® F127 (X_2) and CDD (X_3) concentrations have synergistic effects on the zeta potential. To select a

suitable model, *F*-value and R_2 should be high, but the lack of fit *F*-value should be low. Therefore, the quadratic model is most appropriate for zeta potential (Tables 14 and 15). The response surface plots in Figure 19 show that the chitosan/alginate mass ratio had the main influence on zeta potential. Increasing the chitosan/alginate mass ratio caused increasingly less negative zeta potential of the CDD-loaded nanoparticles. De and Robinson [35] suggested that a higher percentage of chitosan increased the chance of neutralization of amino groups of chitosan with carboxylate groups of alginate, and consequently increased the zeta potential (less negative). Similar results were observed by Araujo et al [198] and Arora et al [176].

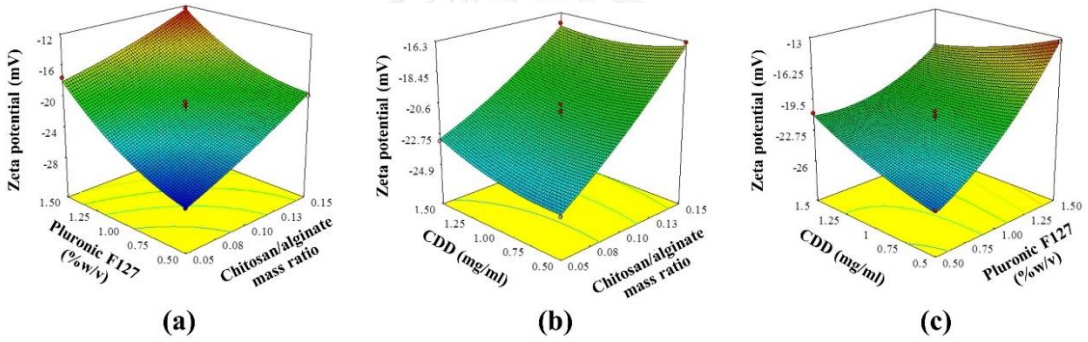

Figure 19 Three dimensional response surface plots showing the effect on zeta potential of (a) chitosan/alginate mass ratio (X_1) and Pluronic® F127 (X_2); (b) chitosan/alginate mass ratio (X_1) and CDD (X_3); (c) Pluronic® F127 (X_2) and CDD (X_3).

The encapsulation efficiency of the CDD-loaded nanoparticles ranged from 13.64% (formulation 4) to 45.11% (formulation 13). The relatively low encapsulation efficiency is due to the hydrophilic nature of the chitosan/alginate nanoparticles, which makes it relatively difficult to encapsulate hydrophobic CDD; and because the hydrophobic nature of CDD results in a larger loss of CDD to the external aqueous phase during formulation. The low encapsulation efficiency is in agreement with the study of Li et al [139], in which the low encapsulation of hydrophobic molecules in

chitosan/alginate nanoparticles was suggested to be due to their incompatibility with the hydrophilic polymers.

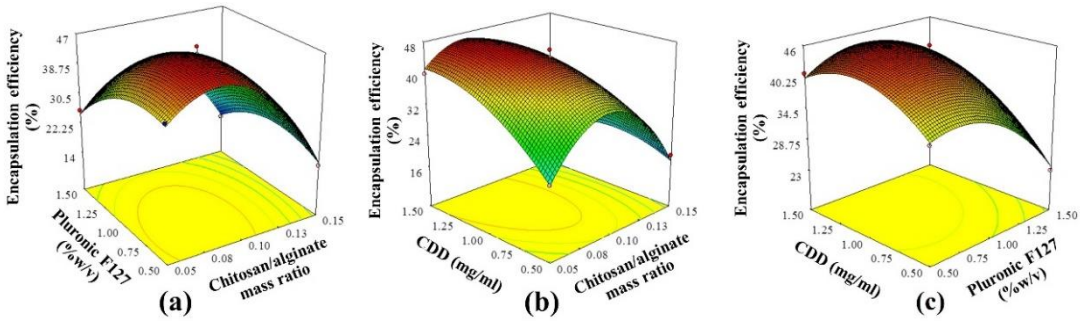

Figure 20 Three dimensional response surface plots showing the effect on encapsulation efficiency of (a) chitosan/alginate mass ratio (X_1) and Pluronic® F127 (X_2); (b) chitosan/alginate mass ratio (X_1) and CDD concentration (X_3); (c) Pluronic® F127 concentration (X_2) and CDD concentration (X_3).

In equation (7), the negative values for X_1 and X_2 represent an antagonistic effect while the positive value of X_3 indicates a synergistic effect. Response surface plots for encapsulation efficiency as a function of chitosan/alginate mass ratio, Pluronic® F127 and CDD concentrations are shown in Figure 20. The encapsulation efficiency depended on all three factors. The value increased as the chitosan/alginate mass ratio increased to 0.10:1, regardless of the Pluronic® F127 and CDD concentrations. This might be because the chitosan layer coated on the surface of alginate nanoparticles reduces leakage of CDD from the nanoparticles to the aqueous phase. Sarmento et al [166] also found that the encapsulation efficiency of chitosan/alginate nanoparticles increased with an increase in chitosan/alginate mass ratio due to the compact structure of the nanoparticle matrix. However, a further increase in the chitosan/alginate mass ratio to 0.15:1 resulted in lower encapsulation efficiency. An increase in Pluronic® F127 up to 1% (w/v) led to an increase in the solubility of the CDD in the aqueous phase by self-assembly in the aqueous environment. The CDD was localized in the hydrophobic core of Pluronic® F127, while

the hydrophilic parts of Pluronic® F127 faced hydrophilic polymers in the aqueous phase. However, the encapsulation efficiency of the CDD-loaded nanoparticles decreased with a further increase of Pluronic® F127 (1.5%, w/v). The encapsulation efficiency was consistently increased by increasing the CDD concentration.

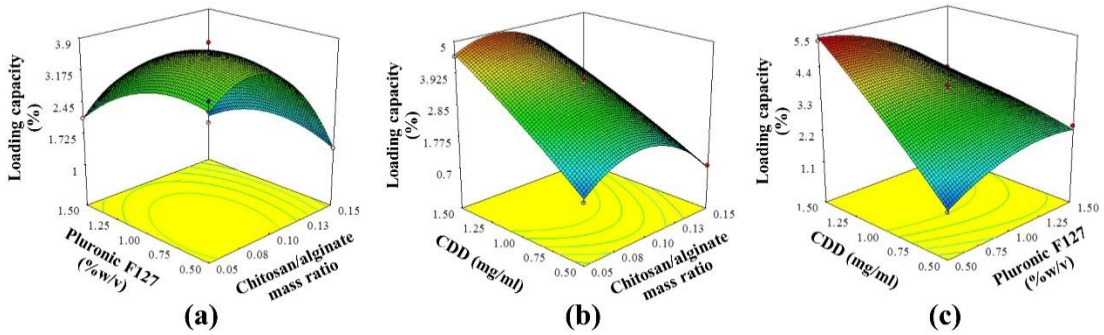

Figure 21 Three dimensional response surface plots showing the effect of factor on loading capacity of (a) chitosan/alginate mass ratio (X_1) and Pluronic® F127 concentration (X_2); (b) chitosan/alginate mass ratio (X_1) and CDD concentration (X_3); (c) Pluronic® F127 concentration (X_2) and CDD concentration (X_3).

The loading capacity of the CDD-loaded nanoparticles ranged from 1.06% (formulation 4) to 5.25% (formulation 11). In equation (8), the negative values of X_1 and X_2 indicate an inverse relationship and the positive value of X_3 indicates a favorable effect of an increase on the loading capacity. That is, an increase in the CDD concentration had a synergistic effect on the loading capacity and caused an increase in loading capacity (Figure 21 (b), 5(c)). Increases of the chitosan/alginate mass ratio and Pluronic® F127 concentrations from low to intermediate levels also resulted in an increase in loading capacity. This might be due to having a sufficient quantity of polymers for encapsulation of CDD. However, high levels of both factors resulted in lower loading capacity.

4.3.4. Optimization and validation of the model

Process optimization was performed with a desirability function (δ) to optimize the four responses simultaneously using Design Expert® software. A high value of the desirability coefficient ($0 \leq \delta \leq 1$) indicates that the operating point can produce acceptable formulation results [199]. The optimal formulation was selected based on the criteria of minimum particle size, zeta potential in the range of -30 to -20 mV, and maximum encapsulation efficiency and loading capacity. The maximum value of the desirability coefficient was obtained at a formulation with a chitosan/alginate mass ratio of 0.05:1, 0.65% (w/v) Pluronic® F127, and 1.5 mg/ml CDD, and this formulation fulfilled the requirements for the optimal formulation. To validate this optimal formulation, CDD-loaded nanoparticles were prepared using the optimized conditions and the observed values of the responses were compared with the predicted values. The results in Table 16 show that the observed and predicted values of the responses were acceptable because of the % error, which showed adequate precision for the prediction of the optimized condition.

Table 16 Optimal formulation, observed and predicted values for the responses, and the % error.

Optimized formulation composition (X_1; X_2; X_3)	Response variable	observed value	Predicted value	% Error[a]
0.05:1; 0.65 % (w/v); 1.5 (mg/ml)	Y_1 (nm)	324 ± 29	335.78	- 3.51
	Y_2 (mV)	-25.24 ± 1.3	-24.16	+4.47
	Y_3 (%)	44.24 ± 3.4	41.91	+5.56
	Y_4 (%)	5.56 ± 0.2	5.32	+4.51

[a] *% Error = (observed value - predicted value)/predicted value x 100*

4.3.5. Characterization of the optimized formulation

CDD-loaded chitosan/alginate nanoparticles produced from the optimal formulation were visualized using TEM (Figure 22). The TEM image confirmed that the CDD-loaded nanoparticles had a well-defined spherical shape, a solid dense structure, and a narrow particle size distribution.

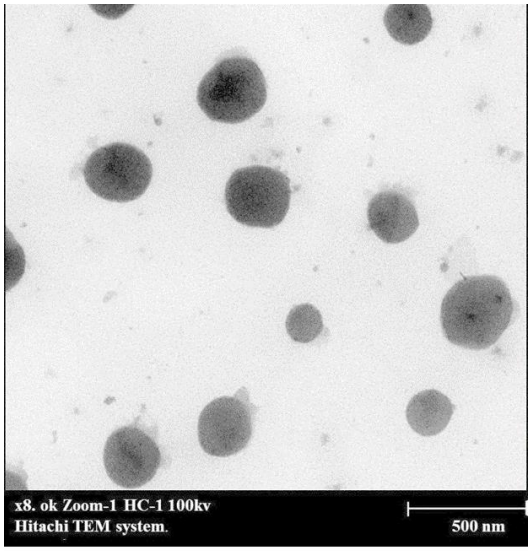

Figure 22 TEM image of CDD-loaded nanoparticles.

Thermal gravimetric analysis (TGA) (Figure 23) showed that CDD powder decomposed at 280°C-400°C, resulting in 60% weight loss. In chitosan/alginate nanoparticles (without CDD), initial weight loss occurred at 25°C -150°C due to evaporation of moisture in the nanoparticles (Figure 23). A second weight loss (~47%) occurred at 200°C-500°C. After encapsulation of CDD in chitosan/alginate nanoparticles, the second weight loss (~40%) occurred at the same temperature as that for the empty nanoparticles, With increasing temperature, the weight of both blank and drug loaded-nanoparticles decreased slowly from 45°C-190°C due to moisture evaporation [200], then decreased rapidly from 190°C-350°C, and then slowly again at higher temperature, possibly due to loss of small molecules and breaking of crosslinking and thermal

degradation of the ionic complex between chitosan and alginate in the polymer matrix [201, 202]. However, the weight of CDD-loaded nanoparticles then rapidly decreased again at 350°C-400°C, resulting in around 70% weight loss. This occurred in the same thermal decomposition range observed for CDD alone, and this weight-loss pattern did not occur for the chitosan/alginate nanoparticles. These results indicate that CDD was encapsulated into nanoparticles. The initial thermal decomposition of CDD shifted from 250°C to 350°C after encapsulation, which suggests that the thermal stability of CDD is enhanced by encapsulation. After thermal decomposition, 25.45% of CDD, 22.24% of chitosan/alginate nanoparticles and 5.15% of CDD-loaded chitosan/alginate nanoparticles remained, indicating high thermal stabilities and confirming the reported slow degradation rate [201].

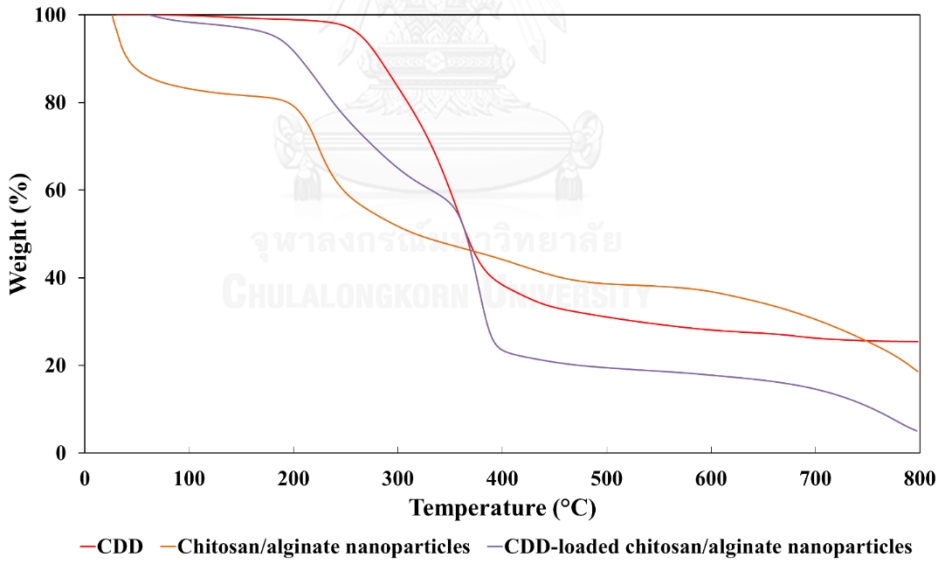

Figure 23 Thermal gravimetric curves for CDD and chitosan/alginate and CDD-loaded nanoparticles.

The encapsulation of CDD suggested in TGA was confirmed by FT-IR (Figure 24) and X-ray diffraction (Figure 25). In FT-IR spectra of CDD, blank nanoparticles and CDD-loaded nanoparticles, characteristic peaks for CDD were observed at 2972-2936, 1765, 1728, 1510 and 1464 $cm^{-1.}$ These peaks were also present in the FT-IR spectrum of CDD-loaded nanoparticles with some broadening and reduction intensity, indicating the absence of chemical interactions between CDD and polymers after nanoparticles formulation. However, disappearance of the bands at 1765 and 1728 cm^{-1} observed in CDD-loaded nanoparticles. Micelle formation in nanoparticles may have resulted in loss of these signals. The additional bands in the spectrum of the CDD-loaded nanoparticles (i.e. 3370, 2884 and 1360 cm^{-1}) are due to OH stretching in alginate and chitosan, and C-H bending and C-H stretching in Pluronic® F127, respectively [180-182]. The characteristic peaks of CDD in the spectrum of the CDD-loaded nanoparticles suggest that CDD was encapsulated in the chitosan/alginate nanoparticles at the molecular level and that micelle formation in the nanoparticle preparation did not cause breakdown of the CDD structure [168].

In X-ray diffraction analysis of CDD powder, chitosan/alginate nanoparticles and CDD-loaded nanoparticles, the peak for CDD was merged and had reduced intensity after encapsulation in the chitosan/alginate nanoparticles, indicating that CDD was encapsulated in the amorphous region.

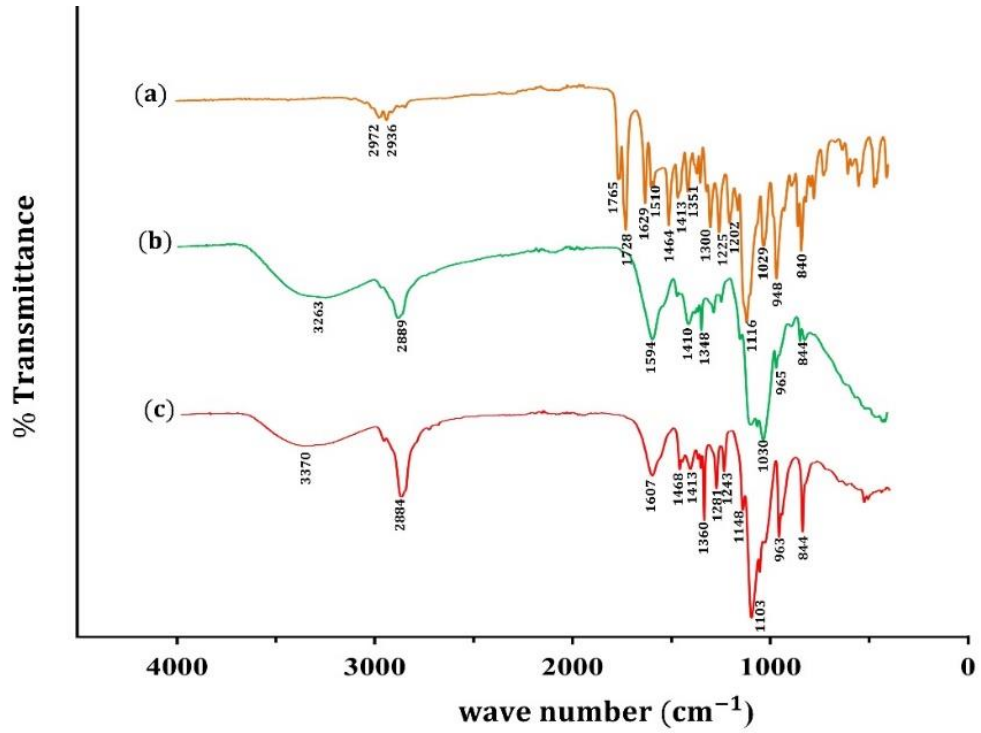

Figure 24 FT-IR spectra of (a) CDD powder, (b) chitosan/alginate nanoparticles and (c) CDD-loaded chitosan/alginate nanoparticles.

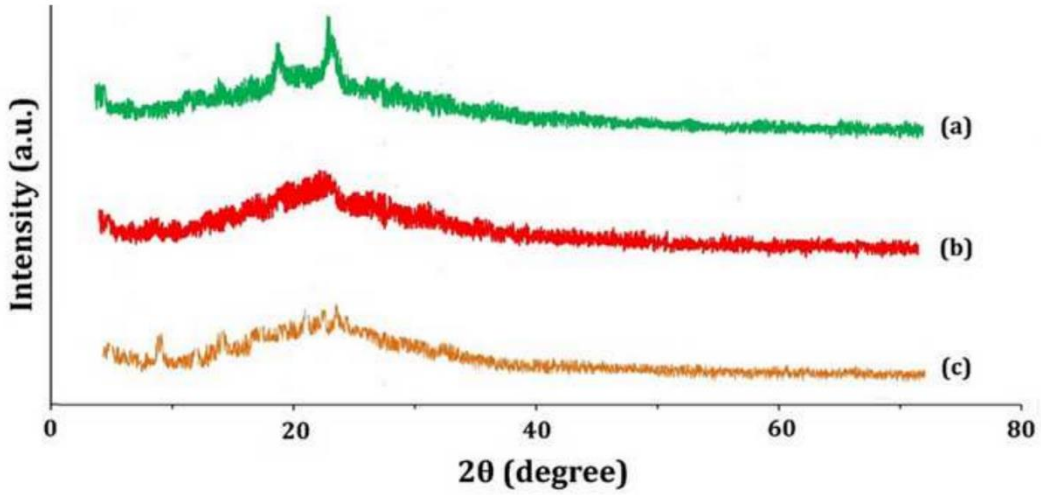

Figure 25 XRD patterns of (a) CDD powder, (b) chitosan/alginate nanoparticles and (c) CDD-loaded chitosan/alginate nanoparticles.

4.3.6. *In vitro* Cytotoxicity studies

The cytotoxicity of the CDD-loaded nanoparticles from the optimal formulation was investigated in MDA-MB-231 cells. Viability of cells after culturing with free CDD and CDD-loaded nanoparticles for 72 h is shown in Figure 26. Both free CDD and CDD-loaded nanoparticles decreased the cancer cell viability, but the CDD-loaded nanoparticles has a stronger effect than free CDD. For example, the viability of MDA-MB-231 cells after treatment with free CDD at 5 μg/ml was about 55%, whereas that of CDD-loaded nanoparticles was about 33%.

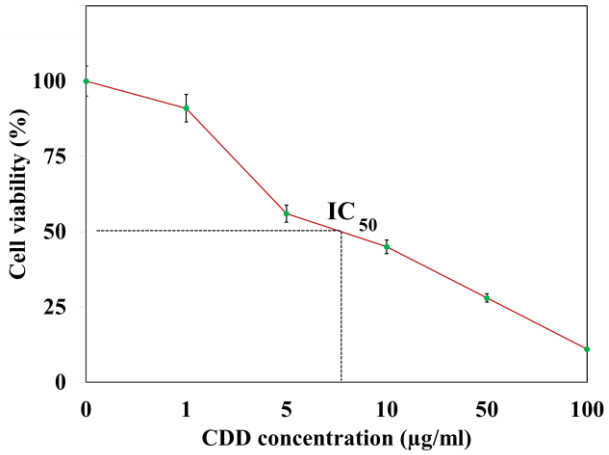

(a)

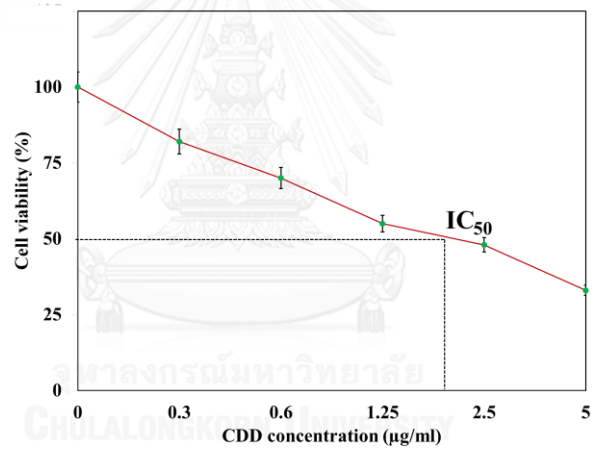

(b)

Figure 26 Survival of MDA-MB-231 cell lines in a MTT assay after treatment with (a) free CDD and (b) CDD-loaded nanoparticles for 72 h.

The IC_{50} of free CDD and CDD-loaded nanoparticles were about 9 and 2 µg/ml, respectively, indicating that both free CDD and CDD-loaded nanoparticles were toxic to these cells. The cytotoxicity of CDD-loaded nanoparticles increased significantly (p<0.05) with increasing CDD concentration. The greater toxicity of the CDD-loaded

nanoparticles might be due to enhanced cellular uptake, as examined in the following section.

Table 17 IC_{50} values for free CDD and CDD-loaded nanoparticles in MDA-MB-231 cells.

Sample	IC_{50} (μg/ml)
Free CDD	9
CDD-loaded nanoparticles	2

4.3.7. *In vitro* cellular uptake studies

The cellular uptake of free CDD and CDD-loaded nanoparticles by MDA-MB-231 cells after incubation for 72 h was visualized using a confocal laser scanning microscope (Figure 27). The fluorescence intensity was markedly higher in cells treated with CDD-loaded nanoparticles compared with those treated with free CDD, and there was no observable fluorescence in cells incubated with blank nanoparticles. This indicates that CDD-loaded nanoparticles were taken up by MDA-MB-231 breast cancer cells more effectively than free CDD, resulting in improved cytotoxicity (Table 17). Bhunchu et al [69] found similar results in Caco-2 cells and concluded that chitosan-alginate nanoparticles can improve cellular uptake and delivery of CDD into Caco-2 cells. The improved uptake and prolonged duration of nanoparticles in cells of up to 72 h are consistent with previous findings for nanoformulation containing hydrophobic molecules such as curcumin [102, 192, 203-205].

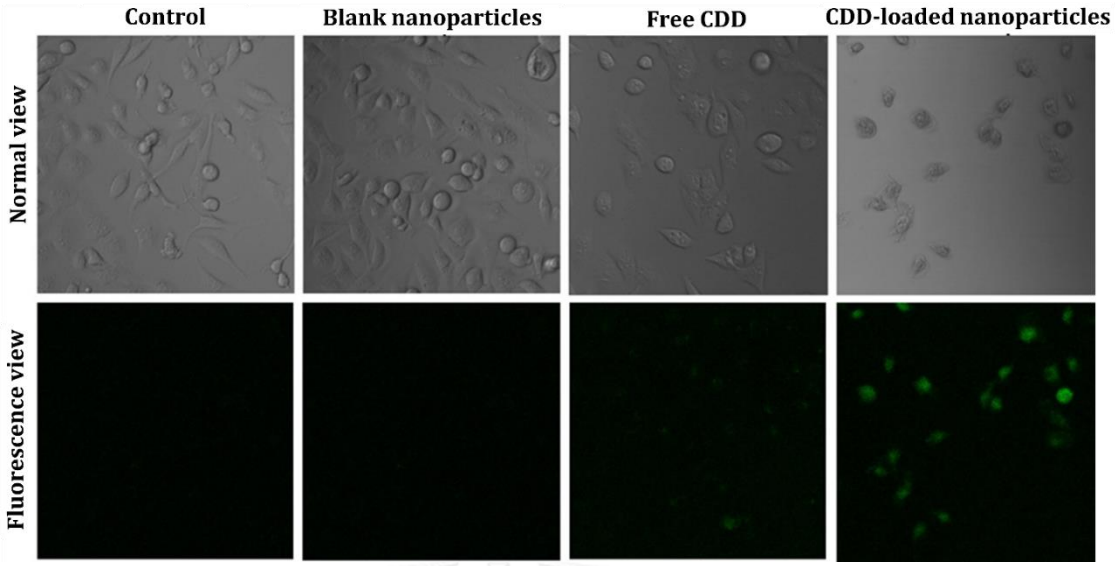

Figure 27 Confocal laser scanning microscopy images of MDA-MB-231 cells after incubation with blank nanoparticles, free CDD and CDD-loaded nanoparticles at 37°C for 72 h.

4.3.8. Stability studies

The stability of nanoparticles produced from the optimal formulation was determined at 4°C and 25°C for 3 months (Table 18). At 4°C, the particle size slightly increased and the negative value of the zeta potential and encapsulation efficiency slightly decreased. However, the zeta potential remained in the range of -20 to -30 mV, which indicates good stability of the particle suspension in aqueous medium [172]. At 25°C, the particle size sharply increased due to aggregation and consequently the negative value of zeta potential and encapsulation efficiency decreased significantly compared to of the changes at 4°C. For example, the encapsulation efficiency after storage at 25°C for 3 months was decreased by about 53%, compared to a decrease of 15% at 4°C. Therefore, storage of the nanoparticles at 4°C is required to reduce the risk of particle aggregation and CDD leakage.

Table 18 Stability study of optimum formulation of CDD-loaded nanoparticles at 25ºC and 4ºC.

Storage condition	Time (months)	Particle size (nm)	Zeta potential (mV)	Encapsulation efficiency (%)
4°C	0	328 ± 35	-26.5 ± 1.3	42.7 ± 3.3
	1	336 ± 19	-27.9 ± 1.1	41.3 ± 0.2
	2	388 ± 33	-24.2 ± 0.5	39.8 ± 3.2
	3	412 ± 29	-22.3 ± 0.8	36.3 ± 1.4
25°C	0	328 ± 35	-26.5 ± 1.3	42.7 ± 3.3
	1	378 ± 47	-24.1 ± 0.7	40.1 ± 0.6
	2	436 ± 28	-20.5 ± 2.1	32.4 ± 2.1
	3	765 ± 39	-15.9 ± 1.9	19.9 ± 1.8

(n = 3)

4.4. Conclusions

Response surface statistical modeling using Box-Behnken design was successfully applied in development of chitosan/alginate nanoparticles for CDD delivery. Variables of chitosan/alginate mass ratio and Pluronic® F127 and CDD concentrations influenced the particle size, zeta potential, encapsulation efficiency and loading capacity of the nanoparticles. The optimized formulation prepared using the predicted levels for these variables had a particle size of 324 nm, zeta potential of - 25.2 mV, encapsulation efficiency of 44.2% and loading capacity of 5.6%. These chitosan-alginate nanoparticles enhanced the cytotoxicity and cellular uptake of CDD in breast cancer cells.

Acknowledgments

The authors express their gratitude to the Ratchadaphiseksomphot Endowment Fund of Chulalongkorn University (RES560530014-AM) and the 90th Anniversary of Chulalongkorn University Fund for providing research funds. We also thank Dr. Ian S. Haworth (University of Southern California) for his comments on the manuscript.

Conflict of interest statement

The authors report no conflicts of interest in this work.

PART III

THESIS CONCLUSION

3.1. Conclusion

This dissertation focuses on the design and optimization of chitosan/alginate nanoparticles loaded with curcumin diethyl disuccinate (CDD). Initially, one-variable-at-a-time was used to screen and identify significant variables that affect the characteristics of CDD-loaded nanoparticles. Subsequently, Box-Behnken experimental design and response surface methodology with desirability function were used to optimize the preparation process. The physical and chemical characteristics of the prepared nanoparticles were investigated. Finally, *in vitro* cellular uptake and cytotoxicity of CDD-loaded chitosan/alginate nanoparticles was examined by confocal laser scanning microscopy in human caucasian colon adenocarcinoma (Caco-2) and human caucasian breast adenocarcinoma (MDA-MB-231) cells.

Anticancer drugs are typically toxic and harmful to healthy cells, which is a major disadvantage of chemotherapy. To overcome this problem, drug delivery systems are required as a novel therapy. Nanoparticles are preferable for delivery of anticancer drugs due to their ease of intracellular uptake, resulting in an increase of therapeutic efficacy. Nanoparticles can be used to deliver drugs to target organs and to improve oral bioavailability, stability of chemotherapy agents against enzymatic degradation, reduction of drug toxicity, and therapeutic efficacy. Due to biodegradability, biocompatibility, non-toxicity and good film formation of chitosan and alginate, they are a good choice as anticancer drug nanocarriers in drug delivery systems that may serve as an alternative approach to conventional cancer chemotherapy.

For encapsulation of CDD, chitosan/alginate nanoparticles were prepared by o/w emulsification and ionotropic gelation (chapter 2-chapter 5). The influence of parameters, including type and concentration of non-ionic surfactants, chitosan/alginate mass ratio, and concentration and rate of CDD addition into the formulation, on the characteristics of the nanoparticles were investigated by one-variable-at-a-time (chapter 2). The results indicate that the characteristics of nanoparticles containing CDD are strongly dependent on the preparation parameters; i.e. type and concentration of surfactants, chitosan/alginate mass ratio, and concentration and rate of CDD addition. Using the optimal conditions, the chitosan-alginate nanoparticles containing CDD showed good physical stability at 4°C and ability to improve cellular uptake of CDD in Caco-2 cells, in comparison with free CDD. Further systematic design and optimization of the preparation process for alginate/chitosan nanoparticles containing CDD using statistical design was performed. The results in chapter 3 and chapter 4 demonstrate that Box-Behnken design and response surface methodology was effective for optimization of the preparation of chitosan/alginate nanoparticles using a limited number of experiments compared to traditional optimization technique i.e. one-variable-at-time. In addition, the physical appearance of CDD-loaded nanoparticles prepared with Pluronic® F127 using the optimized conditions (0.05:1 of chitosan/alginate mass ratio, 0.65% w/v of Pluronic® F127 and 1.5 mg/ml of CDD) were smooth, dense and spherical with a uniform surface. *In vitro* cytotoxicity and intracellular uptake studies also revealed excellent cytotoxicity and uptake in MDA-MB-231 cells compared to free CDD. Stability analysis suggests that the prepared nanoparticles was stable under 4°C for at least 3 months (chapter 4).

REFERENCES

[1] Park W, Na K. Advances in the synthesis and application of nanoparticles for drug delivery. Wiley Interdisciplinary Reviews: Nanomedicine and Nanobiotechnology 2015;7:494-508.

[2] Ryan SM, Brayden DJ. Progress in the delivery of nanoparticle constructs: towards clinical translation. Current Opinion in Pharmacology 2014;18:120-8.

[3] Prasad S, Tyagi AK, Aggarwal BB. Recent Developments in Delivery, Bioavailability, Absorption and Metabolism of Curcumin: the Golden Pigment from Golden Spice. Cancer Research and Treatment 2014;46:2-18.

[4] Bae YH, Park K. Targeted drug delivery to tumors: Myths, reality and possibility. Journal of Controlled Release 2011;153:198-205.

[5] Hu C-MJ, Aryal S, Zhang L. Nanoparticle-assisted combination therapies for effective cancer treatment. Therapeutic Delivery 2010;1:323–34.

[6] Vranić E, Rahić O, Hadžiabdić J, Elezović A, Bošković D. Opportunities and challenges for utilization of nanoparticles as bioactive drug carriers for the targeted treatment of cancer. Folia Medica Facultatis Medicinae Universitatis Saraeviensis 2015;50:34-9.

[7] Bilia AR, Isacchi B, Righeschi C, Guccione C, Bergonzi MC. Flavonoids Loaded in Nanocarriers: An Opportunity to Increase Oral Bioavailability and Bioefficacy. Food and Nutrition Sciences 2014;5:1212-27.

[8] Nitta SK, Numata K. Biopolymer-Based Nanoparticles for Drug/Gene Delivery and Tissue Engineering. International Journal of Molecular Sciences 2013;14.

[9] Prabhu RH, Patravale VB, Joshi MD. Polymeric nanoparticles for targeted treatment in oncology: current insights. International Journal of Nanomedicine 2015;10:1001–18.

[10] Thukral D, Dumoga S, Arora S, Chuttani K, Mishra A. Potential carriers of chemotherapeutic drugs: matrix based nanoparticulate polymeric systems. Cancer Nano 2014;5:1-15.

[11] Ranghar S, Sirohil P, Verma P, Agarwal V. Nanoparticle-based drug delivery systems: promising approaches against infections. Brazilian Archives of Biology and Technology 2014;57:209-22.

[12] Lee KY, Mooney DJ. Alginate: Properties and biomedical applications. Progress in Polymer Science 2012;37:106-26.

[13] Onoue S, Yamada S, Chan H-K. Nanodrugs: pharmacokinetics and safety. International journal of nanomedicine2014. p. 1025-37.

[14] Ayre AP, Pawar HA, Khutle NM, Lalitha KG. Polymeric nanoparticles articles in drug delivery systems critical review and concepts. International Journal Of Pharmacy&Technology 2014;5:2809-23.

[15] Morgen M, Bloom C, Beyerinck R, Bello A, Song W, Wilkinson K, et al. Polymeric Nanoparticles for Increased Oral Bioavailability and Rapid Absorption Using Celecoxib as a Model of a Low-Solubility, High-Permeability Drug. Pharm Res 2012;29:427-40.

[16] Łukasiewicz S, Szczepanowicz K, Błasiak E, Dziedzicka-Wasylewska M. Biocompatible Polymeric Nanoparticles as Promising Candidates for Drug Delivery. Langmuir 2015;31 6415–25.

[17] Dadwal M. Polymeric Nanoparticles as Promising Novel Carriers for Drug Delivery: An Overview. Journal of Advanced Pharmacy Education & Research 2014;4:20-30.

[18] Mahapatro A, Singh DK. Biodegradable nanoparticles are excellent vehicle for site directed in-vivo delivery of drugs and vaccines. Journal of Nanobiotechnology 2011;9:1-11.

[19] Balaji RA, Raghunathan S, Revathy R. Levofloxacin: formulation and in-vitro evaluation of alginate and chitosan nanospheres. Egyptian Pharmaceutical Journal 2015;14:30-5.

[20] Azevedo MA, Bourbon AI, Vicente AA, Cerqueira MA. Alginate/chitosan nanoparticles for encapsulation and controlled release of vitamin B2. International Journal of Biological Macromolecules 2014;71:141-6.

[21] Lertsutthiwong P, Noomun K, Jongaroonngamsang N, Rojsitthisak P, Nimmannit U. Preparation of alginate nanocapsules containing turmeric oil. Carbohydrate Polymers 2008;74:209-14.

[22] Paques JP, van der Linden E, van Rijn CJM, Sagis LMC. Preparation methods of alginate nanoparticles. Advances in Colloid and Interface Science 2014;209:163-71.

[23] Bhunchu S, Rojsitthisak P. Biopolymeric alginate-chitosan nanoparticles as drug delivery carriers for cancer therapy. Die Pharmazie - An International Journal of Pharmaceutical Sciences 2014;69:563-70.

[24] Ramana BV, Parameswari CS, Triveni C, Arundathi T, Reddy V, Nagarajan G. Formulation and evaluation of sodium alginate microbeads of simvastatin. International Journal of Pharmacy and Pharmaceutical Sciences 2013;5:410-6.

[25] Sagiri S, Pal K, Basak P, Rana U, Shakir I, Anis A. Encapsulation of Sorbitan Ester-Based Organogels in Alginate Microparticles. AAPS PharmSciTech 2014;15:1197-208.

[26] Zhang N, Li J, Jiang W, Ren C, Li J, Xin J, et al. Effective protection and controlled release of insulin by cationic β-cyclodextrin polymers from alginate/chitosan nanoparticles. International Journal of Pharmaceutics 2010;393:213-9.

[27] Lertsutthiwong P, Rojsitthisak P, Nimmannit U. Preparation of turmeric oil-loaded chitosan-alginate biopolymeric nanocapsules. Materials Science and Engineering: C 2009;29:856-60.

[28] Younes I, Rinaudo M. Chitin and Chitosan Preparation from Marine Sources. Structure, Properties and Applications. Marine Drugs 2015;13:1133.

[29] Shao Y, Li L, Gu X, Wang L, Mao S. Evaluation of chitosan–anionic polymers based tablets for extended-release of highly water-soluble drugs. Asian Journal of Pharmaceutical Sciences 2015;10:24-30.

[30] Croisier F, Jérôme C. Chitosan-based biomaterials for tissue engineering. European Polymer Journal 2013;49:780-92.

[31] Jana S, Gandhi A, Sen KK, Basu S. Natural Polymers and their Application in Drug Delivery and Biomedical Field. Journal of PharmaSciTech 2011;1:16-27.

[32] Patil JS, Mandave SV, Jadhav SM. Ionotropicaly Crosslinked and Chitosan Reinforced Losartan Potassium Loaded Complex Alginate Beads: Design, Characterization and Evaluation. Malaya Journal of Biosciences 2014;1:126-33.

[33] Bhattarai RS, Dhandapani NV, Shrestha A. Drug delivery using alginate and chitosan beads: An Overview. Chronicles of Young Scientists 2011;2:192-6.

[34] Motwani SK, Chopra S, Talegaonkar S, Kohli K, Ahmad FJ, Khar RK. Chitosan–sodium alginate nanoparticles as submicroscopic reservoirs for ocular delivery: Formulation,

optimisation and in vitro characterisation. European Journal of Pharmaceutics and Biopharmaceutics 2008;68:513-25.

[35] De S, Robinson D. Polymer relationships during preparation of chitosan–alginate and poly-l-lysine–alginate nanospheres. Journal of Controlled Release 2003;89:101-12.

[36] Sahoo RK, Biswas N, Guha A, Sahoo N, Kuotsu K. Nonionic Surfactant Vesicles in Ocular Delivery: Innovative Approaches and Perspectives. BioMed Research International 2014;1:1-12.

[37] Sekhon BS. Surfactants: Pharmaceutical and Medicinal Aspects. Journal of Pharmaceutical Technology, Research and Management 2013;1:43–68.

[38] Xue Y, Zhang S, Tang M, Zhang T, Wang Y, Hieda Y, et al. Comparative study on toxic effects induced by oral or intravascular administration of commonly used disinfectants and surfactants in rats. Journal of Applied Toxicology 2012;32:480-7.

[39] Zhang X, Liu J, Qiao H, Liu H, Ni J, Zhang W, et al. Formulation optimization of dihydroartemisinin nanostructured lipid carrier using response surface methodology. Powder Technology 2010;197:120-8.

[40] Nagarwal RC, Kumar R, Pandit JK. Chitosan coated sodium alginate–chitosan nanoparticles loaded with 5-FU for ocular delivery: In vitro characterization and in vivo study in rabbit eye. European Journal of Pharmaceutical Sciences 2012;47:678-85.

[41] Damalas CA. Potential uses of turmeric (Curcuma longa) products as alternative means of pest management in crop production. Plant Omics Journal 2011;4:136-41.

[42] Anand P, Kunnumakara A, Sundaram C, Harikumar K, Tharakan S, Lai O, et al. Cancer is a Preventable Disease that Requires Major Lifestyle Changes. Pharm Res 2008;25:2097-116.

[43] Gangwar M, Gautam MK, Sharma AK, Tripathi YB, Goel RK, Nath G. Antioxidant Capacity and Radical Scavenging Effect of Polyphenol Rich Mallotus philippenensis Fruit Extract on Human Erythrocytes: An In Vitro Study. The Scientific World Journal 2014;2014:1-12.

[44] Borra SK, Gurumurthy P, Mahendra J, KM J, CN C, Chand R. Antioxidant and free radical scavenging activity of curcumin determined by using different in vitro and ex vivo models. Journal of Medicinal Plants Research 2013;7:2680-90.

[45] Moghadamtousi SZ, Kadir HA, Hassandarvish P, Tajik H, Abubakar S, Zandi K. A Review on Antibacterial, Antiviral, and Antifungal Activity of Curcumin. BioMed Research International 2014;2014:1-12.

[46] Wang Z, Zou P, Li C, He W, Xiao B, Fang Q, et al. Synthesis and biological evaluation of novel semi-conservative monocarbonyl analogs of curcumin as anti-inflammatory agents. MedChemComm 2015;6:1328-39.

[47] Shanmugam M, Rane G, Kanchi M, Arfuso F, Chinnathambi A, Zayed M, et al. The Multifaceted Role of Curcumin in Cancer Prevention and Treatment. Molecules 2015;20:2728.

[48] Naksuriya O, Okonogi S, Schiffelers RM, Hennink WE. Curcumin nanoformulations: A review of pharmaceutical properties and preclinical studies and clinical data related to cancer treatment. Biomaterials 2014;35:3365-83.

[49] Wang N-P, Wang Z-F, Tootle S, Philip T, Zhao Z-Q. Curcumin promotes cardiac repair and ameliorates cardiac dysfunction following myocardial infarction. British Journal of Pharmacology 2012;167:1550-62.

[50] Palipoch S, Punsawad C, Koomhin P, Suwannalert P. Hepatoprotective effect of curcumin and alpha-tocopherol against cisplatin-induced oxidative stress. BMC Complementary and Alternative Medicine 2014;14:1-8.

[51] Singh S, Jamal F, Agarwal R, Singh RK. Hepatoprotective Role of Curcumin against Acetaminophen induced toxicity in rats. International Research Journal of Biological Sciences 2013;2:42-9.

[52] Siviero A, Gallo E, Maggini V, Gori L, Mugelli A, Firenzuoli F, et al. Curcumin, a golden spice with a low bioavailability. Journal of Herbal Medicine 2015;5:57-70.

[53] Altunbas A, Lee SJ, Rajasekaran SA, Schneider JP, Pochan DJ. Encapsulation of curcumin in self-assembling peptide hydrogels as injectable drug delivery vehicles. Biomaterials 2011;32:5906-14.

[54] Chen KL, Mylon SE, Elimelech M. Aggregation Kinetics of Alginate-Coated Hematite Nanoparticles in Monovalent and Divalent Electrolytes. Environmental Science and Technology 2006; 40 1516–23.

[55] Kim TH, Jiang HH, Youn YS, Park CW, Tak KK, Lee S, et al. Preparation and characterization of water-soluble albumin-bound curcumin nanoparticles with improved antitumor activity. International Journal of Pharmaceutics 2011;403:285-91.

[56] Manju S, Sreenivasan K. Hollow microcapsules built by layer by layer assembly for the encapsulation and sustained release of curcumin. Colloids and Surfaces B: Biointerfaces 2011;82:588-93.

[57] Dey S, Sreenivasan K. Conjugation of curcumin onto alginate enhances aqueous solubility and stability of curcumin. Carbohydrate Polymers 2014;99:499-507.

[58] Thomas C, Pillai L, Krishnan L. Evaluation of Albuminated Curcumin as Soluble Drug Form to Control Growth of Cancer Cells in Vitro. Journal of Cancer Therapy 2014;5:723-34.

[59] Wichitnithad W, Nimmannit U, Wacharasindhu S, Rojsitthisak P. Synthesis, Characterization and Biological Evaluation of Succinate Prodrugs of Curcuminoids for Colon Cancer Treatment. Molecules 2011;16:1888.

[60] Wongsrisakul J, Wichitnithad W, Rojsitthisak P, Towiwat P. Antinociceptive Effects of Curcumin Diethyl Disuccinate in Animal Models. Journal of Health Research 2010;24:175-80.

[61] Yang X, Li Z, Wang N, Li L, Song L, He T, et al. Curcumin-Encapsulated Polymeric Micelles Suppress the Development of Colon Cancer *In Vitro* and *In Vivo*. Scientific Reports 2015;5:1-15.

[62] Teong B, Lin C-Y, Chang S-J, Niu GC-C, Yao C-H, Chen IF, et al. Enhanced anti-cancer activity by curcumin-loaded hydrogel nanoparticle derived aggregates on A549 lung adenocarcinoma cells. Journal of Materials Science: Materials in Medicine 2015;26:1-15.

[63] Teixeira CCC, Mendonça LM, Bergamaschi MM, Queiroz RHC, Souza GEP, Antunes LMG, et al. Microparticles Containing Curcumin Solid Dispersion: Stability, Bioavailability and Anti-Inflammatory Activity. AAPS PharmSciTech 2015:1-10.

[64] Krausz AE, Adler BL, Cabral V, Navati M, Doerner J, Charafeddine RA, et al. Curcumin-encapsulated nanoparticles as innovative antimicrobial and wound healing agent. Nanomedicine: Nanotechnology, Biology and Medicine 2015;11:195-206.

[65] Zhao Z, Xie M, Li Y, Chen A, Li G, Zhang J, et al. Formation of curcumin nanoparticles via solutionenhanced dispersion by supercritical CO_2. International Journal of Nanomedicine 2015;10:3171-81.

[66] Pandit R, Gaikwad S, Agarkar G, Gade A, Rai M. Curcumin nanoparticles: physico-chemical fabrication and its in vitro efficacy against human pathogens. 3 Biotech 2015:1-7.

[67] Priyadarsini K. The Chemistry of Curcumin: From Extraction to Therapeutic Agent. Molecules 2014;19:20091.

[68] Cridge BJ, Larsen L, Rosengren RJ. Curcumin and its derivatives in breast cancer: Current developments and potential for the treatment of drug-resistant cancers. Oncology Discovery 2013;1.

[69] Bhunchu S, Rojsitthisak P, Rojsitthisak P. Effects of preparation parameters on the characteristics of chitosan–alginate nanoparticles containing curcumin diethyl disuccinate. Journal of Drug Delivery Science and Technology 2015;28:64-72.

[70] Tadayon A, Jamshidi R, Esmaeili A. Delivery of tissue plasminogen activator and streptokinase magnetic nanoparticles to target vascular diseases. International Journal of Pharmaceutics 2015;495:428-38.

[71] Ghari T, Mortazavi SA, Khoshayand MR, Kobarfard F, Gilani K. Preparation, optimization, and in vitro evaluation of azithromycin encapsulated nanoparticles by using response surface methodology. Journal of Drug Delivery Science and Technology 2014;24:352-60.

[72] Huang Y, Yuan Y, Zhou Z, Liang J, Chen Z, Li G. Optimization and evaluation of chelerythrine nanoparticles composed of magnetic multiwalled carbon nanotubes by response surface methodology. Applied Surface Science 2014;292:378-86.

[73] Zhao X, Jiang R, Zu Y, Wang Y, Zhao Q, Zu B, et al. Process optimization studies of 10-Hydroxycamptothecin (HCPT)-loaded folate-conjugated chitosan nanoparticles by SAS-ionic crosslink combination using response surface methodology (RSM). Applied Surface Science 2012;258:2000-5.

[74] de Coninck J, Bouquelet S, Dumortier V, Duyme F, Verdier-Denantes I. Industrial media and fermentation processes for improved growth and protease production by Tetrahymena thermophila BIII. J Ind Microbiol Biotech 2000;24:285-90.

[75] Dutta JR, Dutta PK, Banerjee R. Optimization of culture parameters for extracellular protease production from a newly isolated Pseudomonas sp. using response surface and artificial neural network models. Process Biochemistry 2004;39:2193-8.

[76] Namal Senanayake SPJ, Shahidi F. Lipase-catalyzed incorporation of docosahexaenoic acid (DHA) into borage oil: optimization using response surface methodology. Food Chemistry 2002;77:115-23.

[77] Ghoreishi SM, Saeidinejad F, Behpour M, Masoum S. Application of multivariate optimization to electrochemical determination of methyldopa drug in the presence of diclofenac at a nanostructured electrochemical sensor. Sensors and Actuators B: Chemical 2015;221:576-85.

[78] Morton SW, Poon Z, Hammond PT. The architecture and biological performance of drug-loaded LbL nanoparticles. Biomaterials 2013;34:5328-35.

[79] Subrahmanyam S, Guerreiro A, Poma A, Moczko E, Piletska E, Piletsky S. Optimisation of experimental conditions for synthesis of high affinity MIP nanoparticles. European Polymer Journal 2013;49:100-5.

[80] Hanrahan G, Lu K. Application of Factorial and Response Surface Methodology in Modern Experimental Design and Optimization. Critical Reviews in Analytical Chemistry 2006;36:141-51.

[81] Box GEP, Hunter JS, Hunter WG. Statistics for experimenters: an introduction to design, data analysis, and model building. New York: John Wiley & Sons, Inc; 1978.

[82] Francis F, Sabu A, Nampoothiri KM, Ramachandran S, Ghosh S, Szakacs G, et al. Use of response surface methodology for optimizing process parameters for the production of α-amylase by Aspergillus oryzae. Biochemical Engineering Journal 2003;15:107-15.

[83] Chopra S, Motwani SK, Iqbal Z, Talegaonkar S, Ahmad FJ, Khar RK. Optimisation of polyherbal gels for vaginal drug delivery by Box-Behnken statistical design. European Journal of Pharmaceutics and Biopharmaceutics 2007;67:120-31.

[84] Herráez JV, Dolz M, Sobrino P, Belda R, González F. Modification of rheological behavior of cellulose gels with NaCl concentration. Application of Ostwald's model. Pharmazie 1993;48:359–62.

[85] Sharma D, Maheshwari D, Philip G, Rana R, Bhatia S, Singh M, et al. Formulation and Optimization of Polymeric Nanoparticles for Intranasal Delivery of Lorazepam Using Box-Behnken Design: *In Vitro* and *In Vivo* Evaluation. BioMed Research International 2014;2014:1-14.

[86] Hao J, Fang X, Zhou Y, Wang J, Guo F, Li F, et al. Development and optimization of solid lipid nanoparticle formulation for ophthalmic delivery of chloramphenicol using a Box-Behnken design. International Journal of Nanomedicine 2011;6 683–92.

[87] Gajra B, Dalwadi C, Patel R. Formulation and optimization of itraconazole polymeric lipid hybrid nanoparticles (Lipomer) using box behnken design. DARU Journal of Pharmaceutical Sciences 2015;23:1-15.

[88] Noori Koopaei M, Khoshayand MR, Mostafavi SH, Amini M, Khorramizadeh MR, Jeddi Tehrani M, et al. Docetaxel Loaded PEG-PLGA Nanoparticles: Optimized Drug Loading, In-vitro Cytotoxicity and In-vivo Antitumor Effect. Iran J Pharm Res 2014;13:819-33.

[89] Elmizadeh H, Khanmohammadi M, Ghasemi K, Hassanzadeh G, Nassiri-Asl M, Garmarudi AB. Preparation and optimization of chitosan nanoparticles and magnetic chitosan nanoparticles as delivery systems using Box–Behnken statistical design. Journal of Pharmaceutical and Biomedical Analysis 2013;80:141-6.

[90] Chaudhary H, Kohli K, Amin S, Rathee P, Kumar V. Optimization and formulation design of gels of Diclofenac and Curcumin for transdermal drug delivery by Box-Behnken statistical design. Journal of Pharmaceutical Sciences 2011;100:580-93.

[91] Jambrak AR. Experimental Design and Optimization of Ultrasound Treatment of Food Products. Food Processing & Technology 2011;2:1-3.

[92] Decker-Baumann C, Buhl K, Frohmüller S, Herbay AV, Dueck M, Schlag PM. Reduction of chemotherapy-induced side-effects by parenteral glutamine supplementation in patients with metastatic colorectal cancer. European Journal of Cancer 1999;35:202-7.

[93] Chellat F, Merhi Y, Moreau A, Yahia LH. Therapeutic potential of nanoparticulate systems for macrophage targeting. Biomaterials 2005;26:7260-75.

[94] Haley B, Frenkel E. Nanoparticles for drug delivery in cancer treatment. Urologic Oncology: Seminars and Original Investigations;26:57-64.

[95] Singh R, Lillard Jr JW. Nanoparticle-based targeted drug delivery. Experimental and Molecular Pathology 2009;86:215-23.

[96] Mohanraj V, Chen Y. Nanoparticles-A review. Tropical Journal of Pharmaceutical Research 2006;5:561-73.

[97] Kumari A, Yadav SK, Yadav SC. Biodegradable polymeric nanoparticles based drug delivery systems. Colloids and Surfaces B: Biointerfaces 2010;75:1-18.

[98] Gazori T, Khoshayand MR, Azizi E, Yazdizade P, Nomani A, Haririan I. Evaluation of Alginate/Chitosan nanoparticles as antisense delivery vector: Formulation, optimization and in vitro characterization. Carbohydrate Polymers 2009;77:599-606.

[99] Lertsutthiwong P, Rojsitthisak P. Chitosan-alginate nanocapsules for encapsulation of turmeric oil. Die Pharmazie - An International Journal of Pharmaceutical Sciences 2011;66:911-5.

[100] Li P, Dai Y-N, Zhang J-P, Wang A-Q, Wei Q. Chitosan-alginate nanoparticles as a novel drug delivery system for nifedipine. Int J Biomed Sci 2008;4:221-8.

[101] Malesu V, Sahoo D, Nayak P. Chitosan-sodium alginate nanocomposites blended with cloisite 30B as a novel drug delivery system for anticancer drug curcumin. International Journal of Applied Biology and Pharmaceutical Technology 2011;2:402-11.

[102] Das RK, Kasoju N, Bora U. Encapsulation of curcumin in alginate-chitosan-pluronic composite nanoparticles for delivery to cancer cells. Nanomedicine: Nanotechnology, Biology and Medicine 2010;6:153-60.

[103] Douglas KL, Tabrizian M. Effect of experimental parameters on the formation of alginate–chitosan nanoparticles and evaluation of their potential application as DNA carrier. Journal of Biomaterials Science, Polymer Edition 2005;16:43-56.

[104] Kumar M. Nano and microparticles as controlled drug delivery devices. Journal of Pharmacy & Pharmaceutical Sciences 2000;3:234–58.

[105] Society AC. Cancer Facts & Figures 2011. Atlanta: American Cancer Society; 2011.
[106] Anand P, Sundaram C, Jhurani S, Kunnumakkara AB, Aggarwal BB. Curcumin and cancer: An "old-age" disease with an "age-old" solution. Cancer Letters 2008;267:133-64.
[107] Mittelberg KN, Tucker RD, Loening SA, Moseley PL. Effect of radiation and hyperthermia on prostate tumor cells with induced thermal tolerance and the correlation with HSP70 accumulation. Urologic Oncology: Seminars and Original Investigations;2:146-51.
[108] Gelperina S, Kisich K, Iseman MD, Heifets L. The Potential Advantages of Nanoparticle Drug Delivery Systems in Chemotherapy of Tuberculosis. American Journal of Respiratory and Critical Care Medicine 2005;172:1487-90.
[109] Kukowska-Latallo J, Candido K, Cao Z, Nigavekar S, Majoros I, Thomas T, et al. Nanoparticle targeting of anticancer drug improves therapeutic response in animal model of human epithelial cancer. . Cancer Research 2005;65:5317-24.
[110] Pandey R, Khuller GK. Oral nanoparticle-based antituberculosis drug delivery to the brain in an experimental model. Journal of Antimicrobial Chemotherapy 2006;57:1146–52.
[111] Davis ME. Nanoparticles for systemic medicines and imaging agents. Nanotechnology Law & Business 2006;3:255–61.
[112] Juillerat-Jeanneret L. The targeted delivery of cancer drugs across the blood–brain barrier: chemical modifications of drugs or drug-nanoparticles? Drug Discovery Today 2008;13:1099-106.
[113] Bawa R. Nanoparticle-based therapeutics in humans: a survey. Nanotechnology Law & Business 2008;5:135-55.
[114] Oberdörster G, Oberdörster E, Oberdörster J. Nanotoxicology: an emerging discipline evolving from studies of ultrafine particles. Environ Health Perspect 2005;113:823-39.
[115] Colvin VL. The potential environmental impact of engineered nanomaterials. Nat Biotech 2003;21:1166-70.

[116] Derfus AM, Chan WCW, Sangeeta N. Bhatia SN. Probing the Cytotoxicity of Semiconductor Quantum Dots. Nano Letters 2004;4:11-8.

[117] Shukla RK, Tiwari A. Carbohydrate polymers: Applications and recent advances in delivering drugs to the colon. Carbohydrate Polymers 2012;88:399-416.

[118] Coppi G, Iannuccelli V. Alginate/chitosan microparticles for tamoxifen delivery to the lymphatic system. International Journal of Pharmaceutics 2009;367:127-32.

[119] Jayakumar R, Menon D, Manzoor K, Nair SV, Tamura H. Biomedical applications of chitin and chitosan based nanomaterials—A short review. Carbohydrate Polymers 2010;82:227-32.

[120] Lu Z, Yeh T, Tsai M, Au J, Wientjes M. Paclitaxel-loaded gelatin nanoparticles for intravesical bladder cancer therapy. Clinical Cancer Research 2004;15:7677–84.

[121] Gulyaev A, Gelperina S, Skidan I, Antropov A, Kivman G, Kreuter J. Significant Transport of Doxorubicin into the Brain with Polysorbate 80-Coated Nanoparticles. Pharm Res 1999;16:1564-9.

[122] Derakhshandeh K, Erfan M, Dadashzadeh S. Encapsulation of 9-nitrocamptothecin, a novel anticancer drug, in biodegradable nanoparticles: Factorial design, characterization and release kinetics. European Journal of Pharmaceutics and Biopharmaceutics 2007;66:34-41.

[123] Fonseca C, Simões S, Gaspar R. Paclitaxel-loaded PLGA nanoparticles: preparation, physicochemical characterization and in vitro anti-tumoral activity. Journal of Controlled Release 2002;83:273-86.

[124] Teixeira M, Alonso MJ, Pinto MMM, Barbosa CM. Development and characterization of PLGA nanospheres and nanocapsules containing xanthone and 3-methoxyxanthone. European Journal of Pharmaceutics and Biopharmaceutics 2005;59:491-500.

[125] Redhead HM, Davis SS, Illum L. Drug delivery in poly(lactide-co-glycolide) nanoparticles surface modified with poloxamer 407 and poloxamine 908: *in vitro* characterisation and *in vivo* evaluation. Journal of Controlled Release 2001;70:353-63.

[126] Nicoli S, Santi P, Couvreur P, Couarraze G, Colombo P, Fattal E. Design of triptorelin loaded nanospheres for transdermal iontophoretic administration. International Journal of Pharmaceutics 2001;214:31-5.

[127] Gómez-Gaete C, Tsapis N, Besnard M, Bochot A, Fattal E. Encapsulation of dexamethasone into biodegradable polymeric nanoparticles. International Journal of Pharmaceutics 2007;331:153-9.

[128] Mitra S, Gaur U, Ghosh PC, Maitra AN. Tumour targeted delivery of encapsulated dextran–doxorubicin conjugate using chitosan nanoparticles as carrier. Journal of Controlled Release 2001;74:317-23.

[129] Tokumitsu H, Ichikawa H, Fukumori Y. Chitosan-Gadopentetic Acid Complex Nanoparticles for Gadolinium Neutron-Capture Therapy of Cancer: Preparation by Novel Emulsion-Droplet Coalescence Technique and Characterization. Pharm Res 1999;16:1830-5.

[130] Shikata F, Tokumitsu H, Ichikawa H, Fukumori Y. *In vitro* cellular accumulation of gadolinium incorporated into chitosan nanoparticles designed for neutron-capture therapy of cancer. European Journal of Pharmaceutics and Biopharmaceutics 2002;53:57-63.

[131] Parveen S, Mitra M, Krishnakumar S, Sahoo SK. Retraction notice to ``Enhanced Antiproliferative Activity of Carboplatin loaded Chitosan-Alginate Nanoparticles in Retinoblastoma Cell Line'' [Acta Biomaterialia 6 (2010) 3120–3131]. Acta Biomaterialia 2010;6:3120-31.

[132] Lapasin R, Pricl S. Rheology of Industrial Polysaccharides: Theory and Applications. UK: Blackie Academic and Professional.; 1995.

[133] Phillips G, Williams P, Wedlock D. Gums and stabilizers for the food industry 5: Applications of alginates. New York: IRL Press at Oxford University Press; 1990.

[134] Tønnesen HH, Karlsen J. Alginate in Drug Delivery Systems. Drug Development and Industrial Pharmacy 2002;28:621-30.

[135] Agnihotri SA, Mallikarjuna NN, Aminabhavi TM. Recent advances on chitosan-based micro- and nanoparticles in drug delivery. Journal of Controlled Release 2004;100:5-28.

[136] Sarmento B, Ferreira DC, Jorgensen L, van de Weert M. Probing insulin's secondary structure after entrapment into alginate/chitosan nanoparticles. European Journal of Pharmaceutics and Biopharmaceutics 2007;65:10-7.

[137] George M, Abraham TE. Polyionic hydrocolloids for the intestinal delivery of protein drugs: Alginate and chitosan — a review. Journal of Controlled Release 2006;114:1-14.

[138] Richardson T, Murphy W, Mooney D. Polymeric delivery of proteins and plasmid DNA for tissue engineering and gene therapy. Critical Reviews™ in Eukaryotic Gene Expression 2001;11:47-58.

[139] Li X, Kong X, Shi S, Zheng X, Guo G, Wei Y, et al. Preparation of alginate coated chitosan microparticles for vaccine delivery. BMC Biotechnol 2008;8:1-11.

[140] Jain A, Jain SK. *In vitro* and cell uptake studies for targeting of ligand anchored nanoparticles for colon tumors. European Journal of Pharmaceutical Sciences 2008;35:404-16.

[141] Gazori T, Haririan I, Fouladdel S, Namazi A, Nomani A, Azizi E. Inhibition of EGFR expression with chitosan/alginate nanoparticles encapsulating antisense oligonucleotides in T4 7 D cell line using RT-PCR and immunocytochemistry. Carbohydrate Polymers 2010;80:1042-7.

[142] Liu L-S, Liu S-Q, Ng SY, Froix M, Ohno T, Heller J. Controlled release of interleukin-2 for tumour immunotherapy using alginate/chitosan porous microspheres. Journal of Controlled Release 1997;43:65-74.

[143] Mladenovska K, Raicki RS, Janevik EI, Ristoski T, Pavlova MJ, Kavrakovski Z, et al. Colon-specific delivery of 5 - aminosalicylic acid from chitosan-Ca-alginate microparticles. International Journal of Pharmaceutics 2007;342:124-36.

[144] Peng C, Zhao Q, Gao C. Sustained delivery of doxorubicin by porous CaCO3 and chitosan/alginate multilayers-coated CaCO3 microparticles. Colloids and Surfaces A: Physicochemical and Engineering Aspects 2010;353:132-9.

[145] Zhao Q, Han B, Wang Z, Gao C, Peng C, Shen J. Hollow chitosan-alginate multilayer microcapsules as drug delivery vehicle: doxorubicin loading and in vitro and in vivo studies. Nanomedicine: Nanotechnology, Biology and Medicine 2007;3:63-74.

[146] Ringe K, Walz C, Sabel B. Nanoparticle drug delivery to the brain. Encyclopedia of Nanoscience and Nanotechnology 2004;7:91–104.

[147] Shoaib M, Tazeen J, Merchant H, Yousuf R. Evaluation of drug release kinetics from ibuprofen matrix tablets using HPMC. Pakistan Journal of Pharmaceutical Sciences 2006;19:119-24.

[148] Ak T, Gülçin İ. Antioxidant and radical scavenging properties of curcumin. Chemico-Biological Interactions 2008;174:27-37.

[149] Chen D-Y, Shien J-H, Tiley L, Chiou S-S, Wang S-Y, Chang T-J, et al. Curcumin inhibits influenza virus infection and haemagglutination activity. Food Chemistry 2010;119:1346-51.

[150] Saja K, Babu MS, Karunagaran D, Sudhakaran PR. Anti-inflammatory effect of curcumin involves downregulation of MMP-9 in blood mononuclear cells. International Immunopharmacology 2007;7:1659-67.

[151] Ghosh D, Choudhury ST, Ghosh S, Mandal AK, Sarkar S, Ghosh A, et al. Nanocapsulated curcumin: Oral chemopreventive formulation against diethylnitrosamine induced hepatocellular carcinoma in rat. Chemico-Biological Interactions 2012;195:206-14.

[152] Černý D, Lekić N, Váňová K, Muchová L, Hořínek A, Kmoníčková E, et al. Hepatoprotective effect of curcumin in lipopolysaccharide/-galactosamine model of liver injury in rats: Relationship to HO-1/CO antioxidant system. Fitoterapia 2011;82:786-91.

[153] Prakash P, Misra A, Surin WR, Jain M, Bhatta RS, Pal R, et al. Anti-platelet effects of Curcuma oil in experimental models of myocardial ischemia-reperfusion and thrombosis. Thrombosis Research 2011;127:111-8.

[154] Srivastava RM, Singh S, Dubey SK, Misra K, Khar A. Immunomodulatory and therapeutic activity of curcumin. International Immunopharmacology 2011;11:331-41.

[155] Anand P, Kunnumakkara AB, Newman RA, Aggarwal BB. Bioavailability of curcumin: problems and promises. Molecular Pharmaceutics 2007;4:807–18.

[156] Song L, Shen Y, Hou J, Lei L, Guo S, Qian C. Polymeric micelles for parenteral delivery of curcumin: Preparation, characterization and in vitro evaluation. Colloids and Surfaces A: Physicochemical and Engineering Aspects 2011;390:25-32.

[157] Wan Z, Ke D, Hong J, Ran Q, Wang X, Chen Z, et al. Comparative study on the interactions of cationic gemini and single-chain surfactant micelles with curcumin. Colloids and Surfaces A: Physicochemical and Engineering Aspects 2012;414:267-73.

[158] Madan T, Munshi N, De TK, Maitra A, Usha Sarma P, Aggarwal SS. Biodegradable nanoparticles as a sustained release system for the antigens/allergens of Aspergillus fumigatus: preparation and characterisation. International Journal of Pharmaceutics 1997;159:135-47.

[159] Mahkam M. Modification of nano alginate-chitosan matrix for oral delivery of insulin Nature and Science 2009;7:1-7.

[160] Mi F-L, Sung H-W, Shyu S-S. Drug release from chitosan–alginate complex beads reinforced by a naturally occurring cross-linking agent. Carbohydrate Polymers 2002;48:61-72.

[161] DeGroot AR, Neufeld RJ. Encapsulation of urease in alginate beads and protection from α-chymotrypsin with chitosan membranes. Enzyme and Microbial Technology 2001;29:321-7.

[162] Liu P, Krishnan TR. Alginate-pectin-poly-L-lysine particulate as a potential controlled release formulation. Journal of Pharmacology and Pharmacotherapeutics 1999;51:141-9.

[163] Bilensoy E, Sarisozen C, Esendağlı G, Doğan AL, Aktaş Y, Şen M, et al. Intravesical cationic nanoparticles of chitosan and polycaprolactone for the delivery of Mitomycin C to bladder tumors. International Journal of Pharmaceutics 2009;371:170-6.

[164] Na JH, Lee S-Y, Lee S, Koo H, Min KH, Jeong SY, et al. Effect of the stability and deformability of self-assembled glycol chitosan nanoparticles on tumor-targeting efficiency. Journal of Controlled Release 2012;163:2-9.

[165] Finotelli PV, Da Silva D, Sola-Penna M, Rossi AM, Farina M, Andrade LR, et al. Microcapsules of alginate/chitosan containing magnetic nanoparticles for controlled release of insulin. Colloids and Surfaces B: Biointerfaces 2010;81:206-11.

[166] Sarmento B, Ribeiro AJ, Veiga F, Ferreira DC, Neufeld RJ. Insulin-Loaded Nanoparticles are Prepared by Alginate Ionotropic Pre-Gelation Followed by Chitosan Polyelectrolyte Complexation. Journal of Nanoscience and Nanotechnology 2007;7:2833-41.

[167] Zhang Y, Wei W, Lv P, Wang L, Ma G. Preparation and evaluation of alginate–chitosan microspheres for oral delivery of insulin. European Journal of Pharmaceutics and Biopharmaceutics 2011;77:11-9.

[168] Kharia AA, Singhai AK. Formulation and Evaluation of Gastroretentive Drug Delivery System of Acyclovir as Mucoadhesive Nanoparticles. International Journal of PharmTech Research 2013;5:1538-45.

[169] Sarmento B, Ferreira D, Veiga F, Ribeiro A. Characterization of insulin-loaded alginate nanoparticles produced by ionotropic pre-gelation through DSC and FTIR studies. Carbohydrate Polymers 2006;66:1-7.

[170] Yuan CL, Xu ZZ, Fan MX, Liu HY, Xie YH, Zhu T. Study on characteristics and harm of surfactants Journal of Chemical and Pharmaceutical Research 2014;6:2233-7

[171] Kim S, Fernandes MM, Matamá T, Loureiro A, Gomes AC, Cavaco-Paulo A. Chitosan–lignosulfonates sono-chemically prepared nanoparticles: Characterisation and potential applications. Colloids and Surfaces B: Biointerfaces 2013;103:1-8.

[172] Wu L, Zhang J, Watanabe W. Physical and chemical stability of drug nanoparticles. Advanced Drug Delivery Reviews 2011;63:456-69.

[173] Schmidts T, Dobler D, Nissing C, Runkel F. Influence of hydrophilic surfactants on the properties of multiple W/O/W emulsions. Journal of Colloid and Interface Science 2009;338:184-92.

[174] Othayoth R, Kumar KS, Karthik V. Development and Characterization of Chitosan-Pluronic Polymeric Nanoparticles for the Breast Cancer Treatment. International Journal on Mechanical Engineering and Robotics 2013;1:2321-5747.

[175] Ekambaram P, Abdul Hasan Sathali A. Formulation and evaluation of solid lipid nanoparticles of ramipril. Journal of Young Pharmacists 2011;3:216-20.

[176] Arora S, Gupta S, Narang RK, Budhiraja RD. Amoxicillin loaded chitosan-alginate polyelectrolyte complex nanoparticles as mucopenetrating delivery system for h. Pylori. Sci Pharm 2011;79:673-94.

[177] Bathool A, Vishakante GD, Khan MS, Shivakumar HG. Development and characterization of atorvastatin calcium loaded chitosan nanoparticles for sustain drug delivery. Advancesd Materials Letters 2012;3:466-70.

[178] Pal R. Rheology of simple and multiple emulsions. Current Opinion in Colloid & Interface Science 2011;16:41-60.

[179] Paruchuri R, Trivedi S, Joshi SV, Pavuluri G, Kumar MS. Formulation optimization and irinotecan nanoparticles. International Journal of Pharmaceutical, Chemical and Biological Sciences 2012;2:1-10.

[180] Sankalia MG, Mashru RC, Sankalia JM, Sutariya VB. Reversed chitosan–alginate polyelectrolyte complex for stability improvement of alpha-amylase: Optimization and physicochemical characterization. European Journal of Pharmaceutics and Biopharmaceutics 2007;65:215-32.

[181] Sugama T, Cook M. Poly(itaconic acid)-modified chitosan coatings for mitigating corrosion of aluminum substrates. Progress in Organic Coatings 2000;38:79-87.

[182] Yang Y-T, Di Pasqua AJ, He W, Tsai T, Sueda K, Zhang Y, et al. Preparation of alginate beads containing a prodrug of diethylenetriaminepentaacetic acid. Carbohydrate Polymers 2013;92:1915-20.

[183] Al-Shdefat R, Yassin AEB, Anwer K, Alsarra L. Preparation and characterization of biodegradable paclitaxel loaded chitosan microparticles. Digest Journal of Nanomaterials and Biostructures 2012;7:1139-47.

[184] Vera Candioti L, De Zan MM, Cámara MS, Goicoechea HC. Experimental design and multiple response optimization. Using the desirability function in analytical methods development. Talanta 2014;124:123-38.

[185] Ali A, Sinha K. Exploring the Opportunities and Challenges in Nanotechnology Innovation in India. Journal of Social Science for Policy Implications

2014;2:227-51.

[186] Ukil A, Maity S, Karmakar S, Datta N, Vedasiromoni JR, Das PK. Curcumin, the major component of food flavour turmeric, reduces mucosal injury in trinitrobenzene sulphonic acid-induced colitis. British Journal of Pharmacology 2003;139:209-18.

[187] Cousins M, Adelberg J, Chen F, Rieck J. Antioxidant capacity of fresh and dried rhizomes from four clones of turmeric (Curcuma longa L.) grown in vitro. Industrial Crops and Products 2007;25:129-35.

[188] Yang R, Zhang S, Kong D, Gao X, Zhao Y, Wang Z. Biodegradable Polymer-Curcumin Conjugate Micelles Enhance the Loading and Delivery of Low-Potency Curcumin. Pharm Res 2012;29:3512-25.

[189] Bisht S, Feldmann G, Soni S, Ravi R, Karikar C, Maitra A, et al. Polymeric nanoparticle-encapsulated curcumin ("nanocurcumin"): a novel strategy for human cancer therapy. Journal of Nanobiotechnology 2007;5:1-18.

[190] Ghalandarlaki N, Alizadeh AM, Ashkani-Esfahani S. Nanotechnology-applied curcumin for different diseases therapy. BioMed Research International 2014;2014:1-23.

[191] Lertsutthiwong P, Haworth IS, Rojsitthisak P. Alginate: A promising polysaccharide for delivery of essential oils In: Ryouichi I, Youta M, editors. Handbook of Carbohydrate Polymers: Development, Properties and Applications. New York: Nova Science Publishers; 2010. p. 621-38.

[192] Kunwar A, Barik A, Mishra B, Rathinasamy K, Pandey R, Priyadarsini KI. Quantitative cellular uptake, localization and cytotoxicity of curcumin in normal and tumor cells. Biochimica et Biophysica Acta (BBA) - General Subjects 2008;1780:673-9.

[193] Amenaghawon NA, K.I. N, F.A. A, Ogbeide SE, C.O. O. Application of Box-Behnken design for the optimization of citric acid production from corn starch using Aspergillus niger. British Biotechnology Journal 2013;3:236-45.

[194] Vega-Avila E, MK. P. An overview of colorimetric assay methods used to assess survival or proliferation of mammalian cells. Proceedings of the Western Pharmacology Society 2011;54:10-4.

[195] Umthong S, Phuwapraisirisan P, Puthong S, Chanchao C. In vitro antiproliferative activity of partially purified Trigona laeviceps propolis from Thailand on human cancer cell lines. BMC complementary and alternative medicine2011. p. 37.

[196] Segurola J, Allen NS, Edge M, Mc Mahon A. Design of eutectic photoinitiator blends for UV/visible curable acrylated printing inks and coatings. Progress in Organic Coatings 1999;37:23-37.

[197] Woitiski CB, Veiga F, Ribeiro A, Neufeld R. Design for optimization of nanoparticles integrating biomaterials for orally dosed insulin. European Journal of Pharmaceutics and Biopharmaceutics 2009;73:25-33.

[198] Araujo V, Gamboa A, Caro N, Abugoch L, Gotteland M, Valenzuela F, et al. Release of prednisolone and inulin from a new calcium-alginate chitosan-coated matrix system for colonic delivery. Journal of Pharmaceutical Sciences 2013;102:2748-59.

[199] Ranjan AP, Mukerjee A, Helson L, Vishwanatha JK. Scale up, optimization and stability analysis of Curcumin C3 complex-loaded nanoparticles for cancer therapy. Journal of Nanobiotechnology 2 2012;10:1-18.

[200] Paula HCB, Sombra FM, Abreu FOMS, Paul RCMd. Lippia sidoides essential oil encapsulation by angico gum/chitosan nanoparticles. Journal of the Brazilian Chemical Society 2010;21:2359-66.

[201] Gomathi T, Govindarajan C, Rose H.R MH, Sudha PN, Imran PKM, Venkatesan J, et al. Studies on drug-polymer interaction, in vitro release and cytotoxicity from chitosan particles excipient. International Journal of Pharmaceutics 2014;468:214-22.

[202] Kanti P, Srigowri K, Madhuri J, Smitha B, Sridhar S. Dehydration of ethanol through blend membranes of chitosan and sodium alginate by pervaporation. Separation and Purification Technology 2004;40:259-66.

[203] Sun J, Bi C, Chan HM, Sun S, Zhang Q, Zheng Y. Curcumin-loaded solid lipid nanoparticles have prolonged in vitro antitumour activity, cellular uptake and improved in vivo bioavailability. Colloids and Surfaces B: Biointerfaces 2013;111:367-75.

[204] Chuah LH, Roberts CJ, Billa N, Abdullah S, Rosli R. Cellular uptake and anticancer effects of mucoadhesive curcumin-containing chitosan nanoparticles. Colloids and Surfaces B: Biointerfaces 2014;116:228-36.

[205] Punfa W, Yodkeeree S, Pitchakarn P, Ampasavate C, Limtrakul P. Enhancement of cellular uptake and cytotoxicity of curcumin-loaded PLGA nanoparticles by conjugation with anti-P-glycoprotein in drug resistance cancer cells. Acta Pharmacol Sin 2012;33:823-31.

APPENDIX

VITA

Mr. Settapon Bhunchu was born on June 10th, 1985 in Bangkok, Thailand. He graduate with a Bachelor of Engineering Degree in Electrical Engineering in 2008 and a Master Degree of Environmental Engineering, Faculty of Engineering, Chulalongkorn University in 2011. He has further studied for the Doctor of Philosophy Degree in Nanoscience and Technology, Graduate School, Chulalongkorn University since 2012.

Published Publications

1. S. Bhunchu, P. Rojsitthisak, Biopolymeric alginate-chitosan nanoparticles as drug delivery carriers for cancer therapy, Die Pharmazie - An International Journal of Pharmaceutical Sciences, 69 (2014) 563-570.

2. S. Bhunchu, P. Rojsitthisak, P. Rojsitthisak, Effects of preparation parameters on the characteristics of chitosan–alginate nanoparticles containing curcumin diethyl disuccinate, Journal of Drug Delivery Science and Technology, 28 (2015) 64-72.

3. S. Bhunchu, P. Rojsitthisak, P. Rojsitthisak, Response Surface Methodology to Optimize the Preparation of Chitosan/Alginate Nanoparticles Containing Curcumin Diethyl Disuccinate, Advanced Materials Research, 1119 (2015) 398-402.

Submitted Publication

4. S. Bhunchu, P. Rojsitthisak, C. Muangnoi, P. Rojsitthisak, Design of chitosan/alginate nanoparticles containing curcumin diethyl disuccinate of cytotoxicity in MDA-MB-231 human breast cancer cells.